Dublin City University

School of Electronic Engineering

Surface Modification of Cyclic Olefin Polymers Using Atmospheric Pressure Jet

Candidate: Faraj Abubaker Elammari (M. Eng)

A Thesis Submitted in Partial Fulfilment of The Requirement
For the Degree of Doctor of Philosophy

Supervisor: Prof. Stephen Daniels

Co-Supervisor: Dr. Connor McArdle

March 2022

Declaration

I hereby certify that this material, which I now submit for assessment on the programme of study leading to the award of Doctor of Philosophy is entirely my own work, and that I have exercised reasonable care to ensure that the work is original, and does not to the best of my knowledge breach any law of copyright, and has not been taken from the work of others save and to the extent that such work has been cited and acknowledged within the text of my work.

Signed:

Student Number: 14210705

Date:

Acknowledgements

First and foremost, I am eternally grateful to God for his abundant blessings, providence, and mercy, which enabled me to complete this work. Second, I'd like to thank my wife Radiya for her patience and encouragement throughout my studies.

Throughout the years, I've been grateful to Professor. Stephen Daniels, my immediate supervisor, for all his help with guidance, support, and patience. Throughout my PhD at DCU, I owe a great deal to Stephen for his guidance and mentoring. Additionally, I want to express my gratitude to Dr. Rajani K. Vijayaraghavan for her involvement, guidance, and sisterly affection throughout the project. I am at a loss for words to express my gratitude and appreciation for her contribution to the completion of this work.

I would like to thank all the staff of various research centres in DCU specifically National Centre for Plasma Science and Technology (NCPST).

Finally, I'd like to acknowledge the Libyan government for the financial support of this work.

Introduction and Motivation

This is a collaborative project with the primary objective of improving the wetting properties of surfaces on cyclic olefin polymer (COP) surfaces by introducing new functional groups into the surface structures without affecting the bulk structure, as well as modifying the surface topography. The second part will provide an overview of gold nanoparticles deposited on glass for surface plasmon and sensing applications. Due to the need for more economical and cost-effective ways for material surface modifications to overcome their disadvantages and become functional in the biomedical, textile, aerospace, and food packaging industries, the importance of Atmospheric Pressure Plasma Jets (APPJs) is due to the variation of active species generation that may be beneficial for sterilisation, decontamination, and food handling processes. Several of the primary factors underlying the renaissance are listed below. As opposed to low pressure plasma systems, APPs do not require expensive vacuum equipment. They are capable of being operated outdoors, allowing for continuous feed processing. Air can be used as the feed gas for APPs, significantly lowering the cost and making them more affordable. They produce high concentrations of reactive species, which are required for surface modification and metal nanoparticles. The study aims to investigate the possibility of improving the cyclic olefin polymer (COP) properties using an atmospheric pressure plasma jet APPJ, with a particular emphasis on operating parameters such as the type of gas used, the gas flow rate, the power supply conditions, and the distance between the jet and the substrate, which all play a significant role in plasma species and lead to changes in the properties. The primary objective of this research project was to increase the wettability of the

COP polymer surface, as COP's naturally hydrophobic surface precludes its use in biomedical applications such as microfluidic devices that require a hydrophilic surface. As a result, we worked to accomplish the following goals:

1. Investigating and analysing the physical and chemical properties of the COP pre- and post-plasma treatment, including surface roughness, surface wettability, and introducing functional groups.
2. We aimed to achieve the same or better COP surface wettability by substituting air for expensive plasma gases such as argon and helium that are typically used to modify polymers.
3. Electrical and optical characteristics of plasma jets were determined using current-voltage probes and optical emission spectroscopy in order to gain a better understanding of plasma physics and chemistry and how they affect polymer surfaces.
4. Increase the hydrophobic recovery time (ageing effect) of plasma-treated COP. Recent research indicates that it can take up to four weeks for COP to regain its initial wettability.
5. Optimise the APPJ's operational parameters in order to achieve the optimal plasma conditions while conserving time, effort, and money.
6. We carried out an experimental design using the software package 'Design Expert V.12'.
7. Finally, we used the air APPJ to control glass-coated gold nanoparticles for bio sensor applications. The promising results obtained were the creation of approximately 8 nm particles.

Thesis Contributions

In this thesis, economic and simple methodologies are employed to gain a super hydrophilic COP surface where the lowest water contact angle obtained was 6° of operation of various atmospheric pressure jet parameters. Contact angle measurements revealed that the hydrophobicity of the COP film decreased and stabilised after several weeks at around 20° and about 40° for approximately 6 months. These promising results provide additional industrial usage capabilities compared with previous research (Dudek, Gandhiraman et al. 2009). This is the first time that design experts have been used in APPJ to modify the surface of polymers, resulting in significant time and cost savings (e.g. gas costs, part replacement, and electricity consumed), all of which are directly related to the operation's quality and quantity. The primary objective of this study is to determine ways to further increase the hydrophilicity of the surface while minimising time and costs. The final outcomes of this thesis demonstrate that an APPJ device may be used for nanoparticles in biosensing applications. Tailoring of the plasmonic enhancement of gold-coated glass has been demonstrated by varying the thickness of the gold deposited as well as the plasma parameters of gold nanoparticles; although only a small shift in optical peeks was observed on the treated surfaces. However, the nanoparticle size of the treated substrates was about 10 nm and this is a very promising result, but the number of these particles was not sufficient.

Structure of the Thesis

The organisational structure of the thesis is as follows. The history of atmospheric pressure plasma, as well as its classification, are discussed in the first chapter.In addition, previous research in polymer surface modification has been carried out in the past. The experimental procedures and results of the COP surface modification experiments are discussed in detail in the second chapter. In the third chapter, we will discuss the software Design Expert, which is used to optimise experiments. The fourth chapter is devoted to describing the characteristics of the APPJ that was used in this study. The stability of the COP surface will be discussed in detail in Chapter 5. Then, in chapter six, APPJ was used to coat glass nanoparticles with gold, which was a first in the field. Finally, conclusions are drawn, and future prospects are discussed in detail.

Publications

- "Cold Atmospheric Pressure Air Plasma induced functionalization of Cyclic Olefin Polymer Substrates: An Investigation of Long-Term Stability". Faraj A. Elammari, Rajani K. Vijayaraghavan, Stephen Daniels. Journal of Applied Surface Science, (Ready for publication).

- "Optimization Of Air Atmospheric Pressure Plasma Jet treated Cyclic Olefin Polymer Surface". Faraj. Elammari, Stephen Daniels. Multi-Knowledge Electronic Comprehensive Journal For Education And Science Publications (MECSJ). June 2020

- Book chapter. Polymers surface modifications. Elsevier (Encyclopedia of Materials: Plastics and Polymers). Published 2021 https://doi.org/10.1016/B978-0-12-820352-1.00194-2

Table of Contents

Declaration ii
Acknowledgements iii
Introduction and Motivation iv
Thesis Contributions vi
Structure of the Thesis vii
Publications viii
Table of Contents ix
List of Abbreviation xiv
List of Figures xv
List of Tables xviii
Abstract xix
1 Introduction to Atmospheric Pressure Plasma and It's Application 1
1.1 Introduction 2
1.2 Definition of Plasma 2
1.3 Equilibrium and Non-equilibrium Atmospheric Pressure Plasma 3
1.4 Atmospheric Pressure Plasma Sources 12
1.4.1 Corona Discharge (CD) 13
1.4.2 Dielectric Barrier Discharge (DBD) 13
1.4.3 Radio Frequency Discharge Plasma 16
1.4.4 Atmospheric Pressure Plasma Jets (APPJ) 18
1.5 Applications of Atmospheric Pressure Plasma 19
1.5.1 Gas treatments 20
1.5.2 Spectroscopic analysis 20
1.6 Polymer Surface Modification 22
1.6.1 Polymer surface modification using atmospheric pressure plasma jet 24
1.7 Polymer Surface Modification Techniques 31

1.8 Previous Studies on Surface Modification of Different Polymeric Materials Using an Atmospheric Pressure Plasma 32

1.8.1 Treating a polypropylene (PP) polymer surface 34

1.8.2 Treating polythene (PE) polymer surface 35

1.8.3 Surface modification of polydimethylsiloxane (PDMS) 37

1.8.4 Cyclic Olefin Polymers (COPs) and Surface Modification 38

2 Cyclic Olefin Polymers Surface Modification, Experiments Procedures and Results 46

2.1 Introduction 47

2.2 Materials 47

2.2.1 Cyclic olefin polymer samples 47

2.2.2 Plasma gases 48

2.2 48

2.3 Experimental plasma jet and plasma processing procedure 48

2.3.1 **Plasma jet design** 49

2.4 Surface Characterisation Techniques 51

2.4.1 Contact Angle Goniometry 51

2.4.2 Atomic Force Microscopy (AFM) 53

2.5 Results and Discussion 53

2.5.1 Characterization of APPJ 54

2.6 Effect of the APPJ parameters on COP surface 54

2.6.1 Plasma fed gas impact 55

2.6.2 APPJ plasma treatment function of distance 58

2.6.3 APPJ treatment function of power supply frequency 59

2.6.4 Gas flow rate impact on COP surface 60

2.7 Ambient humidity effect on COP surface wettability 61

2.8 COP Surface Topography Analysis 63

2.8.1 Scanning Electron Microscopy (SEM).....63

2.8.2 Atomic Force Microscopy (AFM) 64

2.9 Conclusions.....66

3 Optimization of Atmospheric Pressure Plasma Treatment on COP Surfaces …… 68

3.1 Introduction.....69

3.2 Methodology 71

3.2.1 Response Surface Methodology 71

3.2.2 Experimental Design 72

3.2.3 Desirability Approach.....74

3.3 Experimental design.....75

3.3.1 Experimental work Faraj, you need to check the numbering of your sections as at present, 1.3 has no text in it. 77

3.3.2 Operating cost calculation 77

3.4 Results and Discussion.....80

3.4.1 Development of mathematical models. 80

3.4.2 Final equation in terms of actual factors.....82

3.5 Effect of Process Parameters on the Responses.....83

3.5.1 Water Contact Angle (WCA) 83

3.5.2 Impact on cost.....88

3.6 Optimization.....88

3.7 Conclusions.....90

4 Characterization of the Atmospheric Pressure Plasma Jet 91

4.1 Plasma characterization.....93

4.2 Experimental Set-up and Investigation.....94

4.2.1 Current-voltage measurements 94

4.2.2 Optical emission spectroscopy measurements.....98

4.2.3 Plasma plume temperature.....102

4.2.4 APPJ plume length as a function of operating parameters.....103

4.3 Summary.....106

5 Cyclic Olefin Polymers Post Air Atmospheric Pressure Plasma Treatment 107

5.1 Introduction:.....108

5.2 Known surface functionalization methods.....108

5.3 Surface ageing or hydrophobic recovery 109

5.4 Effect of hydrogen peroxide (H_2O_2) treatment on plasma COP polymer surface 112

5.5 Post-plasma oxidation.....114

5.6 Influence of humidity storage affecting the ageing behaviour of the COP surface.....115

6 Air Atmospheric Pressure Plasma Jet Treatment of A Gold-Coated Glass Substrate for Use with Sensors 119

6.1 Introduction.....120

6.2 SPR Sensor in Planar, Array-based Form.....122

6.3 The Use of Noble Metals as a Primary Component of Nanoparticles 124

6.4 A Brief Overview of Au NP 124

6.5 Plasma and Nanoparticles - Application of Plasma for the Synthesis and Modification of Nanomaterials.....125

6.6 Film Deposition Technique.....126

6.6.1 Deposition techniques used (vacuum evaporation) 127

6.7 Characterisation Methods 128

6.7.1 UV –VIS absorption spectroscopy 129

6.7.2 Scanning Electron Microscopy (SEM).....130

6.8 Experimental Set-up.....131

6.8.1 Sample preparation 131

6.9 Results and Dissections.....132
6.9.1 Morphological properties.....132
6.10 Conclusion.....135
7 Conclusion and Recommendations for Future Work 136
7.1 Conclusions.....137
7.2 Future Work:.....139
References.....139
Appendix.....156

List of Abbreviation

APPJ	Atmospheric Pressure Plasma Jet
APP	Atmospheric Pressure Plasma
COP	Cyclic Olefin Polymers
AC	Alternative Current
DC	Direct Current
E_m	Electron Mass
T_e	Electron Temperature
m_e	Electron Mass
VB	Breakdown Voltage
DBD	Dielectric Barrier Discharge
RF	Radio Frequency
MWF	Microwave Frequency
WCA	Water Contact Angle
FTIR	Fourier Transform Infrared Spectroscopy
AFM	Atomic Force Microscopy
UV-Vis	Ultraviolet–Visible Spectroscopy
XPS	X-ray Photoelectron Spectroscopy
OES	Optical Emission Spectroscopy
N_2	Nitrogen
O_2	Oxygen
Ar	Argon
P	Pressure
RONS	Reactive Oxygen and Nitrogen Species
SLM	Standard Litter per Minute
RSM	Root Mean Square
HDT	Heat Distortion Temperature
PEEK	Polyether Ether ketone
PET	Polyethylene Terephthalate
PTFE	Polytetrafluoroethylene
SEM	Secondary Electron Microscopy
PDMS	Polydimethylsiloxane
RSM	Response Surface Methodology
IPA	Isopropyl Alcohol
NP	Nanoparticles
PVD	Physical Vapour Deposition
CVD	Chemical Vapour Deposition
PECVD	Plasma Enhanced Chemical Vapour Deposition
SPR	Surface Plasmon Resonance
AuNP	Gold Nanoparticles
AuNR	Gold Nanorods
AuNS	Gold Nanospheres
LMWOM	Low Molecular Weight Organic Molecules

List of Figures

Figure 1. 1. Paschen curves for different gases (helium, nitrogen, neon, hydrogen and argon) [12] .....**Error! Bookmark not defined.**
Figure 1. 2. Classification of plasmas based on charge density per unit volume and electron temperature [17].....**Error! Bookmark not defined.**
Table 1. 1. Temperature and pressure ranges of hot and cold plasmas [19]. .....**Error! Bookmark not defined.**
Table 1. 2. Main characteristics of LTE and non-LTE plasma [20]..... **Error! Bookmark not defined.**
Figure 1. 3. shows a typical diagram Corona Discharge .. **Error! Bookmark not defined.**
Figure 1. 4. Basic dielectric-barrier discharge configurations [32]. ..... **Error! Bookmark not defined.**
Figure 1. 5. Electrons and ions frequencies in cold plasmas [40] ..... **Error! Bookmark not defined.**
Table 1. 4. . Examples of APS coatings .....**Error! Bookmark not defined.**
Figure 1. 6. The plasma spray principle. .....**Error! Bookmark not defined.**
Figure 1. 7. Figure 1. 8 Cyclic olefin polymers synthesis [88] **Error! Bookmark not defined.**
Table 1. 5 Surface treatments to reduce hydrophobicity of COP materials **Error! Bookmark not defined.**
Figure 2. 1. Schematic diagram of Atmospheric pressure plasma jet used . **Error! Bookmark not defined.**
Figure 2. 2. Contact angle goniometer (FTA200) ..... **Error! Bookmark not defined.**
Figure 2. 3. The Dimension 3100 atomic force microscopy (AFM) ..... **Error! Bookmark not defined.**
Figure 2. 4. Water contact angles (WCA) before and after helium/oxygen/Nitrogen and air plasma.....**Error! Bookmark not defined.**
Figure 2. 5. FTIR spectra of COP films treated by Ar, He and Air plasma **Error! Bookmark not defined.**
Figure 2. 6. FTIR spectra of COP films treated with Air plasma..... **Error! Bookmark not defined.**
Figure 2. 7. Changes in water contact angles of the COP surface as a function of nozzle distance.....**Error! Bookmark not defined.**
Figure 2. 8. Changes in water contact angles of the COP surface as power supply frequency.....**Error! Bookmark not defined.**
Figure 2. 9. Changes in water contact angles of the COP surface as function APPJ feed gas flow.....**Error! Bookmark not defined.**
Figure 2 10. Relative humidity impact on COP surface wettability.....63

Figure 2. 10. Scanning electron microscopy (SEM) images of COP polymer images of a 1µm wide for control and treated sample..... **Error! Bookmark not defined.**
Figure 2. 11. AFM images of pristine COP (A), air APPJ treated COP polymers (B). .....**Error! Bookmark not defined.**
Figure 3. 1. presents the water contact angle of untreated and air APPJ treated selected samples of COP .....**Error! Bookmark not defined.**
Table 3. 1 Independent variable and experimental design levels used..... **Error! Bookmark not defined.**
Figure 3. 2. Optimization steps [140]. .....**Error! Bookmark not defined.**
Table 3. 3 Design matrix .....**Error! Bookmark not defined.**
Table 3. 4 Experimentally measured responses...**Error! Bookmark not defined.**
Table 3. 5. ANOVA analysis for the water contact angle model ..... **Error! Bookmark not defined.**
Table 3. 6 ANOVA analysis for the operating cost model **Error! Bookmark not defined.**
Figure 3. 3. Perturbation plot showing the effect of all factors on the COP water contact angle. .....**Error! Bookmark not defined.**
Figure 3. 4. Contours plot showing the effect of input voltage V and frequency on the COP water contact angle (A) d=3mm and air flow=20 l/min. (B) d=20mm and air flow= 10 l/min .....**Error! Bookmark not defined.**
Figure 3. 5. Interaction effect between input voltage and frequency on the water contact angle (Red line is high voltage and black line is low voltage)..... **Error! Bookmark not defined.**
Figure 3. 6. (A) Contours plot and (B) Interaction showing the effect of input voltage and air flow on the water contact angle ..**Error! Bookmark not defined.**
Figure 3. 8 Perturbation plot showing the effect of all factors on the COP surface modification cost .....**Error! Bookmark not defined.**
Table 3. 7 Optimal solution as obtained by design-expert based on the first criterion.....**Error! Bookmark not defined.**
Table 3. 8 Optimal solution as obtained by design-expert based on the second criterion.....**Error! Bookmark not defined.**
Figure 4. 1: Photograph of the plasma jet plume**Error! Bookmark not defined.**
Figure 4. 2. The schematic block diagram for measuring current - voltage.**Error! Bookmark not defined.**
Figure 4. 3 Plasma off typical voltage (A) and current (B) waveforms with a 10 kV applied voltage, a 20 kHz driving frequency, and a 20 slm air flow rate. .....**Error! Bookmark not defined.**
Figure 4. 4 The voltage signal observed when the plasma was in the optimal conditions obtained from DOE. .....**Error! Bookmark not defined.**

Figure 4. 5 Figure 3.10: (a) (b) An illustration of a positive voltage drops and current spike. (c) Illustration of a negative voltage drop and current spike. **Error! Bookmark not defined.**
Figure 4. 6. Schematic diagram of the optical emission spectroscopy measurements. ..... **Error! Bookmark not defined.**
Figure 4. 7. Broadband spatially resolved optical emission spectra of APP jet. The measurements were taken at 20kV applied voltage, a 30 kHz driving frequency, and a 20 slm plume flow rate. ..... **Error! Bookmark not defined.**
Figure 4. 8. plasma plume temperature at various operating conditions (A, air flow rate), (B, Distance) and (C, Frequency) ..... **Error! Bookmark not defined.**
Figure 4. 9. plasma plumes length measurement. **Error! Bookmark not defined.**
Figure 4. 10. Plume lengths-scale variation in operating conditions, (. ..... **Error! Bookmark not defined.**
Figure 5. 1. Water contact angle as a function of time over a period of 60 days. (Black) sample treated with air APPJ saved in normal room conditions, ... **Error! Bookmark not defined.**
Figure 5. 2. COP films treated the air APPJ treatment with and without washing with H_2O_2 for 10 minutes..... **Error! Bookmark not defined.**
Figure 5. 3. Evolution of the water contact angle of APPJ-treated COP films stored in at different humidity ambient (A) stored in room temperature and humidity, (B) stored in room temperature and low humidity ... **Error! Bookmark not defined.**
Figure 5. 4. ATR-FTIR of COPs samples treated with air APPJ saved in different humidity conditions. ..... **Error! Bookmark not defined.**
Figure 6. 1. Plasma processing of materials at different length scales [191]. ...126
Figure 6. 2. diverse techniques of thin film deposition [192].....127
Figure 6. 3. A schematic diagram of a vacuum evaporation system [194]. 128
Figure 6. 5. Photograph of the Zeiss EVO LS-15 SEM system. 130
Figure 6. 6. SEM images of gold nanoparticle (micro scalepatterns on glass obtained from plasma treatment at a flow rate of 20 l/min and a distance of 5mm from the nozzle at various treatment times. 133
Figure 6. 7. 200 nm scale of the SEM images of gold nanoparticle patterns on glass 134
Figure 6. 8. Comparison of the UV-vis spectra of as-glass gold coated AuNPs before and after air APPJ treatmente. 134

List of Tables

Table 1. 1. Temperature and pressure ranges of hot and cold plasmas [13]. .....**Error! Bookmark not defined.**
Table 1. 2. Main characteristics of LTE and non-LTE plasma [15]..... **Error! Bookmark not defined.**
Table 1. 3 List of Plasma Processes and Applications [39]**Error! Bookmark not defined.**
Table 1. 4. . Examples of APS coatings .....**Error! Bookmark not defined.**
Table 1. 5 Surface treatments to reduce hydrophobicity of COP materials **Error! Bookmark not defined.**

Table 3. 1 Independent variable and experimental design levels used..... **Error! Bookmark not defined.**
Table 3. 3 Design matrix .....**Error! Bookmark not defined.**
Table 3. 4 Experimentally measured responses…**Error! Bookmark not defined.**
Table 3. 5. ANOVA analysis for the water contact angle model ..... **Error! Bookmark not defined.**
Table 3. 6 ANOVA analysis for the operating cost model **Error! Bookmark not defined.**
Table 3. 7 Optimal solution as obtained by design-expert based on the first criterion.....**Error! Bookmark not defined.**
Table 3. 8 Optimal solution as obtained by design-expert based on the second criterion.....**Error! Bookmark not defined.**

Thesis title: Surface Modification of Cyclic Olefin Polymers Using an Atmospheric Pressure Jet

Faraj Elammari

Abstract

The design and development of the plasma pressure jet is used throughout the thesis. The plasma jet's key components are discussed. Helium, argon, nitrogen, and air plasma were used to study the surface activation and bonding of cyclic olefin polymers. The plasma gas had a temperature less than 50 °C, making it suitable for polymer processing. The substrates were treated between 3 to 20 mm from the plasma exit. Air, as the plasma jet's feeding gas, creates a surface wettability of less than 10°. Water contact angle (WCA), scanning electron microscopy (SEM), atomic force microscopy (AFM), and infrared spectroscopy (IR) were used to characterise the substrate surface properties. This study establishes atmospheric pressure plasma as a cost-effective method for making cyclic olefin polymers hydrophobic and super hyderophilic. Secondly, design expert V12 software was used to optimize the APPJ operating parameters to obtain the lowest COP water contact angle with the lowest pricing. More research is required to optimise the polymer's surface and reduce the number of repetitive experiments. Therefore, the plasma jet was detailed to better facilitate understanding. Voltage and current probes were used for electrical measurements,

and optical characterisation was performed using optical emission spectroscopy. Hydrophobic recovery of polymers is a concern in a variety of applications, most notably microfluidic devices. The work presented in Chapter 5 resulted in a stable surface that remained stable for more than 60 days and was partially stable for approximately 180 days. Finally, we modified the surface of disposable glass for biosensor applications. In order to improve the optical properties, the gold of different thickness can be tailored in this work by varying plasma jet parameters. The surface treated was characterised using UV-VIS spectroscopy and scanning electron microscopy. Although the results were not suitable for biosensor applications, the experiment was worthwhile.

1 Introduction to Atmospheric Pressure Plasma and It's Application

1.1 Introduction

This chapter describes the basic principles of the atmospheric pressure plasma jet (APPJ). There are an enormous number of APPJ designs which are dependent on used excited voltage which includes kHz alternative current (AC), direct current (DC), radio frequency (RF), microwave (MW). Argon helium, nitrogen or mixed with oxygen or air as feed gas. The power supply used in APPJ as it is known, may be either continuous or pulsed. Therefore, in this chapter, a brief discussion of the atmospheric pressure plasma will be showcased.

1.2 Definition of Plasma

The fourth state of matter is usually referred to as plasma, while others are solid, liquid and gas. Plasma is one of the world's most abundant forms of common matter. In the rarefied intergalactic regions, especially intra-cluster media and stars, including the sun, the majority of plasma occurs; more than 99% of visible matter in the universe consists of plasmas. They consist of ions that are positive, electron or negative and neutral particles [1], [2]. When a solid gets energy from an external source (e.g. heat), the particles within it will have enough energy to loosen its structure and thereby melt into a liquid (the second state of matter). The par tubes in liquid escape from the gas (third state of matter) after obtaining enough energy to vaporise to gas. This results in transition of the phases that occur at a certain pressure and a constant temperature and this energy is known as latent heat for the phase transition. Those electors that escape from atoms or molecules will not only allow ions to move more freely, but also produce more electrons and ions by means of collisions following the rapid reactor in an electric field, where significant

amounts of power are then used by ~~to~~ the gas ~~by~~ through mechanisms such as an electric discharge. The higher electrons and ions eventually change the electrical property of the gas to ionized gas or plasma. This transition from ~~a~~ gas to a plasma is nonetheless a thermodynamic phase transition-due to the progressive rising of the temperature.

1.3 Equilibrium and Non-equilibrium Atmospheric Pressure Plasma

Different gas pressures can generate plasma in a laboratory and for this to be done at lower pressures, it will therefore need a vacuum system. In recent decades, plasmas are generated at atmospheric pressures to avoid the expensive and complicated vacuum system. The neutral particulate density is approximately $2.4 \times 1025/m^3$ at a pressure of one atm, where the electron-neutral collision frequency $\upsilon_{en} = n_0(2kT_e/m_e)^{1/2}\sigma_0$ is of the order of 10^{11-12}/s, where n_0 is the neutral particle density, T_e electron temperature, me electron mass and σ_0 electron-neutral collision cross section, and k is considered the Boltzmann constant [3]. If the electric field is used to generate plasma, the electrons receive more energy from the electric field than they lose by collision with neutral particles. This leads to accelerating the electrons, which can cause an avalanche that eventually leads to gas breakdowns. Many factors are considered to play a role in the breakdown voltage (V_B), such as gas composition, pressure (P) and the gap spacing (D) between the electrodes [4], [5].

As illustrated in Figure 1.1, the increase in ambient pressure increased the voltage needed for breakdown at constant gap lengths in varying gases. Breakdown voltages are calculated using a pressure-distance product. Pd is a two-dimensional

parameter that is used because it represents the particle density in the spark gap. The mechanism of Townsend's breakdown is a cascading avalanche of electrons. The mechanism of breakdown is a cascading avalanche of electrons, S, following the application of an electric field across the spark gap, Electrons are emitted from the cathode and travel towards the anode. With an increase in the applied voltage across the spark gap, the electrons travelling between the cathode and anode gain enough energy to cause ionisation and subsequent electron release, resulting in an electron avalanche [6], [7]. When the applied voltage across the spark gap becomes sufficiently high, breakdown occurs and a glow discharge occurs, this is referred to as the breakdown voltage. As the particle density increases because of an increase in pressure, electrons crossing the spark gap from the cathode to the anode will lose their energy as a result of an increase in collision frequency. The applied voltage across the spark gap must be increased to generate sufficient energy to cause further ionisation and thus breakdown [8].

The Pd parameter is a representation of the Knudsen Number K_n, shown in Equation (1.1) below, which is the ratio of a particle mean free path (the distance travelled by an electron between collisions).

$$K_n = \frac{\lambda}{d} \tag{1.1}$$

where λ is the mean free path and d is the electrode gap spacing.

By following the processes in equations (2-1)- (4-1) that lead to equation (5-1), this Knudsen number equation can be used to compute the Pd. parameters utilized in Paschen scaling using the ideal gas equation.

$$P = nK_bT \tag{1.2}$$

$$n = \frac{1}{\sigma\lambda} \tag{1.3}$$

$$Pd = nK_b Td = \frac{K_b Td}{\sigma\lambda} = \frac{K_b T}{\sigma}\frac{d}{\lambda} \tag{1.4}$$

$$Pd = \frac{K_b T}{\sigma}\frac{1}{K_n} = \frac{C}{K_n} \tag{1.5}$$

where K_b = Boltzmann's Constant, n = number of molecules, T = gas temperature and σ = collisional cross section swept by a particles travelling in space.

To have enough energy to ionise particles when they collide, the electron's mean free path must be sufficiently long, resulting in a low collision frequency. With increasing pressure, the electron's mean free path shortens [9], [10]. Due to the increased collision frequency, the energy of the electron is dissipated, reducing its ability to ionise gas particles. As illustrated in Figure 1, shorter spark gaps result in a higher breakdown voltage. This is because the Knudsen Number is large, or the electron mean free path is too long, in comparison to the electrode gap spacing d. Each gas or combination of gases has a unique E/N ratio, which is constant for glow discharges. The E/N ratio is the relationship between the electric field, E, and the neutral particle density, N. E/N is a function of the average energy of electrons travelling across the gap. To keep the E/N value constant as the gas density N increases owing to pressure, the applied electric field E must likewise increase by the same factor [11], [12].

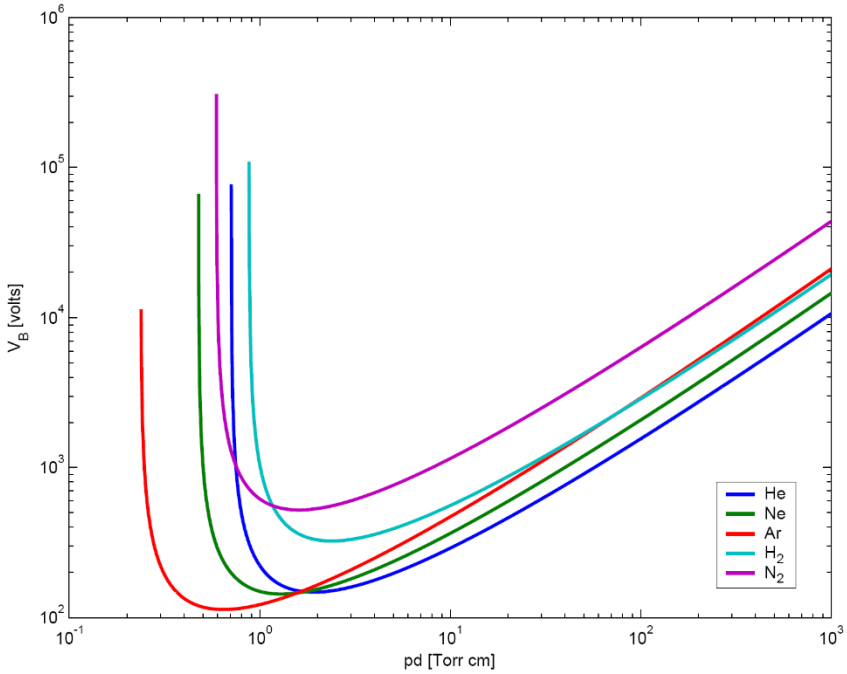

Figure 1. 1: Paschen curves for different gases (helium, nitrogen, neon, hydrogen and argon) [13]

The characteristic dependence of V_B on P.d, at high frequencies of electron-neutral collision, where a significant portion of the electron power is transmitted to the neutral particles. If the temperature of the neutral particle T_n is increased significantly and becomes closer to the electron temperature of T_e, then the plasma is classified as an equilibrium plasma. In general, the neutral particle T_n temperature and the arc plasma electron temperature T_e are several thousand Kelvin. The plasma arc is known to be used in various applications, such as welding, cutting and waste materials. However, other applications, for example, biomedical (one of the fastest growing fields), contamination, sterilizing and surface modification and others, all need low temperatures as atmospheric pressure plasma (APP), where the T_n temperature is necessary to remain close to room temperature, and in this case, the

T_n temperature will be much lower than Te and will be classified as a non-equilibrium plasma.

Thermal plasmas are almost totally ionised, and due to the high rate of collisions between electrons and neutral types, a thermal equilibrium will be reached, in which the electron temperature (T_e) is considered approximately equal to the neutral temperature (T_n). The high temperatures in thermal plasmas, for example, barrier low discharge, have deficient concentrations of free electrons. In this situation, there are insufficient collisions between the electrons and neutral species for thermal equilibrium. Electrons are accelerated to a high kinetic energy, a 1 – 2 eV arc, rendering them unsuitable for machining. On the other hand, possibly a non-thermal plasma or weak (1 eV = 11,600 K), while Tn remains 400 K. Therefore, these weakly ionised plasmas are considered suitable for the treatment of thermally sensitive materials such as polymers and integrated circuits. Thermal plasmas are almost totally ionised, and because of the high rate of collisions between electrons and the neutral type, a thermal equilibrium is reached in which the electron temperature (T_e) is approximately equal to the neutral temperature (T_n). The high temperatures in thermal plasmas, for example, barrier low discharge, have deficient concentrations of free electrons. In this situation, there are insufficient collisions between the electrons and neutral species for thermal equilibrium. The electrons are accelerated to a high kinetic energy, with 1 to 2 eV arches, which makes them unsuitable for machining. On the other hand, possibly a non-thermal plasma or weak (1 eV = 11,600 K), while Tn remains 400 K. Therefore, weakly ionised plasmas are very suitable for the treatment of thermally sensitive materials such as polymers and integrated circuits. [14], [15].

There are several types of kinetic plasmas, but the ion temperature, which is approximately equivalent to the electron temperature ($T_e \approx Ti_)$, is the most commonly used term for a hot plasma since the neutral atoms and molecules may be at a lower temperature [16]. There is little interaction between electrons and ions, hence the mean free path of a particle in a kinetic plasma (λ) is long (i.e. the period between collisions is high, and the frequency of collisions is low). Kinetic plasmas include electron and ion beams at low pressures utilized in semi-conductor manufacturing, welding, and melting.

The reason for plasmas' unique properties and relevance to high-energy processes is illustrated in Figure 1.2, where the electron temperature T_e is plotted as a function of the electron number density for various plasma processes. The Boltzmann constant establishes a relationship between energy and temperature.

kB: $\frac{1}{2}mu^2 = k_B T$.

where $k_B = 1.38 \times 10^{-23}$ J /K^{-1} [10], [17].

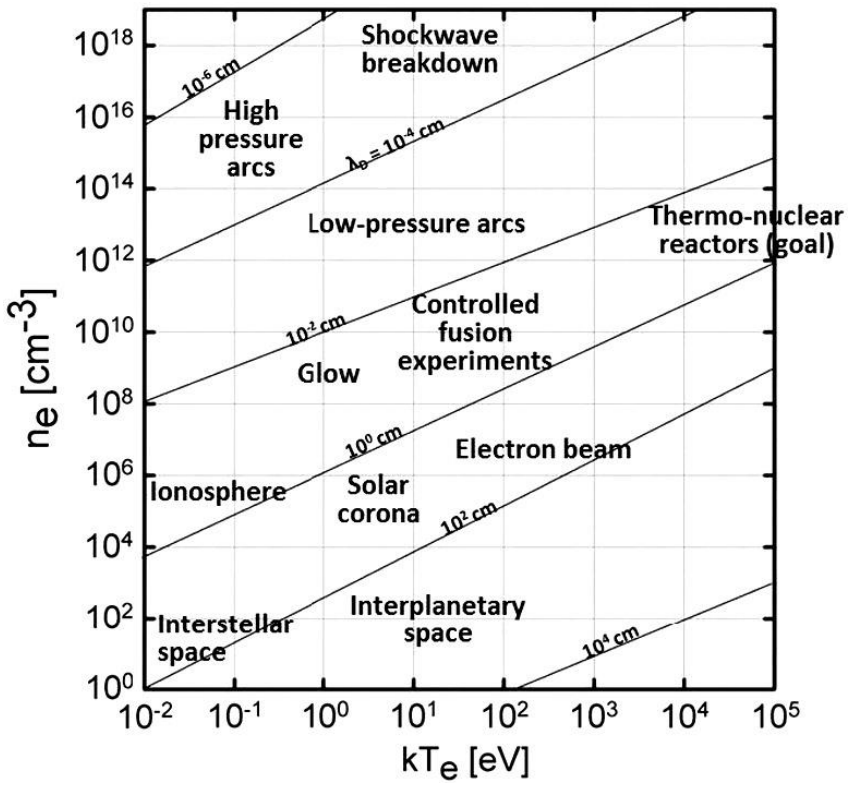

Figure 1.2: Classification of plasmas based on charge density per unit volume and electron temperature [18]

In a cold plasma, such as that found in a neon lamp, the kinetic energy is almost entirely equivalent to the electron energy and while the mean electron temperature may be several times that of the surrounding air, the number of hot electrons is a relatively insignificant fraction of the total and their thermal mass is relatively minimal [19].

Table 1. 1: Temperature and pressure ranges of hot and cold plasmas [20]

Low-temperature thermal cold plasmas	Low-temperature thermal cold plasmas	High-temperature hotplasmas
$T_e \approx T_i \approx T < 2 \times 104$ K	$T_i \approx T_e \approx 300$ K $T_i << T_e << 105$ K	$T_i \approx T_e > 106$ K
Arcs at 100 kPa Low	pressure ~100 Pa glow and arc	Kinetic plasmas, fusion plasmas

The temperature of a DBD is typically a few electron volts (eV), and a DBD's gas temperature is usually slightly greater than, or nearer to, room temperature. The typical maximum electron density of a DBD is 10^{11} cm^{-3}. Another popular method of temporal control is the use of pulsed voltage at nanoseconds for driving the discharge [18]. Pulsed voltage at nanoseconds produces plasma only if voltage is applied. Total energy is therefore limited as well. In addition, there are several pulsed nanosecond discharges. Because of the fast-rising time of the applied voltage, the electric field applied to the discharge gap can achieve a significantly higher overvoltage, and this can lead to considerably higher electron temperatures with a high peak discharge current. The peak electron temperature and electron density of an atmospheric pressure plasma driven by nanosecond pulsed applied voltages can reach about 10 eV and 10^{13} cm^{-3}. Because of the high electron temperature and high peak current, the reactive species concentration generated by nanosecond pulsed voltage will be higher. In addition, studies have found that uniform atmospheric pressure can be generated at atmospheric pressure even when

air is used as the working gas. Finally, various plasma parameters, such as reactive species concentration and gas temperature, can be precisely adjusted by controlling the pulse rising time, pulse frequency, pulse width, and amplitude of the applied voltage. Table 1.2 presents some differences between LTE and non-LTE plasmas. The electron temperature T_e in a typical low-power ion source plasma is in the range of 30 000–40 000 K, whereas the ion temperature T_i is in the range of 500–1000 K [14].

Table 1.2: Main characteristics of LTE and non-LTE plasma [21]

	LTE plasmas	**Non-LTE plasmas**
Current name	Thermal plasmas	Cold plasmas
Properties	T_h=T_e High electron density: 10^{21}–10^{26} m^{-3} Inelastic collisions between electrons and heavy particles create the plasma reactive species whereas elastic collisions heat the heavy particles (the electrons energy is thus consumed).	T_h>>T_e Lower electron density: $<10^{19}$ m^{-3} Inelastic collisions between electrons and heavy particles induce the plasma chemistry. Heavy particles are slightly heated by a few elastic collisions (that is why the electrons energy remains very high).
Examples	Arc plasma (core) T_e=T_h≈10,000 K	Glow discharges T_e≈10,000– 100,000 K T_h≈300– 1000 K

In a typical low-power ion source plasma, the electron temperature T_e is of the order 30 000 - 40 000 K, while the ion temperature T_i is around 500 - 1000 K [22].

The electron and ion gyro radius size depends on the local magnetic field, which can vary dramatically between different plasmas. We can, however, say that the ion gyro radius is nearly always significantly higher than the electron gyro radius, as long as the electron temperature is not dramatically larger than the ion temperature [23].

1.4 Atmospheric Pressure Plasma Sources

Atmospheric pressure plasma (APP) are plasma sources that generate cold non-equilibrium plasma typically in a noble gas flow through a dielectric tube into ambient air [24]. The generation of the plasma inside the noble gas jet produces a much larger ionisation level of noble gas compared to the ambient air surrounding the jet. However, fast moving ionisation waves with the duration of several hundred nanoseconds pass through the dielectric tube and gas jet every half-period, or per applied voltage pulse [24]-[26]. These ionisation waves are highly luminous and move at a velocity in the range of 10-103 km/s, which is several orders of magnitude higher than the gas flow rate [18]. Different sources with different types of frequencies can be used to produce atmospheric plasma. Such sources can be mainly classified into three categories: DC (direct current) discharges, continuous or pulsed low frequency discharges, RF (radio wave frequency) discharges, and microwave discharges. We can have arc plasma torches in low frequency DC discharges with a continuous working mode, but we can have dielectric barrier discharges if we have a pulsed operating mode. Such discharges can be filamentary or glow, depending on other parameters. RF discharges can also work with low and high-power supplies. DBD discharges are the most widely used among these different types of discharges.

1.4.1 Corona Discharge (CD)

Corona Discharge is characterised by an asymmetric electrode and a pair of inhomogeneous electric fields. The high electric field strength in the vicinity of the electrode exceeds the gas breakdown threshold, resulting in the formation of plasma toward the planar electrodes. Figure 1.3 shows a typical diagram of the Corona Discharge. It is a positive corona when the sharp point electrode is connected to the positive terminal of the power supply and the negative corona with negative output polarity. Dust processing, purification of water, electrocameras, printers and powder coating are the areas used for corona discharge [27].

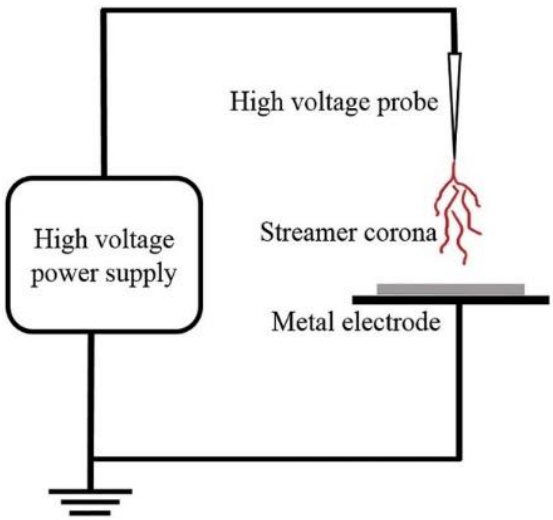

Figure 1. 3: Typical diagram of a Corona Discharge

1.4.2 Dielectric Barrier Discharge (DBD)

Dielectric barrier discharge is usually formed between two parallel electrodes with a 0.1 to 10 mm range separation, where one or both electrodes are coated with a

layer of the dielectric barrier due to dielectric charging problems associated with direct current (DC). They are usually carried out with square wave currents, sine wave flows or pulse waves with frequencies of a few Hz to MHz, but often in the KHz range [28]. In any case, the DBD scheme must be presented as a capacitive component. The displacement current is defined by the total capacity of the DBD system and by the time the voltage was applied. DBDs have unique features and characteristics that enable them to be used in a wide variety of applications, including ozone production, plasma display panels, surface engineering procedures, scrubbing, and excimer lamps [29], [30]. Examples of the DBD characteristics are described in [31], [32] and demonstrated with low power (< 1 W), low gas temperature (~ 600K) and excellent dissociation capability for molecular species. Typical DBDs configurations are shown in Figure 1.4 below.

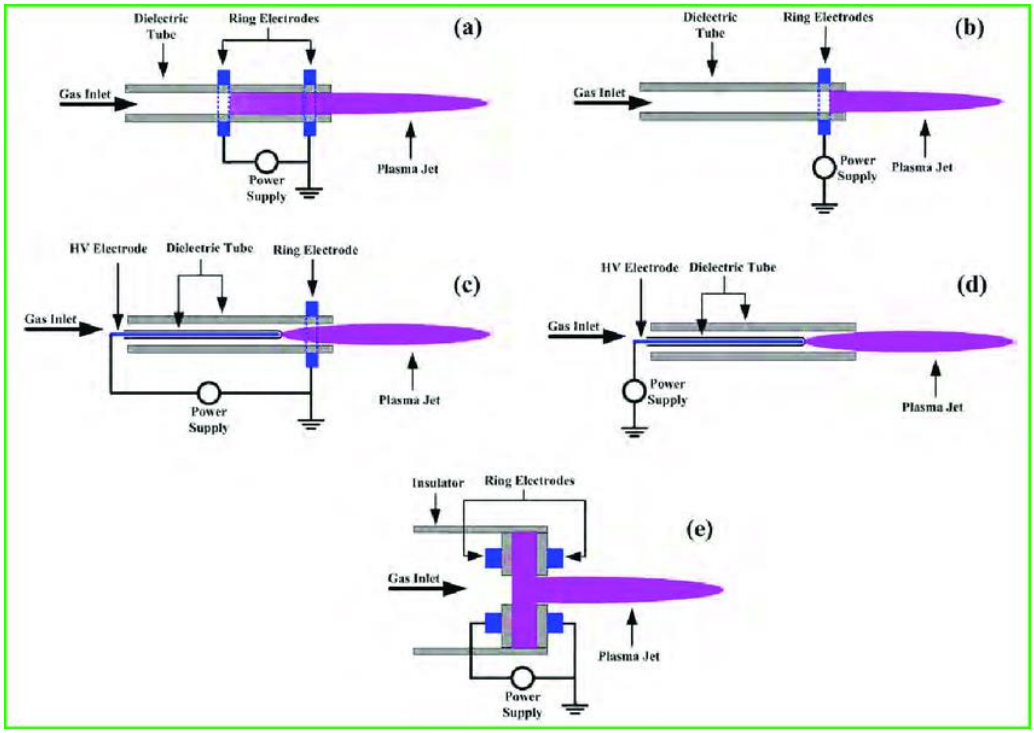

Figure 1.4: Basic dielectric-barrier discharge configurations [33]

These sources are usually non-thermal equilibrium with energy linked via the conductive material of the capillary wall of external ring electrodes. Plasma and neutral gas species provide these sources for applications in health care and life science, as well as applications on thermally sensitive surfaces. This method has been used in the detection of chemical warfare analysis and for the detection of gas-phase connections [34], drugs and explosives, medical applications [35], pollution control [36] and process control, food and safety [37]. The type of discharge gas determines the stability of the glow plug. For example, helium leads to a stable homogenous glow discharge, whereas nitrogen, oxygen and argon simply lead to the transition to a continuous discharge. However, by changing the electrode configuration, it is still possible to operate them in a homogeneous glow discharge regime [35], [38].

1.4.3 Radio Frequency Discharge Plasma

Radio Frequency discharge can be generated either by capacitive or inductive connecting energy to an AC power supply in the radio frequency range (1 KHz to 103 MHz; the most common value 13.56 MHz) [39]. The organisational structure of the thesis is as follows.

A. Inductively coupled RF discharge:

For a long time, inductive discharges have been known, for example, the RF torch, in which the plasma is initiated and maintained by an RF-fed helical coil. [21]. The current in the RF transmission coil induces a time-varying magnetic field in the vicinity of the plasma zone. The resulting electricity ring area (Faraday Law) accelerates the electrons and therefore maintains the discharge. If the frequency of the generated plasma exceeds 1 MHz, this frequency level implies that electrons follow the fluctuations in the electric field and that neither ions nor electrons can reach the torch on the wall, as shown in Figure 1.5.This lack of contact between the plasma and the wall reduces the contamination of plasma and torch walls that work with various gases: inert, restricted, oxidising, and nitriding gases [40]. The inductive torches are employed over a wide range of power, from an average of 20 kW - 1000 kW, with a flow of 10 - 200 slm.

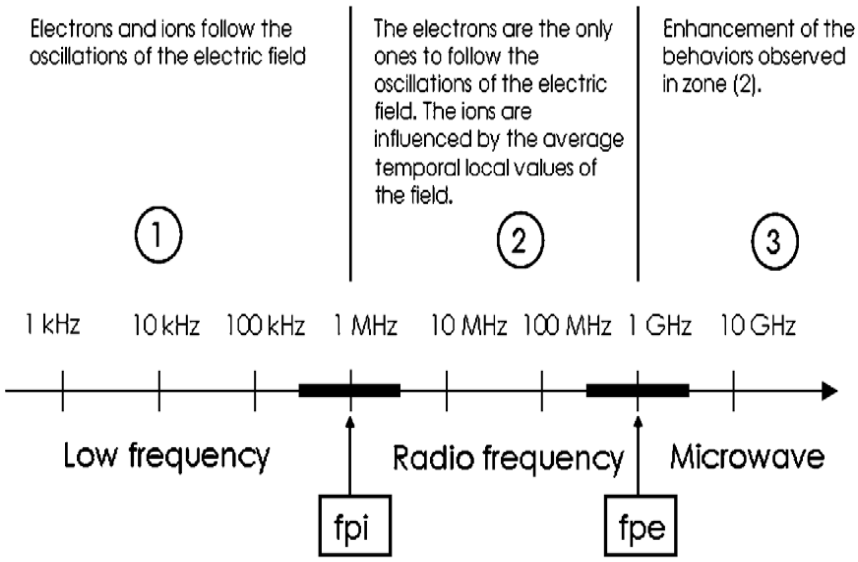

Figure 1.5: Electron and ion frequencies in cold plasmas [41]

B. Capacitive coupled radio-frequency discharges

This is a capacitively coupled radio frequency that is characterized by glow discharge electrodes during performance. When one or both of the electrodes are non-conductive, As a result of the accumulation of positive or negative charges on the electrodes, the glow discharge is extinguished. This problem can be solved by an AC voltage between the two electrodes and in both situations the electrodes act as a glow cold cathode or as a cathode in an arc of a cathode spot. In either case, the electrode is transformed from cathode to anode and reversed every half cycle.In practice, many RF glow discharge procedures use 13.56 MHz, and because this frequency is assigned by the international communications public, it can emit a certain amount of energy while not interfering with communication [42]. For plasma processing applications, capacitive coupled RF discharges are also called "RF diodes" and are shown to exist in the easiest case of a vacuum chamber

containing two planar electrodes that are separated by a distance of a few centimetres.

1.4.4 Atmospheric Pressure Plasma Jets (APPJ)

The atmospheric pressure plasma jet APPJ is one of the most common and vital types of dielectric discharge barriers. The APPJ was developed and will be used in the open air. It operates in a capacitive coupling mode and consists of two electrodes and a dielectric layer. Typically, one electrode connects to a high voltage power source with an excitation frequency between a few kHz and RF. Although the electrode is grounded, the plasma jets are typically used to generate effective chemicals by means of inert gases such as helium and argon with minor impurities of molecular gases, which are not reactive, to improve their industrial and biological capacities. The APPJ is not only limited to the electrodes, but also extends forward. It is fitted with standard, stable and homogeneous discharge characteristics and is far from the spark condition. The mechanics describing the propagation of the APPJ under the external electric field are still not fully understood. Neither are the mechanics describing the propagation of the APPJ under the external electric field. The mechanics describing the propagation of the APPJ under the external electric field are also not fully understood.

The atmospheric pressure plasma jet was first produced in the 1960's as a local thermodynamic equilibrium plasma jet. The APPJ was subsequently produced in different designs and under considerably different conditions. Koinuma et al. discovered APPJ in a plasma-generator with a microbeam in 1992 [43] , which cold torch plasma. later dubbed a "cold torch plasma" [44]. contributed to the

development of an APPJ non-equivalent by using a radio frequency unit using two coaxial metal electrodes where the gas flow through the discharged area was supported by a strong gas jet. Teschke et al [45] investigated the future development of various portable APPJ devices such as jet needles, plasma pencils, and so on, and discovered a new type of plasma jet that is typically generated by using a dual dielectric electric electrode. Recently, various alternative tribal techniques to improve jet generation have been presented. For instance, by using non-sinusoidal exertion and altering the electrode structure. The latter approach includes a barrier torch plasma jet with plate electrodes, two parallel thin cop torch electrodes inserted in a dielectric cylindrical tube and so on. In recent times, floating electrodes have been used so that they have a long plume length, a low operating voltage, and a long operating time. Fridman et al [46],recently developed a floating electrode with numerous advantages over the traditional production method. Hamid et al [47], investigated the impact of the flow rate and tube diameter on improved jet length.

1.5 Applications of Atmospheric Pressure Plasma

The recent rapid development of plasma technology allows its use to be applied in many industrial sectors. Many papers on the topic of generating ozone have been published, including those on gas decontamination [48], [49], and those with biological applications for several decades. Recently, the topic of APPJ has been widely used in polymer research, thin film deposition, food decontamination, control of the concentration of items in liquids, classification and identification of substance composition, manufacture of semi-conductor devices and others.

1.5.1 Gas treatments

The cleaning of gas is an enormous economic and environmental problem. There are different pollutants. These pollutants are derived from exhaust gas engines, electric power stations, the chemical industry (solvents, paints, varnishes) and the petrochemical industry. These compounds are released into the environment, and cause environmental problems.

1.5.2 Spectroscopic analysis

RF inductively coupled plasmas are particularly of interest, as they can further integrate with complementary devices on one ’chip’ and therefore result in a miniaturized total analytics system [36]. Plasmas are used as sources of stimulation for a spectroscopic analysis [37]. There are two primary types of spectroscopy analysis: (i) Hydrocarbons: these are formed from acetylene using an arc plasma in the presence of hydrogen in hydrocarbon cracking. It has been used in industrial applications for many years and is extremely adaptable to acetylene requirements, with its manufacturing adaptable to those requirements [38]. This is extremely flexible: manufacturing can be adapted to acetylene requirements; (ii) Ozone: ozone is used in a variety of industries, including the chemical, pharmaceutical, water, paper dough and food treatment sectors [50]. (iii) Plasma material treatments: there are five major categories to consider when it comes to plasma material treatment:

- Cleaning of surfaces by elimination of organic contaminants and surface sterilization.
- Material surface etching leads to the removal of top layers and surface restructuring with an increase in corrugation and surface area.

- Cross-linking of surface molecules which cause surface chemistry changes surface composition.
- Coating deposition.
- Introducing certain functional groups and formulating a chemical modification of the presence of some or all of these effects makes plasma ideal for treating surfaces in a variety of applications, as shown in Table 1.3.

Table 1. 3: List of Plasma Processes and Applications [51]

Surface Modification	Application
Etching	Surface structuring surface cleaning
Functionalization	Hydrophilization, Hydrophilization, Graftability, Adhesnability, Printability.
Structural Modification	Diffusion and bonding, implantation for hardening
Deposition	Change of hardness, toughness, change tribological properties, corrosion protection architecturing, crystal growth (diamond, graphene …), scaffolds for biomedicine
Tribological Properties	Wear coefficient, erosion rate, coefficient of friction
Optical	Refractive index, optical loss, absorption coefficient extinction coefficient
Electrical	Spark gap switches, circuit breakers
Heat	Welding/cutting arcs, plasma spray, thermoelectric drivers

1.6 Polymer Surface Modification

Because of their excellent properties, such as low density, high flexibility, elasticity, conductivity, strength, easy manufacturing, low material cost and performance production, polymers have gained considerable attention from various industries including automotive, aeronautical, medical, construction and packaging [52], [53]. Polymers often have poor surface characteristics due to their inertia, which limits their use in various biomedical applications. Techniques required in the modification of the surface need to preserve the desirable bulk properties, which involves the alteration of the outer layer of the surface by adding certain functional groups and altering the surface morphology to respond to specific requirements. It usually improves its interaction with the biological environment, increasing its compatibility with bio/blood, barrier properties and adherents, while retaining the polymer's appropriate bulk properties. Plasma treatment is the most suitable process amongst the various surface-modifying techniques available because of its advantages, such as managed surface-modification at a depth between a few μm and nm, multi-layer film creation, highly cross-linking polymers, irrespective of geometries, an environmentally friendly dry, lower temperature method, and not changing the bulk properties, where previous research has shown that plasma treatment can be used to alter the polymer surface properties without affecting its bulk properties [54]-[60].

Different active plasma species are strong enough to break the bonds between the covalent polymers. Surface modification of plasma treatment is a well-known method used in a variety of applications, including textiles, biomedical applications, and membrane separation [61], [62].

Atmospheric plasmas have been proven to possess many applications in surface modification of polymers. Existing research has proven that microwave plasmas have a wide range of applications in polymer surface modification [63], while inductive and arc plasmas are most appropriate where high power is required. Radio and low-frequency plasmas have been found to be most suitable for applications that need low temperatures and active species. Existing studies have shown that pre-treatment of polymers with atmospheric pressure plasmas changes their surface properties so as to improve their adhesive strength and wettability [64], [65]. As mentioned earlier, plasmas can generate high or low temperatures, so they can be used in various industrial applications, including surface activation. Therefore, atmospheric plasmas can treat the unique surface properties of polymers to overcome the surface drawbacks of their properties and to continue to attract more research.

Plasma jets, also known as plasma plumes, are typical of atmospheric pressure plasma that discharges in a situation where the plasma is extended past its generation region into the surrounding area [66]. The plasma jet length can reach up to a couple of centimetres and, as a result, can be controlled by the electrical field, pressure gradient or gas flow. Therefore, the interaction between the atmospheric pressure plasma jet and the polymer surface can improve various reactive species that may be employed in modifying the surface chemistry and, as a result, these plasma techniques will need to be developed further. This further work will need to rely on atmospheric plasma jets as the main work for further research development.

1.6.1 Polymer surface modification using atmospheric pressure plasma jet

Atmospheric plasma jets are known to be used in material processing, such as bulk material treatment and surface treatments [67]. Bulk material treatment includes toxic waste treatment, machining, and powder treatment. Surface treatments include etching, activation, cleaning, and coating. Table 1.3 below outlines some examples of applying atmospheric plasma jets to coatings, whereas Figure 1.6 shows the plasma spray principle used in coatings.

Table 1. 4: Examples of APS coatings

APS coating	Function	Examples of applications
Zn, Al	Resistance to wet corrosion	Water or gas pipes (petrochemistry), bridge metallic structures. . .
Al2O3	Electromagnetic protection for electronic equipment	Computers
CoCrAlY	Electrical insulation	Ozonors, oven inductors
Zn, Sn, Cu	Electrical conductivity	Connecting welding
Al2O3 Hydroxyapatite	Biocompatibility	Biomedical: artificial limb (hip, knee. . .), implants (tooth. . .)
ZrO2–Y2O3	Thermal barrier	Turbine combustor, rocket
Cr2O3 ZrO2–NiCrAlY	Wear resistance	metallurgy, paper industry, Mechanic, army, aeronautic, petrochemistry

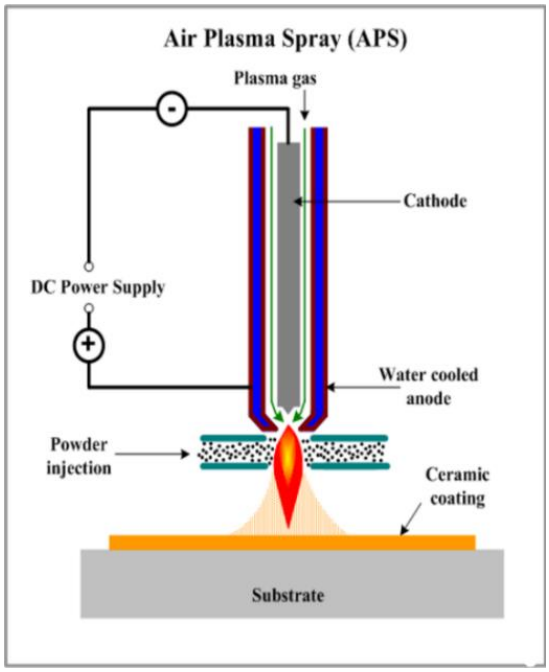

Figure 1.6: The plasma spray principle [68]

Advantages of atmospheric pressure plasma processes:

a. The change is limited to the upper surface layer and does not affect the bulk properties of the polymer.

b. The amendment by the plasma processes is largely independent of the structure or chemical reactivity of the substrate.

c. Varied functional groups can be deposited on the treated surface by varying the gas that is used.

d. In general, the amendment is entirely homogeneous over the entire substrate.

e. The plasma treatment or polymerisation is a one-step procedure and is a drying process.

f. In comparison to other techniques, it is a friend to the environment so far.

g. There is no need for an expensive vacuum system.

- **Disadvantages of atmospheric pressure plasma processes:**

1. Due to the complexity of plasma processes, it is difficult to have proper control of the chemical composition of the modified surface.

2. When treating localized regions, it can only process a small size.

Surface contamination removal is required to promote adhesion, which is why the adhesive treatment is used. In order to have good adhesion, strong interfacial forces are required through chemical compatibility and/or chemical bonding, including the need for material structure and hydrophilicity, which are considered important as well. Hydrophilicity plays an important role, as it determines the interaction between the surface and epoxy or similar polar adhesives and then the degree of bond ability [69]. Surfaces are to be carefully prepared before bonding for the removal of contaminants. It implies, therefore, that dangerous chemicals are commonly used for surface cleaning to increase their hydrophilicity for the removal of thin layers of hydrocarbon-based contaminants [70], [71]. There is also the need for less harmful, toxic and eco-friendly methods. Hence, plasma surface treatment is considered beneficial as it can help the interfacial adhesion process in creating chemically active functional groups such as amine, carbonyl, hydroxyl, and carboxyl groups [72]. As it is known that plasma improves bonding on substrates like glass, polymers and different metals, plasma treatment is then applied to carbon

fibre-induced polymers to increase wettability of polymer surface roughness in oxygen-based functional groups [73].

Usually, polymer chains are very flexible coiled cables with free participation in between and are mostly unadorned chains of a linear skeletal structure that can be represented by a chain with two ends. Branched polymers have side-chains of great length that are connected to the main chain of the coupling points. These are distinguished by the number and size of their branches. Network polymers are three-dimensional structures in which each chain is connected to all the others by a series of clutch points and other chains. These polymers are known as cross-linked polymers [38]. Polymers are successfully used in a wide range of industrial applications including packaging, adhesion, thin films, biomaterials, coatings, and others.

Polymer applications are considered as absorption materials and these include:

- Adhesion
- Print on films
- Dyeing of fabrics
- Static dissipation
- Oil repellency in the air
- Oil released into detergent solutions
- Food packaging

The industrial applications are highlighted further below:

- Ion exchange
- Chromatographic Separations

- Membrane separators
- Catalysis
- Electrical conduction
- Light reflection
- Analytical sensors
- Biotechnological applications
- Medical and Cell Culture Dishes
- Cell supports in fermentation processes
- Degradable polymers biosensors and diagnostic assays
- Sterile packaging
- Proteins and cells separations
- Blood and urine catheters
- Bandages
- Healing reactions on surfaces of implants
- Hemostatic sponges and tissue
- Blood circulation devices
- Drug delivery devices.

Accordingly, it is not only desirable but also necessary to modify polymer surfaces [74] by physical, chemical, mechanical or biological methods and the subsequent surface interactions and reactions required depend on the certain application considered. Sometimes it is desirable to have surface modifications in specific patterns on a surface with special techniques borrowed from lithography. This is a growing area of surface modification, especially at the micro- and nano-scales.

The polymer surface often has low surface energy and high chemical inertia, which means that they frequently have poor wettability and adhesion qualities. An overview of the objectives of modification of polymer surfaces is:

- Hydrophilicity (wettability).
- Ionic charge or PH (where the adsorption of molecules is of consideration).
- Adhesion of micro-organisms.
- Permeation of molecules.
- Chemical or biological reaction kinetics.
- Roughness or friction.
- Electric, optical or acoustic properties.
- Impurities, domains or patterns of the above.

The surface properties can be changed by modifying the molecular structure with low energy consumption. Here, plasma treatment converts the hydrophobic polymer to a hydrophilic surface. Studies on plasma polymer interactions for improvement of wetting and adhesion of metal-polymer laminates have also been conducted [64], [75]. Polymers are used for a wide range of applications in food packaging and decorative products and also in electronic equipment insulation materials. The adhesion of the substances to polymeric substrates is essential for these applications. Not all surfaces of polymers are suitable for adhesion to the required physical and chemical properties. Plasma treatment is a modification of polymer surfaces to improve adhesion while maintaining the other properties of the required applications.

Depending on the gas and plasma used, ions, electrons, fast neutrons, radicals and UV radiation contribute to the polymer, making the etching, activation and cross-linking [64], [76]. Plasma treatment of polymer surfaces causes not only a change in the plasma exposure, but also active sites on the surfaces that cause post-reactions; this is also called ageing [76]. Ageing effects depend on external influences such as adsorption or oxidation as well as on the internal tendency of the system to obtain energy-favourable (thermodynamic equilibrium) conditions by restructuring and diffusion. High surface energy is inclined to adsorb contaminants from the atmosphere into the surface energy surface, and this will influence wettability [77]. Although the mechanisms of adhesion enhancement pre-treatment with plasma or ion beams have been investigated extensively in the last three decades, there are more studies on the factors behind the lack of adherence to this phenomenon. Therefore, the processes in a shallow polymer are low during ion bombardment, as well as in the kinetics of post-bombing chemicals that are incomprehensible. So many efforts have been made to improve the microstructure and thermal stability of metal-polymer interfaces with the aim of preventing degradation and improving adhesion [78]. The surfaces prepared for plasma treatment should be characterised by the changes in optical, chemical and structural features induced by the plasma plume on the surfaces to improve their adherence.

These polymers are distinguished by their glass transition temperature (Tg), which is the temperature at which they transition from a glass-like (hard) to a rubber-like (soft) state. Elastomers are cross-linked rubbery polymers that can be stretched easily into high-voltage devices and that quickly recover their original dimensions as the applied voltage is released. Thermosets are rigid network polymers in that chain movement is limited by a high degree of cross-linking [52].

1.7 Polymer Surface Modification Techniques

The polymeric materials used in the manufacture of biosensors and medical equipment should satisfy performance and bio-compatibility requirements. The understanding of the relationship between structure and substance in polymers is sufficiently advanced in order to achieve the desired mechanical properties that should apply a minimum amount of stress to adjacent tissue, a glucose sensor membrane that requires high levels of oxygen permeability. The rationale for modifying the surface of the biomaterials is straightforward: the main physical properties are retained while adjusting only the surface to affect bio-mineral content. The mechanical properties and functionality of the device remain unchanged with well-designed surface modifications, but bio-compatibility, bio-recognition, and bi-functionality are improved. In addition, surface alteration can also be used. Surface modifications can be divided into two main categories:

(1) the chemical or physical modification of existing surface atoms or molecules (including treating, eating and chemical modification).

(2) coating of a material having a new composition over the present surface (solvent coating or deposition of thin films by chemical deposition of vapour, radiation grafting, chemical grafting or RF-plasma).

Relevant criteria need to be discussed when successfully completing all surface alteration categories for biomedical applications. These can be regarded as chemical, surface analysis and biological surface alteration challenges.

There are different methods of modifying polymer surfaces by generating new functional surface groups that preserve the desired properties of bulk polymers [79]. Modification techniques such as plasma polymerization, plasma spray coating, ion implantation and ion beam-assisted deposition [80], flame, corona treatment [81], photon, electron beam, X-rays, and γ-rays [82]. Important characteristics imparted by these technologies include wettability, adhesion, chemical affinity and bio-compatibility. Surface modification plays a significant role in many industrial applications: electronics, packaging, industrial, automotive, aerospace, storage and medical devices [83]. Surface modification techniques can change the chemical and physical characteristics without impacting the polymer surfaces. The surface treatments contribute to the improvement of the surface energy, adhesion characteristics, increasing their hydrophobicity, introducing special functional groups to the surface and/or affecting the surface roughness.

1.8 Previous Studies on Surface Modification of Different Polymeric Materials Using an Atmospheric Pressure Plasma

The potential applications of atmospheric plasma sources are dependent on their plasma properties, particularly their temperature. For example, polymer surface treatment requires low temperatures below T_g [84], Metal plasma cutting and welding necessitates temperatures in excess of 1227 °C. [21]. The low temperatures can be obtained either with low working ability (few hundred watts) or in the plasma plume with higher power (especially for microwave plasmas). However, to have a sufficient density of active species, the distance from the plasma core should be limited. Therefore, low temperatures and an active zone cannot be combined by arc or inductive plasmas. Only a high work capacity is available at high gas

temperatures and the most appropriate plasmas are inductive or microwave. The optimal conditions for polymer surface modification are by using a cold atmospheric plasma jet induced by a plasma jet that is obtained from a dielectric barrier discharge. The different polymers used in the study included polythene (PE), polyethylene terephthalate (PET) [85] and polypropylene (PP) [86]. The samples used in the studies were exposed to a plasma jet with a scanning procedure, allowing the experiment to achieve a rather uniform surface modification.

Existing research shows that treatment of all polymers causes a reduction of above 40 degrees in the contact angle of water. Fourier-Transform IR spectroscopy (FTIR) and X-ray photo-electron spectroscopy were used to investigate changes in chemical bonding and surface composition. The research found that the wettability of PP, PE, and PET polymers was enhanced by using an atmospheric pressure jet in the air. If the time of the plasma exposure and the process conditions are appropriately selected, then the APPJ can modify the selected area of a sample uniformly [51]. For comparison purposes, the researchers treated the same polymers with an air dielectric barrier discharge. The FTIR and XPS analyses revealed that both processes produce carboxylic acids, alcohols, and carbonyls.

Similarly, it was indicated that the polymers processed by the APPJ exhibited more oxygen content and the hydrophilicity was better once treated by the DBD [58][87]. Such a finding can be linked to efficiency in the chemistry of the plasma whereby the interaction of the metastable with the air molecule results in the production of large amounts of reactive species. The findings could also be due to the gas stream of the plasma jet carrying the oxygen species close to the surface. The consequences of the study suggest that the APPJ is an efficient tool in the modification of the

polymer surface. Therefore, the results of the study could be useful in applications that require a rather small treatment area.

1.8.1 Treating a polypropylene (PP) polymer surface

Results of the study indicated that after treatment with both atmospheric pressure plasma and low-pressure oxygen plasma, the presence of carboxyl, hydroxyl, and carbonyl groups of films could be confirmed. However, whenever treatment with atmospheric pressure plasma occurred, the amount of each functional group was larger. This was most evident in the carbonyl group. Additionally, the amount of the functional group was altered whenever methanol washed. When polypropylene PP films underwent treatment under an atmospheric plasma jet, the hydroxyl group was the most obvious [88].

The research concluded that the difference in the effects of plasma treatment position and plasma treatment time in the plasma jet was hard to recognise. It was also concluded that oxygen functional groups could be introduced into the main chain of a polymer during plasma treatment when the time is less than three seconds. The oxygen atom contained in the plasma jet etches into the surface of the polymer and it prevents the introduction of oxygen functional groups. The research also found that surface discharge plasma and the surface treatment on PP film are effective in generating a hydrophilic surface.

1.8.2 Treating polythene (PE) polymer surface

Many polymers, metals and composite materials, require some treatment before painting or adhesive bonding. Treating polymers modifies the properties of the substrate's surface to enhance the durability and strength of an adhesive joint or painting. Atmospheric pressure plasmas and low-pressure plasmas have been found sufficient to pre-treat polymers. As a result, it has piqued the interest of many researchers in the field of polymer treatment. Before experimentation, polythene (PE) samples are cleaned with ultrasonic isopropanol. In the experiment, a plasma jet system was used for treatment. The jet made use of either pure nitrogen or dry air, with an input pressure of around 5.9 bars, and an excitation frequency of between 17-22 kHz. The PE samples were moved through the translation stages via the plasma jet. Surface tension was determined using contact angle measurements such as advancing angle and dynamic mode. Di-iodomethane, water, and glycerol were used as probe liquids. The XPS measurements were carried out using a Kratos Ultra system [89]. Surface analysis on the PE samples was conducted 24 hours after treatment with the plasma jet. For the purpose of adhesive bonding, a methacrylate adhesive was used. The reason for choosing this adhesive was because the material shows some adhesive failure on a non-treated surface and even after treatment. The improvement was linked to an increase in surface tension and the incorporation of functional groups containing nitrogen and oxygen into the polythene surface. As per the AFM measurements, plasma treatment does not change the roughness of the surface significantly. Existing research also indicates that similar effects of plasma treatment on surface roughness have been found on polyethylene terephthalate and polyvinylidene fluoride. These findings show that the chemical composition of the

surface is of more importance than the roughness of the surface concerning adhesive bonding ability.

Research findings correspond to the adhesion mechanism according to the theory of chemical reaction, which has found that the formation of chemical bonds and dipole attraction between the adhesive and the substrate is the primary cause of bond strength [85]. Using two types of gas, it was possible to obtain more information about the activation mechanism, and about the conditions in industrial applications, by experimenting around the plasma and PE sample without a concealed environment. Comparison of surface modifications after treatment with nitrogen plasma and air plasma showed some interesting aspects. For example, treatment with air plasma caused more surface tension than treatment with nitrogen plasma [85]. This is due to the higher concentration of heteroatoms incorporated into the surface of the substrate treated with air plasma. Despite having lower surface energy, nitrogen plasma samples showed more bond strength. An observation such as this indicates that there is no direct correlation between bond strength and surface tension.

APPJ treatment using nitrogen and air improves the PE adhesive bond strength through surface modifications. The differences between air and nitrogen plasmas lead to different surface modifications. Therefore, results from the study indicate that to understand the activation mechanism of the APPJ system used, both the plasma reactions on the surface and post-plasma processes should be taken into account. Therefore, theoretical predictions on optimal process parameters as a result of plasma modelling have become more difficult, since additional reactions that are not directly related to the treatment require consideration [85].

1.8.3 Surface modification of polydimethylsiloxane (PDMS)

Polydimethylsiloxane (PDMS) has been widely used in many devices as microfabrication due to being self-sealable, elastic, inexpensive, and bio-compatible. PDMS has also proven to allow easy fabrication of devices and boasts of having excellent optical transparency. However, its innate hydrophobicity portrays non-specific binding, thereby limiting it to applications involving electro-osmotic flow [90]. Therefore, there is a lot of interest among researchers in how the surface of PDMS can be modified to make it hydrophilic while preserving its bulk-material properties. Plasma treatments using oxygen have been the most commonly used and simple method for modifying the PDMS surface to be hydrophilic. However, hydrophilicity is lost quickly since PDMS oligomers usually migrate from the bulk part to the air-surface interface.

The difficulties in maintaining the hydrophilicity of PDMS for longer periods after treatment have led to developing a method that can modify the PDMS surface and make it hydrophilic for a longer period [90]. In their experiment, two different layers were deposited on a PDMS surface block using plasma-enhanced chemical vapour deposition, abbreviated as PECVD, using TEOS-O2 and CH4 reactants. The characteristics of the surface were determined using surface roughness and static contact angle measurements and chemical bonding/composition determinations. The findings were compared with results from a double layer of a modified PDMS surface.

Results from the study indicate that permanent bonding of PDMS through treatment using oxygen plasma did not make it possible to modify the surface of PDMS

deposited with a double layer. Permanent bonding of PDMS with silicon, glass, or other thermoplastics however, can be induced by treatment formation of siloxane bonds to form silanol groups on the surface. Because the double layer was deposited on a bare PDMS block in cases where atmospheric plasma PECVD modifies the PDMS samples, the molecules of the PDMS cannot be exposed to oxygen plasma. The self-sealing characteristic of the PDMS surface can be preserved through modification by stencils that have patterned through-holes. Results from the study also indicated that surface modification using a double layer and atmospheric plasma PECVD using CH4 and TEOS-O2 is a promising technique that can be applied where a long-lasting hydrophilic surface of a hydrophobic material is needed.

1.8.4 Cyclic Olefin Polymers (COPs) and Surface Modification

1.8.4.1 Cyclic Olefin Polymers (COP_s)

Cyclic Olefin Polymers, COPs, are described as engineering thermoplastics that have a unique combination of properties and are valuable in many applications in packaging, CD-ROM, optics, medical equipment, and toners. Existing research shows that COPs have low density, excellent electrical properties, glass-like transparency, and heat-deflection temperature. They also possess low elongation at breaking, good surface hardness, high tensile modulus, and high rigidity. Furthermore, COPs have the advantage of being highly pure, having a low moisture absorption property, and shrinking and warping slightly, making them more suitable for injection moulding. COP chemicals resist bases on aqueous acids and polar organic. As shown in Figure 1.7, COPs are obtained through

co-polymerization of cyclo-olefin with ethylene or by Mitsui and TOPAS by TOPAS, advanced polymers (TAP: formerly Ticona and Hoechst) [91], [92]. They are prepared via ring-opening metathesis polymerization (ROMP) of cyclo-olefin followed by hydrogenation [93]-[95], and commercialized under the trade names Zeonex and Zeonor by Zeon [96] and Arton by Japan Synthetic Rubber (JSR) [92].

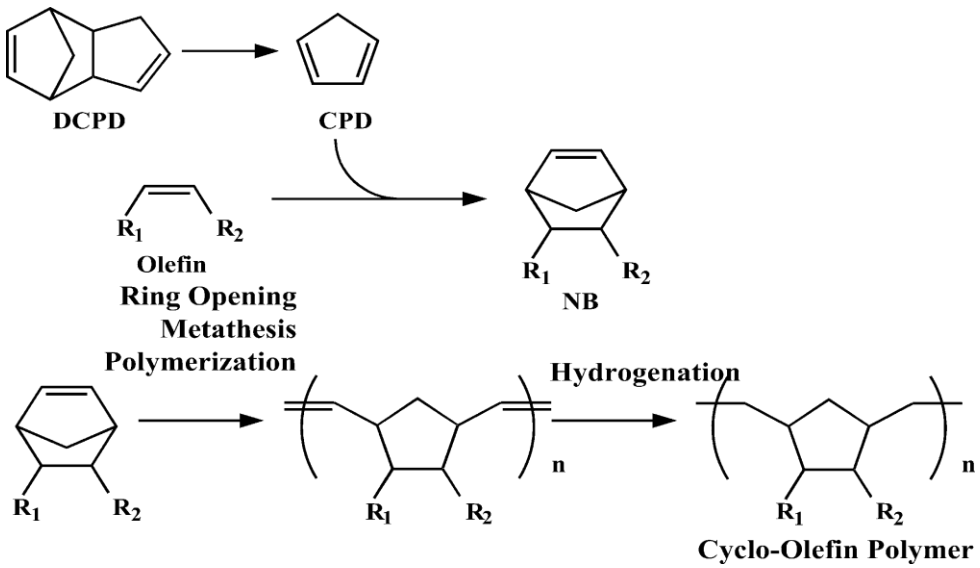

Figure 1. 7: Cyclic-olefin polymer synthesis [95]

Existing literature shows that the initial appearance of COPs in research was in the 1950's, and their first commercial use in catalysis was in the 1980's [97]. The light transmittance of COPs exceeds that of polycarbonate (PC) and polystyrene (PS), and almost equals that of PMMA (poly-methyl methacrylate). They also have low haze, birefringence, and chromatic aberration. When COPs are compared with other amorphous plastics that are transparent, COPs have a higher heat distortion temperature (HDT) with a modulus that is less dense. They are able to replace glass in most optical components since they are less brittle as compared to glass where

the durability of glass is considered an issue. Such applications include flat panel displays, hard disk drives, automotive light guides, and video camcorders [98].

The optical properties of COPs are closely similar to those of PMMA but are better for heat resistance [99]. Because of these properties, COPs are an excellent material for surface replication on new-generation DVDs. COPs are also suitable where optical-quality surfaces are needed, such as in contact lens tooling. COPs are also good at insulating electricity and are non-polar. Their ionic content is negligible, and they have relatively low electron mobility.

1.8.4.2 Surface Modification of Cyclic-Olefin Polymer by Laser Irradiation

Controlled modification of the wettability of a polymer's surface to either hydrophobic or hydrophilic is desirable for many applications, such as in the self-cleaning of a contaminant. Surface wettability is a property that also determines the ease of adhesion in cells and the behaviour of a reagent's flow in microfluidic channels. A hydrophilic surface is able to improve the surface wettability and adhesion, which is a desirable property for joining and coating applications. Cyclic olefin polymers (COPs) are one of the most widely used polymers in bio-technologies and micro-fluidics. Modification of COP surface wettability is controllable, and thereby highly desirable for applications in COP-based devices that are micro-fluidic in nature [100].

Existing literature shows that researchers have employed many techniques, such as corona discharges, plasma treatment, wet-chemical etching, electron beam irradiation, ion beam treatment, and laser irradiation. However, laser irradiation has

proven to be a clean and fast process. Laser irradiation can offer precise control and localised treatment for generating features with little thermal impact on the bulk material. This technology has been applied to the surface modification of semi-conductors, polymers, and metals. The usage of ultra-short pulsed lasers has increased as a technique for surface treatment. A previous study demonstrated that a femtosecond infrared laser could be used to induce both super hydrophilicity and super hydrophobicity on the surface of a COP material using direct laser irradiation and different laser parameters [101].

Investigation of the power deposition rate effects of laser fluence and roughness of the surface of the COP revealed the wettability change that was being induced by laser treatment in different laser conditions was investigated by treating COP substrates with different laser fluencies. Therefore, the fluence can be described as the average energy that is deposited per unit area of a sample of the surface in a single pulse [102]. The study's findings revealed that the water contact angle, WCA, varies with the power deposition rate and the temperature. If the laser conditions are appropriate, the surface wettability of COP can be modified from super-hydrophobic to super-hydrophilic. The modification is achieved when the laser beam scanning speed and pulse energy are controlled and adjusted. The developed process can be applied to the controlled modification of the localised surface wettability of a micro-fluidic device or in the development of high wettability surfaces used in inkjet printing.

1.8.4.3 Surface Modification of A Cyclic Olefin Polymer using Plasma Technique

Few reports have been published on the effects of COP atmospheric pressure plasma treatment. In the previously published work, these types of samples were quickly recovered (within a few days) [103]. Plasma samples are frequently subjected to an additional step towards direct chemical functionality in order to increase or prevent the hydrophobic recovery of the plasma samples [104]. It is therefore desirable, in any plasma process, to induce functional groups on the surface of the COP in a single step so that the hydrophobic recovery times can be extended for a long period of time.

In micro-electronic packages, treatment of polymer surfaces with atmospheric pressure and vacuum plasmas to improve poor wetting and adhesion can occur during critical stages of the manufacturing process, such as putting epoxy moulding compound on the ground and applying epoxy during filling to the Flip Chip module.The packaging industry has long exploited low-pressure fuel system plasmas to active polymer surfaces before glueing. However, atmospheric pressure plasmas (APPS) have been developed as a reactive species concentration that is several hundred times higher than in vacuum plasmas, which suggests that the app treatment can give a higher throughput. A thorough comparison between these two technologies (atmospheric pressure and vacuum discharges) for activation of the flame retardant 4 (FR-4) and polyimide substrates for attachment to epoxy during filling. This accordingly shows information about both low and atmospheric pressure plasmas suitable for the improvement of the attachment. The choice of one

method over the other should be based on other considerations, such as production, costs and benefits.

In the recent past, many researchers interested in investigating flexible electronic devices revealed that cyclic olefin polymer COP modifies using an oxygen atmospheric plasma jet treatment [105]. The COPs used in their research were obtained using metallocene catalysts, and this included glass at high transition temperatures, combined with low moisture absorption, excellent transparency, low dielectric loss and good chemical resistance. Research shows that the key factors that are responsible for effects on the surface in plasma treatments of polymers are vacuum ultraviolet radiation in a chamber, free radicals that are present in the plasma, and impingement of ions on the surface [106]. When plasmas derived from simple gases are used, significant change effects include etching or ablation, branching or cross-linking near the surface molecules, degradation of the polymer molecules and the introduction of newer function groups.

The etching effect meant that the surface of the polymer was ion bombarded by the plasma, while the degradation of the polymer molecules of the surface is known to have been caused by the thermal energy induced during plasma treatment. The simplest way of modifying the physical and chemical states of the surface of the material used was by plasma treatment without necessarily altering any bulk properties [107]. Research has shown that no poisonous gases and chemical solvents used in the modified process can make it a green modification process. To develop the adhesive ability of the COP substrate, oxygen plasma treatment then becomes a necessity. Modification of the COP surface was done using different experimental parameters such as treatment time and RF power. Surface roughness on the COP was investigated using an atomic force microscope and AFM, and at

the same time chemical bonding was done considering X-ray photo-electron spectroscopy (XPS).

The study found that there are apparent morphology and chemical changes on the COP substrate surface once oxygen plasma treatment is carried out. The surface acquired oxygen functionality in the C-O, C=O groups, and this was reflected in a noticeable reduction at a contact film angle from 90 degrees to 17.6 degrees after 10 seconds treatment. The roughness on the COP substrate upon plasma treatment resulted in an increase in ions in terms of bombardment effect. The adhesive characteristics of the COP-based substrate can be enhanced by inserting hydrophilic functional groups on the COP substrate's surface. This research also found that the adhesive performance occurring between the modified surface of polymers and the coated layer was due to the interaction between acceptors and the donor [108].

In microfluidic devices, the hydrophobicity of COPs (water contact angles around 90°) can be problematic as oxygen plasma and chemical coating process studies have shown to reduce the surface hydrophobicity of low-pressure plasma wherein the results are as summarised in Table 1.4 with surface treatments reducing the hydrophobicity of COP materials.

Table 1. 5: Surface treatments to reduce hydrophobicity of COP materials

Surface treatment method	COP material	Native Water contact angle (°)	Treated Water contact angle (°)
Low-pressure plasma	Topas 6071	90	39 [109]
Oxygen plasma	APEX	90	7[110]
UV/ozone	Zeonor 1020 R	95	49[111]

Permanent PVA coating	Zeonor 1020 R	95	74[111]
Corona discharge	ZEONOR	90	27 [112]
Plasma-enhanced chemical vapour deposition	Topas 8007	90	10[113]

2 Cyclic Olefin Polymers Surface Modification, Experiments Procedures and Results

2.1 Introduction

This section describes the experimental set-up and conditions that were used in the research project. This section discusses surface modification of thermoplastic polymers, experimental procedures and characterisation techniques used in the analysis of plasma polymer interaction. The plasma jet nozzle used to generate an atmospheric pressure plasma jet has been described in detail and the primary set-up is outlined in this section. X-ray Photo Electron Spectroscopy (XPS), Fourier transform infrared (ATR-FTIR) spectroscopy, Atomic Force Microscopy (AFM), and Contact Angle Goniometry (WCA) were all used to evaluate the interaction/fundamental chemical properties of plasma polymers.

2.2 Materials

2.2.1 Cyclic olefin polymer samples

The cyclic olefin polymer (COP) samples that were used in the experiment were Zeonor film, which was manufactured by Zeon Europe GmbH and used in the experiment. COPs are well-known for their excellent optical properties, as well as for being a high-purity polymer. With its inert surface, Zeonor Film is well suited to the manufacture of sensitive bio-diagnostic devices. In order to accommodate a wide range of applications, Zeonor film is available in a number of different thicknesses and glass transition temperatures. In this experimental work, the Zeonor

Film grade (ZF14-188), glass transition temperature (136°C), and thickness (188 m) were all used in conjunction with the glass transition temperature [108]

2.2.2 Plasma gases

Process gases purchased from BOC gases in Ireland, such as argon, helium, nitrogen and oxygen, are used in the production of plasma and the treatment of samples in the laboratory. The air compressor was used to collect the air and filter it before it was connected to the plasma jet.

2.3 Experimental plasma jet and plasma processing procedure

Experiments were conducted using COP films that had been cut into small pieces of approximately 2.5 x 2.0 cm in size. To protect the samples, they were wrapped in plastic and peeled just before being used in the experiment. In all experiments, the inter-electrode gap was maintained at 2 mm. To generate the desired air plasma, a high voltage power supply model PVM400 was used. This power supply generates high sinusoidal voltages of up to 20 kV at output frequencies of up to 40 kHz. To control the gas flow to the jet, a digital mass flow controller (0SMC integrated display flow metre 0.5/25 L/min) was used. A high voltage probe (Tektronix P 6015A, 1000X) and a current transformer were used to measure the voltage and current. The voltage and current were measured using a Tektronix tds digital oscilloscope (2024, 200MHz).

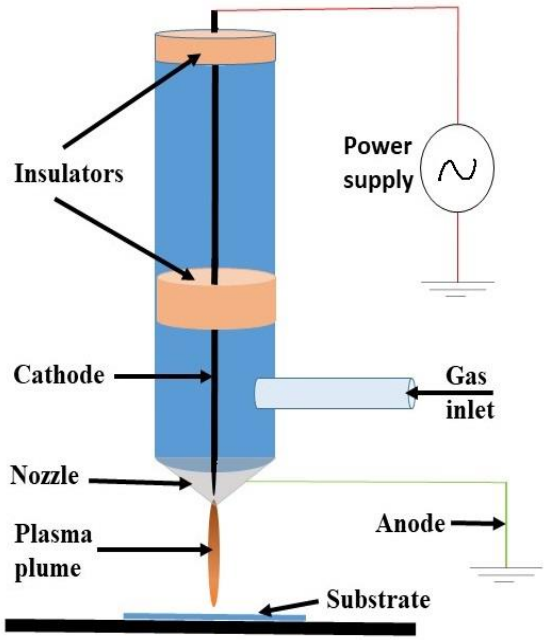

Figure 2.1: Schematic diagram of atmospheric pressure plasma jet used

2.3.1 Plasma jet design

Plasma treatment of COP surfaces were performed using an experimental plasma jet developed by the National Centre for Plasma Science and Technology (NCPST). Figure 2.1 depicts a schematic diagram for this system.

As shown in Figure 2.1, the jet is made of a 120 mm outer plastic tube with a 22 mm inner diameter and a 25 mm outer diameter. Gas can be introduced into the jet chamber via a 5 mm hole cut into the tube's side. A Peek capsule secured at one end of the plastic tube extends 40 mm into the tube.

Electrical power is supplied to the jet by two stainless steel electrodes. The first electrode, a nozzle as shown in Figure 2.1, is threaded into place at the opposite end of the plastic tube and is electrically grounded. The nozzle electrode's interior is

conical in shape, with a small 0.6 mm hole at the bottom for airflow out of the jet chamber.

The second electrode, a pin, is electrically connected to the high voltage line as shown in Figure 3.2. A Polyether Ether Ketone (Peek) capsule secures the pin in place and allows it to be moved closer or further away from the ground electrode. When a sufficiently high voltage is applied between the pin and ground electrodes, plasma is generated and excited species are transported out of the jet chamber to the plume.

As illustrated in Figure 2.1, the outer electrode (nozzle) is grounded while the central electrode receives a high voltage power supply at a frequency of (0-40) KHz, resulting in a discharge. The reactive species produced exits the nozzle at a high rate of speed and travels to the area to be treated. Inside the plastic cylinder, the electrode is placed horizontally. When an alternating current high voltage is applied in the presence of gas flow, an atmospheric pressure plasma jet (APPJ) is generated between the electrode and the grounded cone. Numerous factors contribute to the value of applying power to produce APPJ:

a) Gas type: the use of various gas compositions such as He, N_2, Ar and air also gas mixtures such as Ar/N_2, O_2/N_2 gives different species for applications.

b) Distance between electrodes**.**

c) Gas flow rate and here, the density of the plasma plume depends on neither the gas flow rate nor the tube inner diameter [76]. The gas flow rate used in the experiments varied from 5 l/min up to 25 l/min.

2.4 Surface Characterisation Techniques

Various techniques can be used for the analysis of the surface which has its specific advantages and disadvantages. Dedicated suitability of each method depends on the particular problems as they are reviewed. It is important to examine the sample by various techniques for the detection of the same sample. The numerous technologies offer and assist with the interpretation of the data, different types of information may be obtained if the optical, chemical and structural performance are put under consideration. In the current research on the chemical composition of the X-Ray, (XPS), the assessment of surface–energy, Fourier Transform Infrared Microscopy (FTIR-AR), Atomic Force Microscopy (AFM) and Secondary Electron Microscopy (SEM), all these techniques are employed for chemical and topography analysis. The contact angle measurement was used in analysing ~~of~~ the surfaces to determine changes in properties. Provision of information by the topography and characterisation of the various techniques alongside their operation and specifications are discussed in the following sub-sections.

2.4.1 Contact Angle Goniometry

In 1805 Young, found surface wettability phenomena can be used to determine the surface free energy. Physical quantities such as the contact angle and apparent surface free energy are used to describe the wettability of surfaces [109]. Additionally, the relationship between the contact angle and the apparent surface free energy of a solid was discovered. Numerous theoretical approaches exist for estimating the free energy of the surface [110], [111]. Despite the problems connected with estimation of the apparent surface free energy, it is one of the most frequently determined quantities in industry, is usually called surface tension of

solids and is estimated based on studies of the spreading of calibrated probe liquids over solids using a number of common laboratory solvents; liquids such as: water, ethylene glycol, formamide and di-iodomethane [112], [113]. However, water is typically used to measure the surface hydrophobicity or hydrophilicity [114]

Contact angle measurement is the most popular method of solid surface tension measurement. A contact angle goniometer (FTA 200) was used to measure the contact angle values as shown in Figure 2.2. A droplet of water (3 μl) was placed on the polymer surface using a syringe to measure the contact angle. Each contact angle value was taken on the same sample surface as an average of three different points.

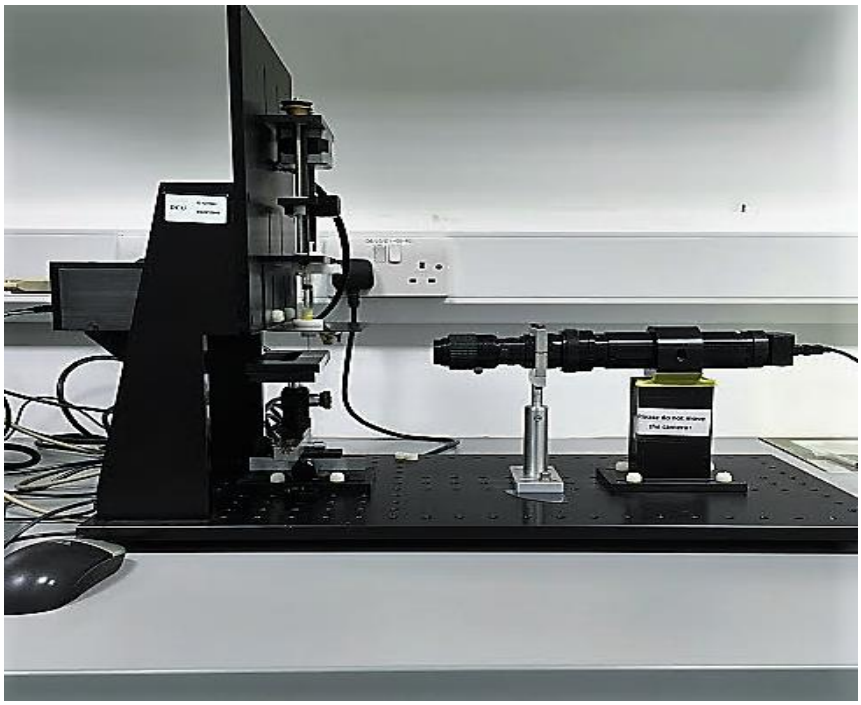

Figure 2.2: Contact angle goniometer (FTA200)

2.4.2 Atomic Force Microscopy (AFM)

A Nano Scope Ilia size system with a Dimension 3100 controller was used ~~to~~ for the polar faces (See Figure 2.3).

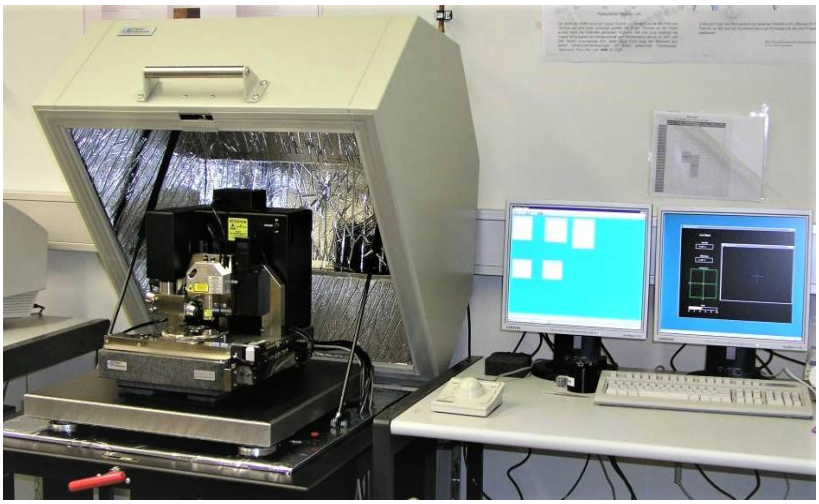

Figure 2.3: The Dimension 3100 atomic force microscope (AFM)

2.5 Results and Discussion

The experimental results of Cyclic Olefin Polymers (COPs) surface treated with an air atmospheric pressure plasma jet (APPJ) are as showcased.

This section discusses the experimental results gained from the treatment of cyclic olefin polymers (COPs) with an air atmospheric pressure plasma jet (APPJ). The study's major goal was to determine the behaviour of surface wettability following air APPJ treatment.

During the experimental research, a large number of experiments were conducted. Each sample treated was submitted to the characteristics instrument in order to get precise results, as the quality obtained deteriorates over time.

2.5.1 Characterization of APPJ

There are a variety of methods for studying and characterising plasma. We may use these approaches to determine plasma parameters such as electron density, temperature and the type of plasma species by observing the plasma.

2.6 Effect of the APPJ parameters on COP surface

A high voltage, high frequency signal is used to generate plasma between two electrodes in the presence of a gas flow. The power supply generates a sinusoidal signal at a frequency of 0-40 KHz. The substrates are positioned downstream of the electrodes so that the surface is exposed to ion bombardment along with the reactive species generated by electron collisions with the molecular gases. Many gases can be good or bad, depending on the application, when one substrate is being treated at a time. Further discussions on atmospheric pressure plasma design can be found in several other research papers [71].

In this work, we investigated the surface modification by an atmospheric pressure plasma jet at different operating conditions to find out the optimal operating parameters to modify the COP surface. Several controllable plasma processing parameters can be optimised to favour the desired processes with high controllability of the plasma processes. These parameters include the distance between the substrate and the nozzle, gas type, the gas flow rate and applied power (P). Thus, optimising a particular plasma process requires systematically studying the dependence of material properties on each relevant parameter.

2.6.1 Plasma fed gas impact

In order to improve the hydrophilic behaviour of COPs, samples were exposed to different gas plasma modifications. AR-FTIR investigation reveals the chemical changes due to differences of the nature of the plasma on the polymers surfaces. WCA of COP shows a significant change from the surface of a pristine COP and after plasma treated samples. Figures 2.4 shows water contact angles (WCA) before and after helium/oxygen/Nitrogen and air plasma treatment. Surface activation of COP with a different APPJ fed gas appears to be quite effective at surface wettability. According to several authors, reactive neutral species such as Oxygen, carbonyl, carboxyl hydroxyl, peroxide groups, and Nitrogen Dioxide play a primary role in the use of plasma for polymers surface modification [115].

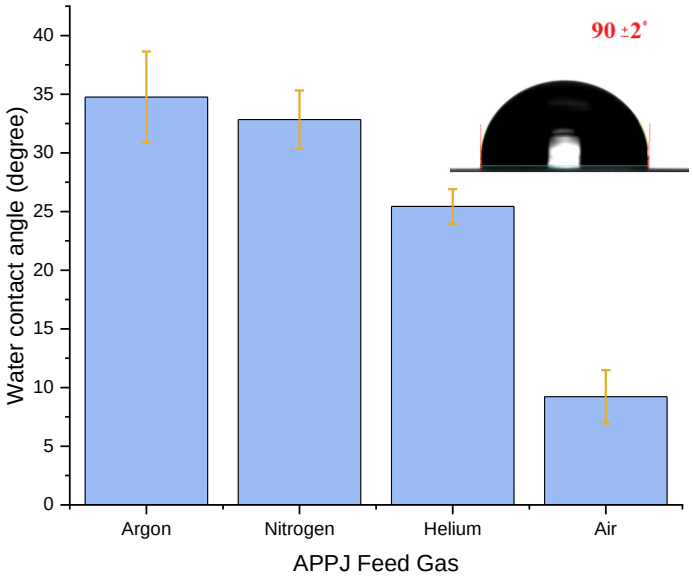

Figure 2.4: Water contact angles (WCA) before and after helium/oxygen/nitrogen and air plasma

FTIR-AR spectra have been used to detect the chemical changes after plasma treatment. Fast electrons produced in a non-thermal plasma can have energies of up to 10 eV, sparking a variety of chemical reactions. In non-thermal plasma processes, energetic photons can play a role in addition to fast electrons. A good example of such a reaction is photoionization in air. Electron impact on bulk gas molecules, on the other hand, is the fundamental source of all reactions, as it forms a vast number of reactive species that can then react with more stable species. OH, O, and N radicals, excited N2 molecules, and atomic and molecular ions (e.g. O^+, O^+_2) are examples of reactive species [116].

From FTIR results, new functional groups have been introduced to the COP surface by different inlet gases in the APPJ. Figures 2.5 and 2.6 depict the FTIR absorption peak that appears between 1600 and 1750 cm^{-1} and is associated with the presence of carbonyl and aldehyde groups caused by oxidation during plasma treatment [117]. It has been reported that various carbonyl-containing species are formed during plasma treatment in the presence of oxygen elements. It was discovered that the oxygenated-argon plasma specimen exhibited an FTIR-ATR peak in the 3500–3600 cm^{-1} range, but not in the argon plasma specimen. This peak indicated the presence of polar hydroxyl groups (–OH) [118], which contributes to the increase in the hydrophilic nature of the COP surface.

As expected, plasma treatment enhances the wettability of polymers by generating OH groups on the treated surface [119]. Likewise, when PP and PET polymers are treated with non-thermal plasma, unique absorption bands at 1548 and 1697 cm^{-1} are found, which correspond to the O-H and C=O stretching vibrations respectively. Furthermore, plasma treatment introduces or enhances oxygen functional groups on

the polymer surface, such as C-O, O-H, and C=O absorption bands between 3200 and 3600 cm^{-1}, enhancing hydrophilicity [120].

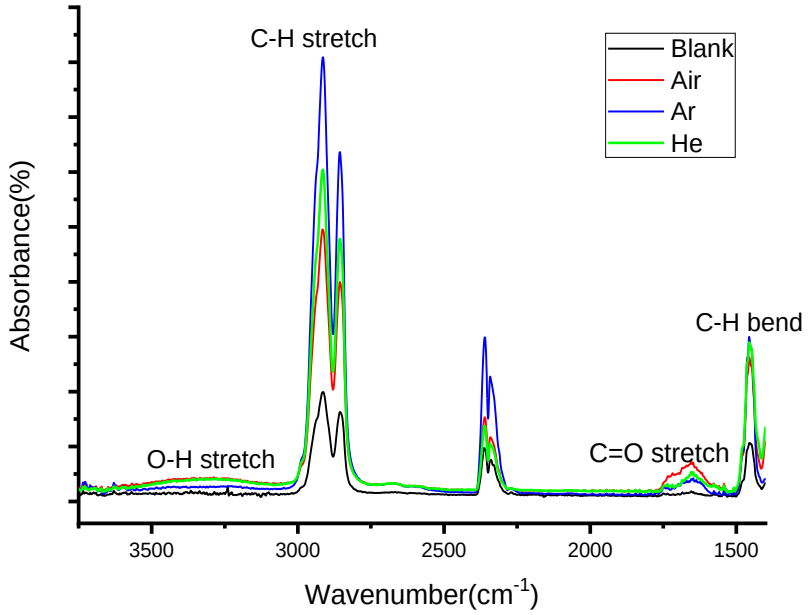

Figure 2.5: FTIR spectra of COP films treated by Ar, He and Air plasma.

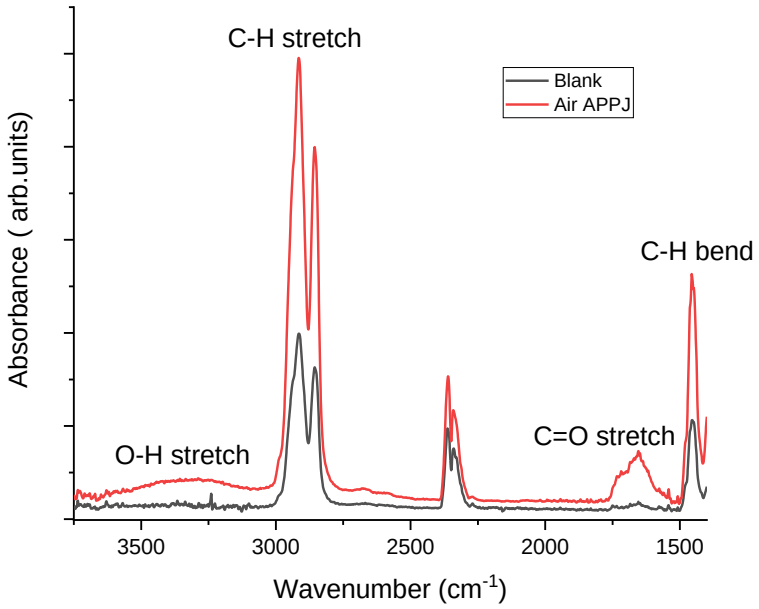

Figure 2.6: FTIR spectra of COP films treated with Air plasma.

The results indicated that plasma chemical reactions had a significant effect on a variety of plasma-fed gases, compared with the other gases used, with air plasma pre-treatment being the most efficient method of achieving an extremely wet COP state.

2.6.2 APPJ plasma treatment function of distance

In this work, COP was treated at varying jet-to-substrate lengths while maintaining all other parameters constant to determine the influence on the COP surface. The connection between the jet-to-substrate distance and the water contact angle is shown in Figure 2.7. When samples were taken close to the nozzle, the WCA rate was almost undetectable due to surface damage. The WCA was lower at 2.5 mm than in other distances. However, it can be observed that the WCA value rose exponentially as the distance between the jet and the substrate increased from 3 mm to 25 mm. The distance between the nozzle and the sample surface influences the WCA of COPs. This could be due to the fact that the concentrations of activated species decrease as they travel downstream away from the nozzle, or it could be due to the fact that the degree of etching is also affected by the polymer surface temperature.

The findings are consistent with those observed by Vesel and his colleagues [121]. Previously published work on WCA representations in an exhaustive study of various PET treatment time and distance settings. They discovered that a shorter treatment distance decreased WCA values, whereas a longer treatment period contributed to the same results. The authors investigated the changes in wettability caused by long-lived oxygen species.

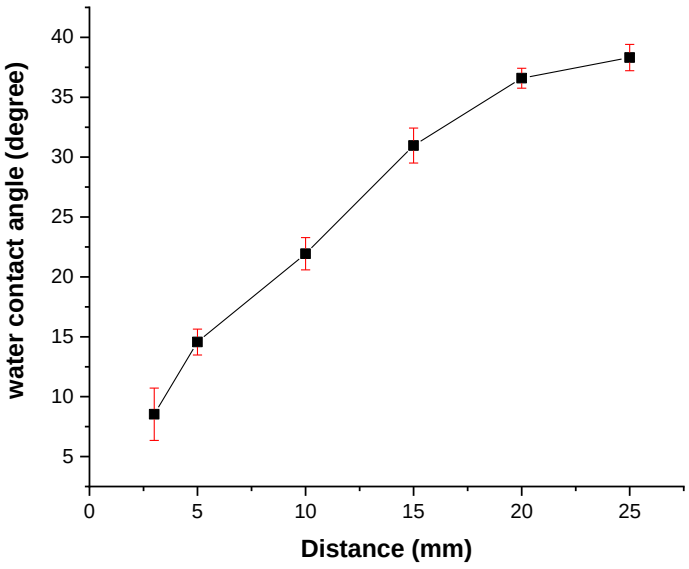

Figure 2.7: Changes in water contact angles of the COP surface as a function of nozzle distance.

2.6.3 APPJ treatment function of power supply frequency

The APPJ power has demonstrated that frequency variation is a critical method for regulating reactive species production and heat flow. Variation in the frequency of APPJ devices, which are generally operated in the MHz range, affects the duration of the plasma and the intensity of the plume, allowing for control of reactive species generation and gas heating. Changes in frequency result in changes in plasma characteristics, which influence the wettability of the COP surface, as seen in Figure 2.8. Whereas a greater plasma frequency results in a lower water contact angle.

An investigation of the effect of surface treatment frequency on the functionality of plasma activation polymer particles, as previously stated [122]. The study demonstrates a substantial dependency on the plasma generator frequencies and a link with the observed plasma's spectrum emission. An investigation into the

influence of plasma processing parameters such as frequency and treatment duration on the amount of surface activation was conducted using water contact angle (WCA) measurements. After 2 minutes of treatment, the WCA of polyethylene terephthalate PTE was decreased from 93° to 32°.

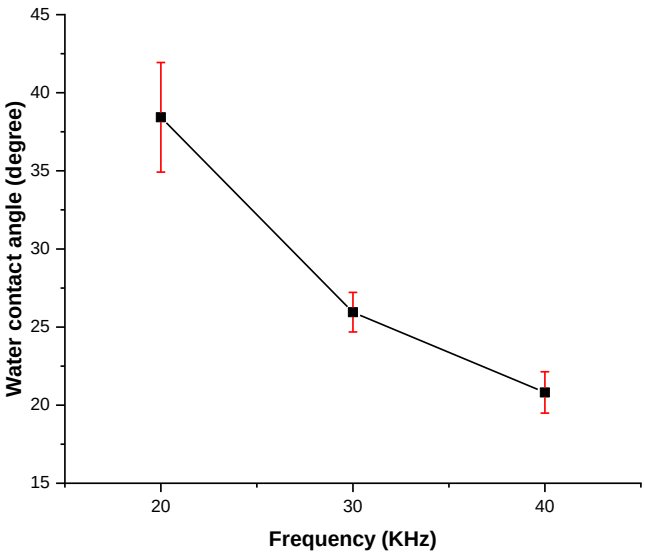

Figure 2.8: Changes in water contact angles of the COP surface as power supply frequencyI don't think this caption makes any sense.

2.6.4 Gas flow rate impact on COP surface

The effect of APPJ air flow rate on surface wettability was investigated; the results are shown in Figure 2.9.The results indicate an inverse relationship between air flow rate and COP wettability. Variability in air flow rate is used to identify the best plasma conditions for surface modification. While a water contact angle is used to determine the wettability of the plasma-treated COP surface, a digital mass flow controller (0SMC Integrated display flow metre 0.5/25 L/min) is used to control the

gas flow to the jet, where the digital output of the gas flow metres connected to the plasma jet system is used. The magnitude of the gas flow has a significant influence on the plasma [123].

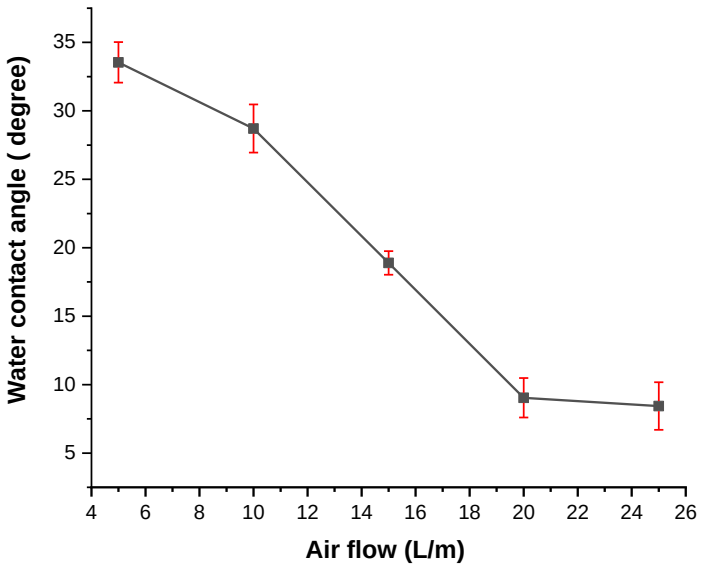

Figure 2.9: Changes in water contact angles of the COP surface as function APPJ feed gas flow.

In our experiments, the plasma gas flow rate can affect the surface wettability of polymers for two primary reasons. The first is that it changes the topography of the surface, causing fluctuations in roughness, and the second is that the plasma active species density in high gas flow is invariably greater than that in low gas flow, invariably affecting the polymer's surface chemistry and topography [124], [125].

2.7 Ambient humidity effect on COP surface wettability

Few studies have been conducted to determine the effect of the environment on surface wettability. The measurement of contact angle is affected by numerous

factors including the liquid used, the volume of the drop, ambient humidity and temperature studied by Zisman [126], Li et al [127], Baek et al [128] and SH Anastasiadis [129].

We investigated the effect of APPJ air plasma ambient humidity on surface wettability; the results are shown in Figure 2.10. Measurements of the temperature and relative humidity RH are made using an Extech 445815 Humidity Meter with an accuracy of 1 °C and 4%, respectively. Controlling the room's moisture by use of a deumidifier resulted in a relative humidity range of 40% to 85%. while the wettability of the plasma-treated COP surface is determined using a water contact angle. The results indicate that the ambient humidity rate and the wettability of COP are proportional. The reason for this is not clear and more investigation needs to be carried out.

Contact angle measurements in a variety of environments provide valuable insight into the properties of polymer surfaces. Measuring the contact angle in an appropriate relative humidity environment is critical because wettability data obtained in environments that are not representative of the materials operating environment can be highly misleading.

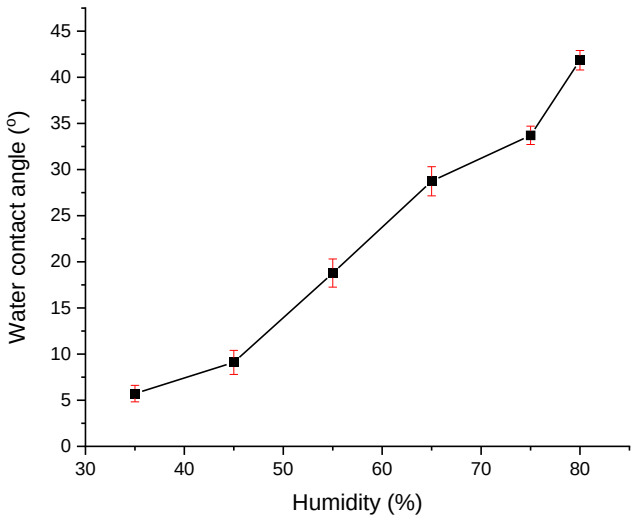

Figure 2.10: Relative humidity impact on COP surface wettability

2.8 COP Surface Topography Analysis

2.8.1 Scanning Electron Microscopy (SEM)

The surface characteristics of untreated and atmospheric plasma treated COP are analysed using scanning electron microscopy (SEM). Conductive samples are required for SEM imaging due to the combined effects of the incident electron beam and electron loss from the sample, which can result in charging effects for non-conductive samples. Due to the non-conductive nature of the COP surface, samples were prepared prior to SEM by sputter coating. Figure 2.11 shows scanning electron microscopy (SEM) images of COP; no difference between treated and untreated samples can be seen in the SEM images; the changes in surface topography were nanoscale. As a result, AFM was used to characterise the surface's topography.

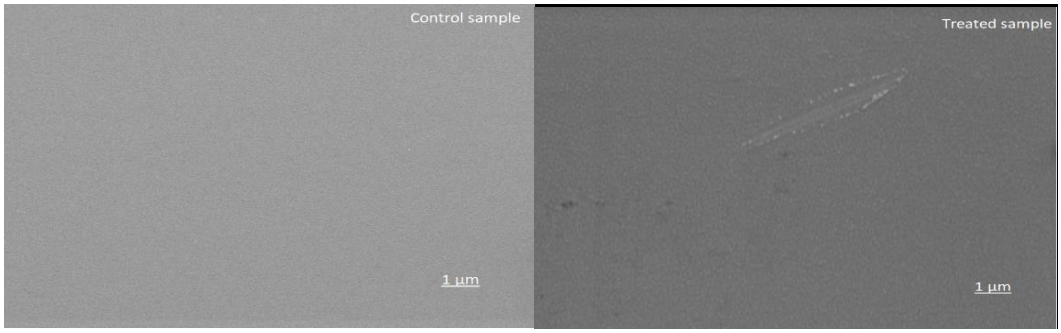

Figure 2.11: Scanning electron microscopy (SEM) images of COP polymer images of a 1µm wide for control and treated sample.

2.8.2 Atomic Force Microscopy (AFM)

The effect of APPJ treatment on COP polymers was represented in a 3D topographic image in Figure 2.12. As one of the important factors in surface enhancement, the better wettability is closely related to the higher surface roughness [130], [131].

Based on the analysis of AFM images, it can be concluded that surface nano-roughness can also contribute to improved wettability. As expected, after air plasma treatment, the COP surface becomes significantly rougher. The correlation between the increase in R_{rms} of plasma-treated films and mass loss measurements indicated that the films underwent a significant etching process. Previously, similar linear conductance was observed in other polymers [79]. As a result, the surfaces of the APPJ structurally modified samples are the result of active species reaching the surface via the gas stream. Additionally, the active oxygen-related species can be dispersed outwards in such a way that the O atoms formed in the plasma plume become incorporated into the polymer chain [132]. The AFM data indicates that treating COP surfaces with air APPJ results in an increase in film roughness, which

results in a decrease in the COP water contact angle from 90° to less than 10°. The following section summarises the results:

1) The plasma-induced process is the etching of a polymeric surface, which is evidenced by the AFM analysis. The removal of the polymeric material to the gas phase is reasonably done by the formation of low molecular weight compounds formed by the products during the oxidation of the polymer and then resulting in the etched surface leading to a rougher surface.

2) The AFM results of the surface topography and local heterogeneity (high and phase images) resulting after the plasma treatment are as displayed in Figures 2.12 (A and B). The surface properties of the sample were measured in three different places, with no extensive differences being observed between these places. The high and phase images of the untreated polymer show no significant differences in the high and phase profiles. The high and phase images of pristine polymers are crude, but there are no discernible inhomogeneities. The R_{rms} values of pristine COP polymers are 4.0 nm and 7.0 nm respectively. The 5/5 μm scan is selected in order to ensure clearly visible changes in the COP surface. The pristine COP exhibits a surface with no apparent irregularities and surface roughness R_a = 46 nm. The plasma-treated sample resulted in the appearance of very fine heterogeneous regions, and then the polymer surface became more irregular. The local heterogeneity after treatment is seen to be more pronounced. The roughness of plasma treated surfaces increases two/three times higher compared to the untreated polymer.

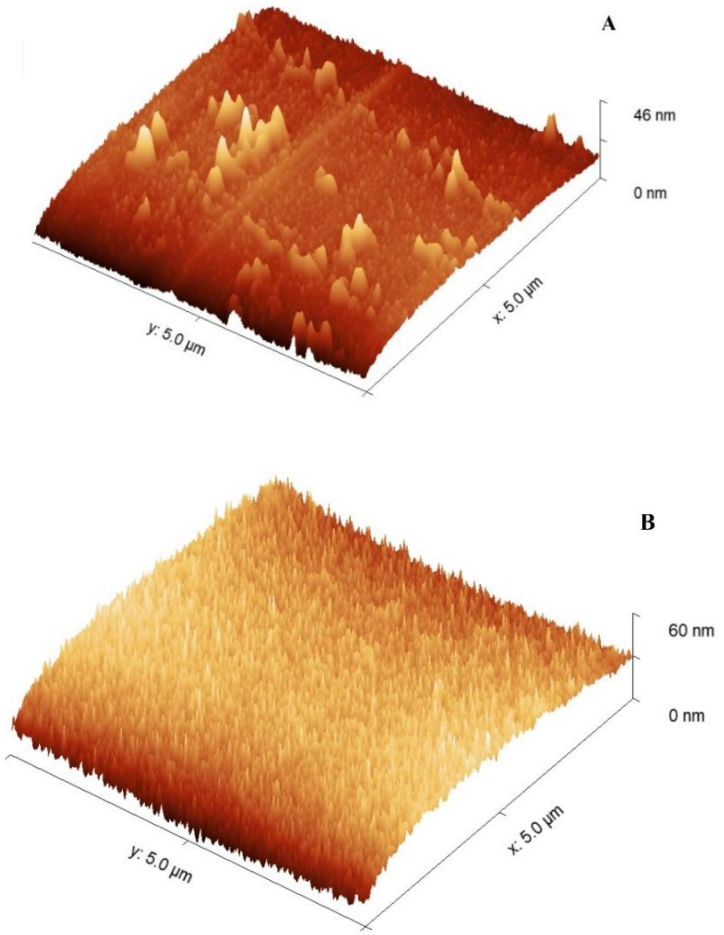

Figure 2.12: (a) AFM images of pristine COP, (b) air APPJ treated COP polymers

2.9 Conclusions

It is shown here how to produce a super hydrophilic surface on COP at a cheap cost by employing air plasma rather than more expensive gases like helium, argon, or nitrogen plasmas, as previously described. The dry method also exhibits quick and effective surface wettability that is repeatable, simple to apply and has no influence on the bulk characteristics of COP. These results may be used for sophisticated polymers that are utilized in adhesion and biological applications, such as microfluidic devices and can be used to analyse them. An investigation of the hydrophilic surface and its energy as well as the APPJ plasma properties indicates

the potential for regulating the wettability of the surface as well as the more direct introduction of specific functional groups, particularly -CH and -OH. When the water contact angle is decreased from roughly 90° to less than 10°, a significant improvement in COP surface wettability is observed.

3 Optimization of Atmospheric Pressure Plasma Treatment on COP Surfaces

3.1 Introduction

Low-temperature atmospheric-pressure plasma jets (APPJs) are increasingly being used in applications such as surface activation, cleaning, wound care, and sterilisation [132]. Successful development of the application of these systems is dependent upon the ability to tailor the active species generated in the plasma jets to the treatment requirements. The purpose of this chapter is to explore optimising the influence of APPJ parameters on the surface wettability of cyclic olefin polymers (COPs), where the surface wettability was shown to be connected to the geometry of the water contact angle. The purpose of this chapter is to explore optimising the influence of APPJ parameters on the surface wettability of cyclic olefin polymers (COPs), where the surface wettability of COPs was shown to be connected to the geometry of the water contact angle. The method was optimised using historical data using the D-optimal criterion, and the influence of plasma parameters such as input voltage, plasma power supply frequency, air flow rate, and distance between the nozzle and the COP surface was also studied. The suggested model was employed and may be further applied in the study to navigate the surface wettability based on the analysis of variance (ANOVA) results. The optimal operating conditions for achieving the lowest water contact angle were predicted and the results indicated that while all of the parameters studied have an effect on the COP surface modification, it is most sensitive to plasma frequency and distance, as well as air flow rate.

Many studies carried out over the years applying these techniques have shown that they could be used for materials that were traditionally unviable for microfluidic devices. Due to their excellent features in optical, mechanical, chemical resistance, low water absorption and low cost, Cyclic Olefin Polymers (COPs) are ideal for

microfluidic applications. Conventionally, the materials employed in microfluidic devices are generally hydrophobic and so also is the cyclic olefin polymer surface. Other techniques, however, are used to create hydrophilic surfaces. These include wet-chemical etching [133], corona discharges [106], [134], laser irradiation [95] and ion beam treatment [135], but in this work, we have chosen the air atmospheric pressure plasma jet (APPJ) as an approach for COP surface modification. As a result of many advantages, they can produce many reactive species which have a great impact on surface factualisation. In addition to reducing the cost of equipment and operation, it is also established that low temperature processes result in low surface damage. Furthermore, they can be used in the treatment of microfluidic channels [136]. This can be a very practical method for modifying surface functional groups without affecting their bulk properties [61]. Whereas the fabrication of polymeric materials for microfluidic applications, such as cyclic olefin polymers (COP), can be achieved by an atmospheric pressure plasma jet by nanoscale surface etching and surface functionality [106], [137].

By spatially increasing the low surface energy of polymers, functional surfaces have a significant impact on surface fabrication [138] and, therefore, result in enhanced wettability of their surfaces as well as an increment in the hydrophilicity of the COP. The operating conditions of the APPJ have a substantial impact on polymer surface modification [139]. The purpose of this work was to investigate the effect of optimising APPJ parameters such as input voltage (V), power supply frequency (kHz), gas flow rate (l/min) and jet to substrate distance (mm) on the COP surface wettability, which is a measure of the water contact angle. Additionally, the cost of sample treatment has been calculated to strike a balance between quality (low water contact angle) and quantity (low cost).

Thus, this chapter's initial objective is to use historical data to establish a relationship between the atmospheric pressure plasma jet input parameters and the two responses (water contact angle and operating cost). The second goal is to find the best factor combination that reduces the water contact angle while staying within a reasonable expense for industrial production. The APPJ parameters used in this study were chosen because they are the only ones controllable by the APPJ equipment used.

3.2 Methodology

The response surface methodology (RSM) is a technique for examining the relationships between multiple explanatory variables and one or more response variables. The main idea behind RSM is to use a series of carefully designed experiments to find the best possible response. Box and Wilson [140] recommend using a first-degree polynomial model to accomplish this. They recognise that this model is only an approximation, but they use it because it is straightforward to estimate and apply, even when little is known about the process.

3.2.1 Response Surface Methodology

Engineers frequently want to define the values of the input process parameters that produce the best results. In terms of process input parameters, the optimal value may be either the minimum or maximum value for a particular function. Design of experiments is a commonly used optimization technique for explaining surface efficiency. It could be used to test atmospheric pressure plasma jet modified polymers and determine optimal responses. This design is a collection of techniques

for predicting interesting responses based on a variety of input variables which can be used to optimise this response [141]. This design also defines the relationships and the controllable variables of inputs between one or more assessed responses [142]. If all independent variables in experiments with negligible errors are observable, regulated and continuous, the response surface can be expressed by Equation (1-3).

$$y = f(x_1, x_2, x_3, \dots\dots\dots, x_k) \quad (1\text{-}3)$$

where k is the number of independent variables.

In order to optimize the" y" response, the true functional relationship between independent variables and the response surface must be accurately approximated. Typically, a second-order polynomial Eq. (2-3) is used in historical data.

$$y = b_0 + \sum b_i x_i + \sum b_{ii} x^2{}_{ii} + \sum b_{ij} x_i x_j + \varepsilon \quad (2\text{-}3)$$

where k is the number of independent variables.

In order to optimize the "y" response, the true functional relationship between independent variables and the response surface must be accurately approximated. Typically, a second-order polynomial Equation (2-3) is used in the design of the experiment.

3.2.2 Experimental Design

The study was conceived on the basis of historical data design available in Design-Expert V12 software. The input variable parameters of the plasma jet are power (input voltage, frequency), gas flow rate of the feed and the distance of the sample from the plasma jet nozzle. The experimental process run has been carried out by modifying one of the process parameters at a time to identify the range of each

parameter and the lack of surface wettability of clear polymers. Figure 3.1 shows the water contact angle of the COP samples treated with air APPJ (14.5°) and the untreated COP surface (96°). The method parameters and actual values are shown in Table 3-1. For the code of variables and the design matrix, as shown in Table 2, the statistical software Design-Expert V12 has been used. Historical data design [143] was employed and for the experimental data, polynomial Equation (3-2) regression equations were fitted for all responses to the experimental data. For each regression equation, the statistical significance of the terms was checked using the sequential F-test, the adaptive test and other adequacy measures with the same software to obtain the best fit.

Figure 3. 1: The water contact angle of untreated and air APPJ treated selected samples of COP.

Table 3. 1 Independent variable and experimental design levels used

Variable	Unit	Limits
Input Voltage	V	155-220
Frequency	KHz	20-40
Air Flow	L\min	5-25
Distance	mm	3-25

3.2.3 Desirability Approach

Several statistical techniques are available for solving multiple response problems, such as overlaying the contour plot for each answer, restricted optimization problems and the desirability approach. Because of its simplicity and flexibility in the system, the desirability approach is recommended and offers consistency in weighting and importance for individual responses. Using this approach to solve these multiple response optimization problems involves using a technique for combining multiple responses into a dimensionless performance metric called the overall desirability function. The desirability method involves transforming each estimated response, Yi, into a unitless utility with a limit of 0< di <1, where a higher di value implies that the response value Yi is more desirable if di = 0 which means a fully undesirable response [144]. In the current work, the individual desirability of each response, di, was calculated using Equations (3-3) - (3-7). The shape of the desirability function can be changed for each goal by the weight field '*wt-i*. Weights are used to give more emphasis to the upper/lower bounds or to emphasize the target value.

The desirability of goals at the highest level will be defined by:

$$di = \begin{cases} 1 & , \quad Y_i \leq Low_i \\ \left(\frac{Y_i - Low_i}{High_i - Low_i}\right)^{wt_i} & , \quad Low_i < Y_i < High_i \\ 0 & , \quad Y_i \geq High_i \end{cases} \tag{3-3}$$

For goal as a minimum, the desirability will be defined by:

$$di = \begin{cases} 1 & , \quad Y_i \leq Low_i \\ \left(\frac{High_i - Y_i}{High_i - Low_i}\right)^{wt_i} & , \quad Low_i < Y_i < High_i \\ 0 & , \quad Y_i \geq High_i \end{cases} \tag{3-4}$$

For goal as a target, the desirability will be defined by

$$di = \begin{cases} \left(\frac{Y_i - Low_i}{T_i - Low_i}\right)^{wt_{1i}} & , Low_i < Y_i < T_i \\ \left(\frac{Y_i - High_i}{T_i - High_i}\right)^{wt_{2i}} & , \quad T_i < Y_i < High_i \\ 0 & , \text{ Otherwise} \end{cases} \tag{3-5}$$

For goal within range, the desirability will be defined by

$$di = \begin{cases} 1 & , \quad Low_i < Y_i < High_i \\ 0 & , \quad Otherwise \end{cases} \tag{3-6}$$

$$D = \left(\prod_{i=1}^{n} {d_i}^{r_i}\right)^{1/(\Sigma r_i)} \tag{3-7}$$

3.3 Experimental design

The optimization element of Design-Expert software V12 searches for a combination of factor rates that simultaneously satisfy the requirements put on each of the responses and process factors (i.e. several-response model) (i.e. optimization requirements). In this work, numerical and graphical methods of optimisation were used by choosing the desired goals for each factor and response. As described previously, the process of numerical optimisation requires integrating the objectives into an overall desirability function (D). In the design-expert package, the numerical optimization functionality seeks one or more points in the factor domain that would

maximize the objective function. The system defines regions in a graphical optimization with multiple answers, where parameters fit the proposed criteria simultaneously. A contour plot may also define the superimposition or overlaying of critical response contours. Instead, it has become possible to search visually for the best compromise. When dealing with a large number of responses, it is recommended that numerical optimization be performed first; otherwise, it may be impossible to find a feasible region. The graphical optimization displays the region in the factor space of the feasible answer values. Regions which do not meet the criteria for optimisation are shaded. Figure 3.2 displays the flow chart of the design-expert program optimisation process.

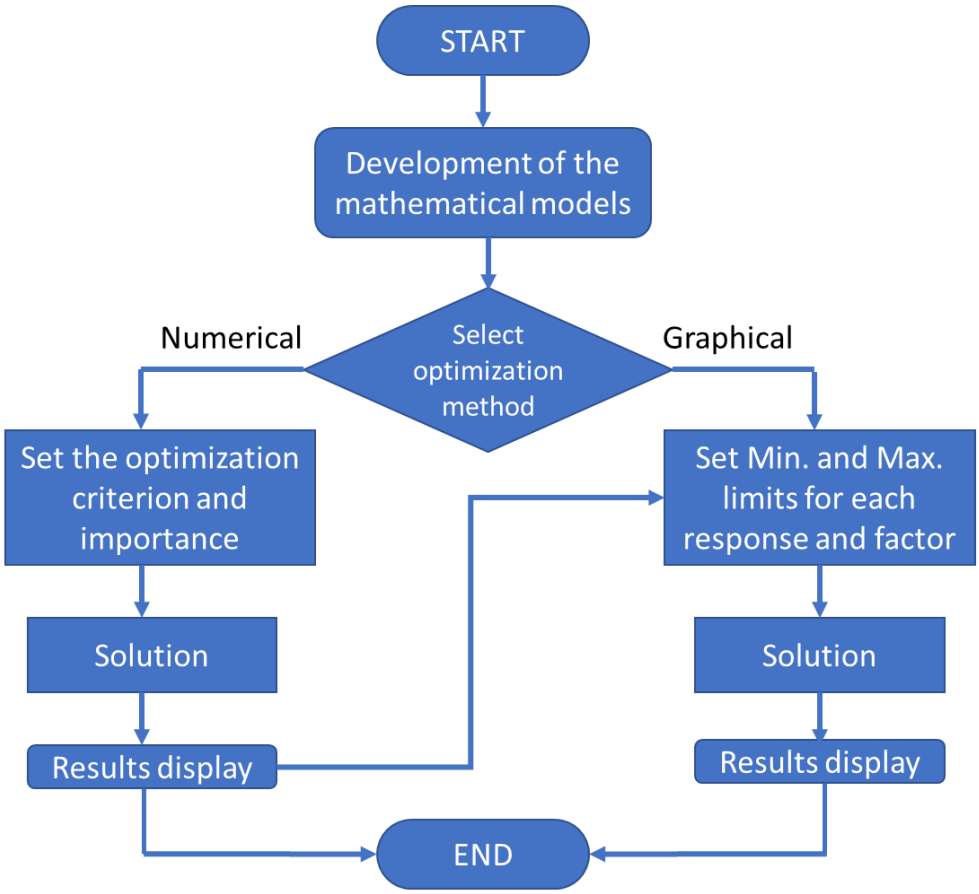

Figure 3.2: Optimization steps [145]

3.3.1 Experimental work Faraj, you need to check the numbering of your sections as at present, 1.3 has no text in it.

Experiments with an air atmospheric pressure plasma jet to modify the COP surface were conducted at a room temperature of 21–23C° and a relative humidity of 50–70%, as detailed in Chapter 2.

There are many factors that play into the value of applying power to produce APPJ, such as the power, frequency, air flow rate and the distance between the nozzle and the treated sample. The outer electrode (nozzle) is grounded, while a high voltage (50-100W) and a frequency of 0-40 KHz are applied to the central electrode to create a discharge. The reactive species generated exits the nozzle at a high velocity and attains the area that is to be treated. The electrode is placed horizontally inside the plastic cylinder. The atmospheric pressure plasma jet (APPJ) is produced between the electrode and the grounded cone when applying a high voltage in the presence of gas flow.

3.3.2 Operating cost calculation

Atmospheric pressure plasma jet operating costs can be estimated per sample. The APPJ system used in this work utilizes air gases at a flow rate of between 5 and 25 l/min. The compressor tank capacity is 24 litres and it consumes 300 W to fill it up, so 1 litre requires 12.5 Watts. The power supply consumption depends on the input voltage and frequency and to calculate the electricity, we use a voltammeter and ammeter and then calculate the power for every run. The operating cost calculation does not consider the system hardware, such as the power supply, the

variac voltage controller and the nozzle. The total approximated operating cost per treated sample is given by Equation (3-8) T

reatment cost =

$$\frac{((Plasma\ power + air\ compressor\ power) \times 250)/1000[KW]}{\left[60\frac{min}{h}\right]} \times 0.2\ (€/\text{sample}) \quad (3\text{-}8)$$

where 250 is the sample dots covered by plasma plume and 0.2 is the presumed |Kilowatt price.

Table 3.2 Design matrix

	Factor 1 (A)	Factor 2 (B)	Factor 3 (C)	Factor 4 (D)		Factor 1 (A)	Factor 2 (B)	Factor 3 (C)	Factor 4 (D)
Run	Input Voltage	Frequency	Air Flow	Distance	Run	Input Voltage	Frequency	Air Flow	Distance
	V	KHz	L/min	mm		V	KHz	l/min	mm
1	220	35	5	3	21	175	20	20	5
2	220	35	10	3	22	175	30	20	5
3	220	35	15	3	23	175	40	20	5
4	220	35	20	3	24	175	20	10	5
5	220	35	25	3	25	175	30	10	5
6	220	20	20	5	26	175	40	10	5
7	220	30	20	5	27	155	40	10	25
8	220	40	20	5	28	175	35	20	25
9	155	35	20	3	29	155	35	10	20
10	175	35	20	3	30	155	35	20	20
11	210	35	20	3	31	175	35	20	20
12	155	20	20	3	32	175	35	10	20

13	155	30	20	3	33	155	35	20	15
14	155	40	20	3	34	155	35	10	15
15	210	35	20	25	35	175	35	20	15
16	210	35	20	20	36	175	35	10	15
17	210	35	20	15	37	155	35	10	10
18	210	35	20	10	38	155	35	20	10
19	210	35	20	5	39	175	35	20	10
20	210	35	20	3	40	175	35	10	10

Table 3.3 Experimentally measured responses

	Response 1	**Response 2**		**Response 1**	**Response 2**
Run	Water contact angle	Cost\sample	**Run**	Water contact angle	Cost\sample
	°	€/sample		°	€/sample
1	33.28	0.099	**21**	35.44	0.240
2	28.45	0.151	**22**	23.8	0.241
3	18.62	0.203	**23**	20.37	0.244
4	8.98	0.255	**24**	39.81	0.136
5	8.93	0.307	**25**	29.01	0.137
6	39.81	0.245	**26**	22.27	0.140
7	29.01	0.250	**27**	69.22	0.134
8	22.3	0.255	**28**	68.33	0.244
9	20.71	0.238	**29**	54.58	0.134
10	18.77	0.244	**30**	42.74	0.238

11	17.54	0.250	**31**	43.88	0.244
12	32.1	0.236	**32**	48.59	0.140
13	32.5	0.237	**33**	37.3	0.238
14	22.64	0.238	**34**	39.38	0.134
15	62.16	0.250	**35**	38.15	0.244
16	42.96	0.250	**36**	39.23	0.140
17	38.87	0.250	**37**	40.47	0.134
18	26.85	0.250	**38**	36.54	0.238
19	19.34	0.250	**39**	27.6	0.244
20	12.73	0.250	**40**	32.84	0.140

3.4 Results and Discussion

3.4.1 Development of mathematical models

The fit summary tab in the design-expert program shows the highest order polynomial where the additional terms are important and the model is not aliased. Selecting a step-by-step regression method automatically eliminates insignificant model terms. The sequential F-test for the importance of both the regression model and the individual model terms, together with the lack of fit testing, was performed using the Design-Expert V12 software. The Analysis of Variance (ANOVA) for the reduced quadratic models summarizes the study of each answer and indicates the significant model terms. Table 3.4 demonstrates the ANOVA findings for the water contact angle and operating costs, respectively. Certain adequacy measures, R2, Adjusted-R2 and Predicted-R2 are also shown in the same table. All the appropriate measures are in logical agreement and indicate a significant relationship. In all

cases, the appropriate precision ratios are greater than 4, indicating an appropriate model. The analysis of the variance results for the water contact angle model shows that the main effective parameter of the APPJ is the distance, followed by the frequency, then the air flow. However, the ANOVA finds that there is no significant effect on the input voltage, but when interaction is considered with the power supply frequency, it becomes significant; so the input voltage was introduced to support the hierarchy. Moreover, there is another interaction effect between the input voltage and the air flow rate. There are significant model terms. However, the main effect of the input voltage was introduced to support the hierarchy.

The Predicted R^2 of 0.9140 is in reasonable agreement with the Adjusted R^2 of 0.9288, i.e. the difference is less than 0.2.

Table 3.4 ANOVA analysis for the water contact angle model

Source	Sum of Squares	V	Mean Square	F-value	p-value	
Model	7974.03	7	1139.15	73.73	< 0.0001	significant
A-Input Voltage	5.32	1	5.32	0.3442	0.5615	
B-Frequency	991.77	1	991.77	64.19	< 0.0001	
C-Air Flow	412.37	1	412.37	26.69	< 0.0001	
D-Distance	5594.54	1	5594.54	362.08	< 0.0001	
AB	157.35	1	157.35	10.18	0.0032	
AC	97.62	1	97.62	6.32	0.0172	
D^2	250.35	1	250.35	16.2	0.0003	
Residual	494.44	32	15.45			
Lack of Fit	482.87	31	15.58	1.35	0.6046	not significant
Pure Error	11.57	1	11.57			
R^2=0.942			Adjusted R^2=0.929			
Predicted R^2=0.914			Adeq Precision=32.626			

Table 3. 5 ANOVA analysis for the operating cost model

Source	Sum of Squares	V	Mean Square	F-value	p-value	
Model	1.93	5	0.3858	241.5	< 0.0001	significant
A-Input Voltage	0.7356	1	0.7356	460.41	< 0.0001	
B-Frequency	0.1305	1	0.1305	81.68	< 0.0001	
C-Air Flow	0.0007	1	0.0007	0.441	0.5111	

AB	0.0373	1	0.0373	23.32	< 0.0001	
AC	0.0048	1	0.0048	3.01	0.0917	
Residual	0.0543	34	0.0016			
Lack of Fit	0.0543	33	0.0016			
Pure Error	0	1	0			
Cor Total	1.98	39				
R^2=0.9726			Adjusted R^2=0.9686			

Nonetheless, the APPJ modified COP wettability parameters have a variable effect on the wettability of COP's surface. According to the results, the main effect of the four factors was the distance, followed by the frequency, then the air flow rate after the quadratic effect of distance and finally, the input. Nevertheless, the main effect of input plasma jet voltage was added to support the hierarchy. The analysis of variance results in the plasma polymers modification operation cost model, Table 3.5, showed that the main effect of the input voltage and frequency along with the air flow are significant model terms. As mentioned above, treatment costs per sample can be calculated using Equation (3.9). In this work, a mathematical model was built to estimate optimization costs. Based on the results obtained, the models developed are statistically accurate and can be used for further analysis. In Equation (3.10), the final models for coded and actual factors are shown.

3.4.2 Final equation in terms of actual factors

Water contact angle = -65.12818+0.711230* Input Voltage+2.05493* Frequency+1.76937* Air Flow +0.179582*Distance-0.01651* Input Voltage* Frequency-0.01297 Input Voltage* Air Flow+0.06294*Distance^2 (3.9)

Cost sample = 0.74838+0.00126* Input Voltage-0.03571* Frequency+0.01725* Air Flow+0.00025* Input Voltage* Frequency (3.10)

3.5 Effect of Process Parameters on the Responses

In the subsequent headings, whenever an interaction effect or a comparison between any two input parameters is being discussed, the other two parameters will be at their levels mentioned in the caption.

3.5.1 Water Contact Angle (WCA)

It is evident from the results that all the process input parameters have a significant effect on the water contact angle of an APPJ. However, Figure 3.3 is a perturbation plot which illustrates the effect of the plasma parameters on the water contact angle. The distance (D) has a positive effect on the water contact angle and the other factors have a negative effect. Both the frequency and the air flow have a negative effect on the impact water contact angle. While in the case of the distance, the result demonstrates that increasing distance leads to increasing the water contact angle.

Actual Factors
A = 187.5
B = 30
C = 15
D = 14

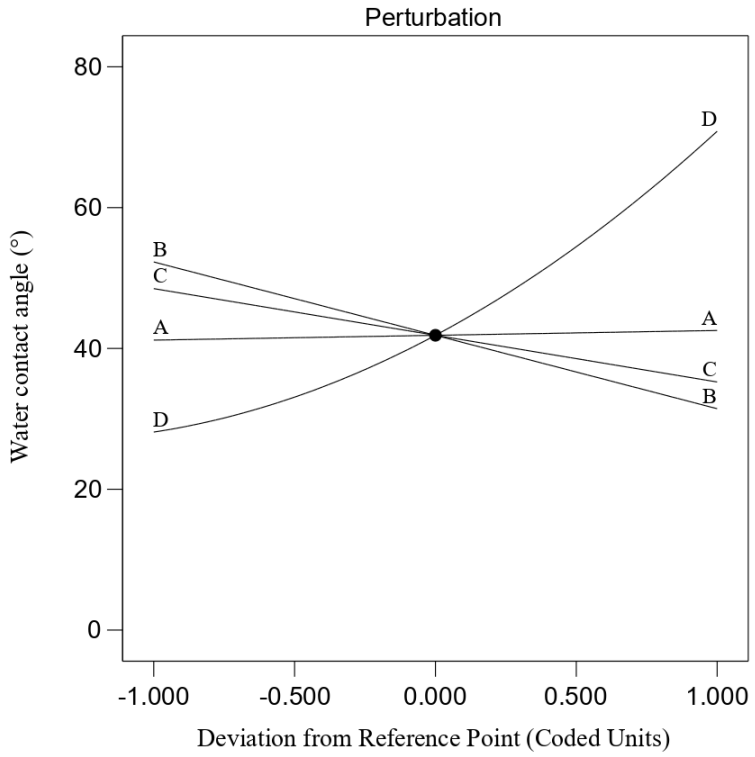

Figure 3.3: Perturbation plot showing the effect of all factors on the COP water contact angle.

Figure 3.4 (A) is an interaction plot showing the interaction effect between the frequency and the input voltage at air flow of 5 l/min and distance of 3 mm. It is evident from plot A that at a frequency range of 20-27.5 KHz when increasing the input voltage that it would lead to a slight increase in the water contact angle. At 27.5 KHz frequency the water contact angle remains at the same value for any input voltage, for higher power supply frequency the COP water contact angle decreases gradually when increasing the input voltage. The same behaviour is observed in Figure 3.4 (B) at air flow 10 l/min and distance 20 mm, the difference is at 35.5 KHz frequency and the water contact angle remains at the same value at any input

voltage value, thenit decreased with increasing the input voltage. This could be related to the fact that it heavily depends on plasma frequencies and a correlation of the plasma active species. The plasma operating parameters, such as frequency, has an effect on the surface activation because of the active species generated which reflect on the polymer surfaces wettability [123], [146]. However, when using a frequency above this threshold, approximately 27 and 35.5 KHz (in our examples), a more desirable contact angle could be achieved by applying a higher input voltage of 220 V. In the meantime, the smallest contact angle of about 7° could be obtained by using the highest frequency of 40 KHz alongside that of an input voltage of 220 V. This is because it is affected by other parameters such as air flow rate and distance from the plasma nozzle to the sample surface [123] and the active species concentration when changing the power supply parameters [147] Figure 3.4. The effect of input voltage and frequency on the water contact angle is shown in Figure 3.5; as the voltage increases, the water contact angle decreases. When a high voltage is applied, the COP surface wettability is clearly improved [148].

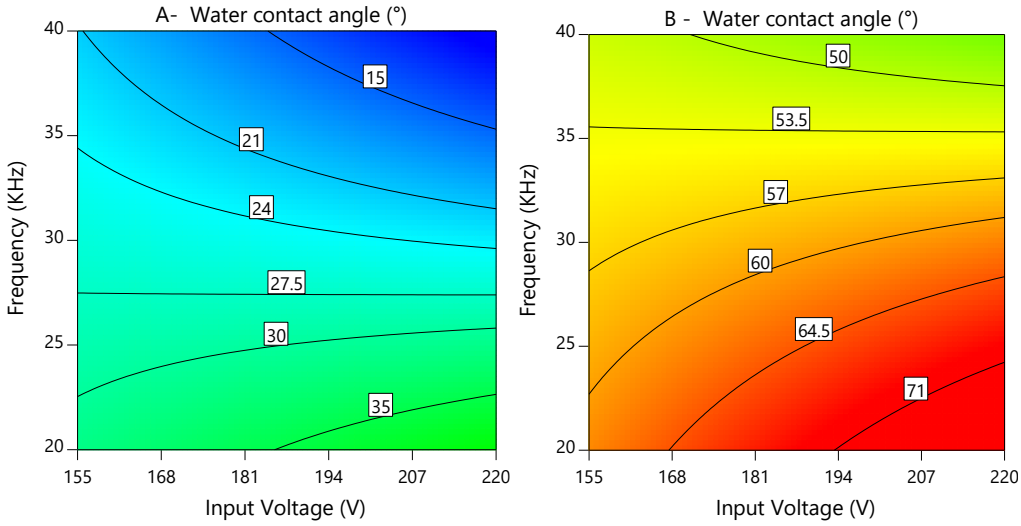

Figure 3.4: Contour plot showing the effect of input voltage V and frequency on the COP water contact angle (A) d=3mm and air flow=20 l/min. (B) d=20mm and air flow= 10 l/min.

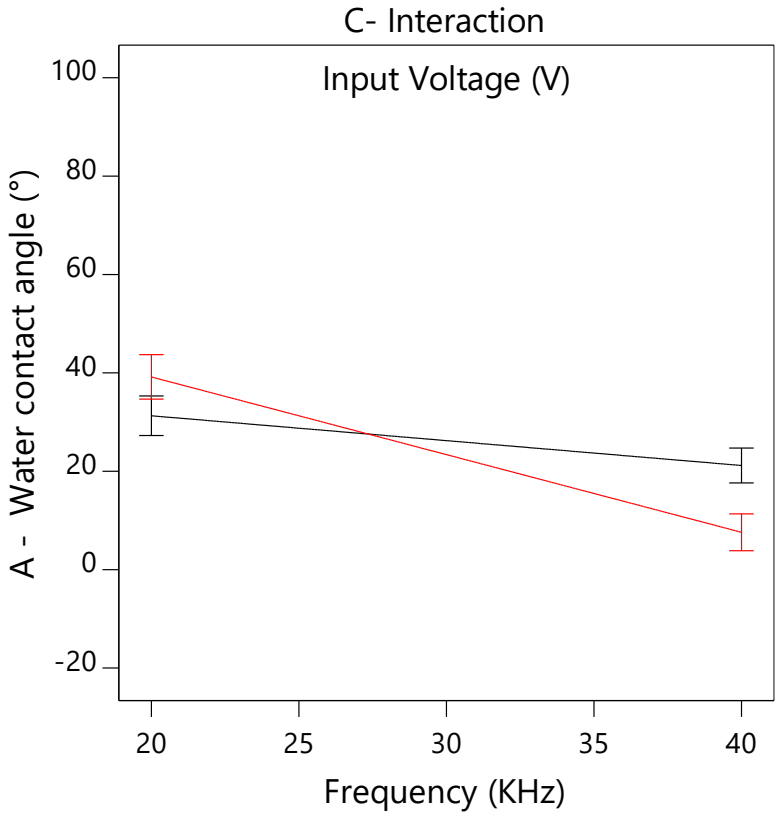

Figure 3.5: Interaction effect between input voltage and frequency on the water contact angle (red line is high voltage and black line is low voltage).

Figure 3.6-A shows the contour plot of the plasma input voltage and air flow rate at a distance of 15 mm and the power supply frequency of 20 KHz. At low flow rate the water contact angle is relatively lower at low input voltage and higher at higher input voltage. This could be because the gas temperature is reduced with the gas flow rate increasing as a result of convective cooling [132]. At a high flow rate, however, the water contact angle increases as the input voltage increases. This observation can be ascribed to the greater incorporation of O groups with higher powers, as there have been no substantial changes in the surface ruggedness. The high air flow provides intensive plasma particles while at a low flow rate, there are not enough particles [149]. Therefore, the gas flow rate must be sufficiently high to provide enough particles travelling towards the polymer surface. Figure 3.6-B

shows the interaction between the air flow rate and the input voltage at 5 l/min (black) and high flow rate 25 l/min (red). From the figure, as mentioned before in [123], it is evident that at a high air flow rate, the water contact angle is lower.

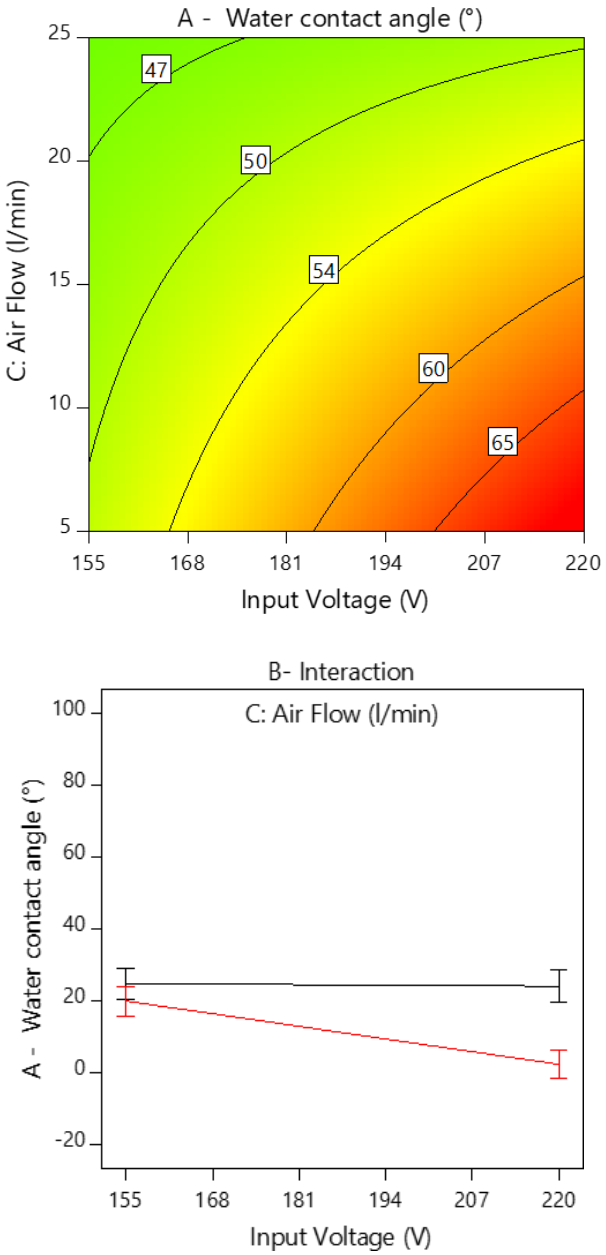

Figure 3.6: (A) Contour plot and (B) Interaction showing the effect of input voltage and air flow on the water contact angle.

3.5.2 Impact on cost

The cost impact shows the interaction effect of the parameters within the investigated range, with the input voltage having the strongest positive effect on the cost. Increasing the voltage from the lowest to the highest value increased the response by 31.25% and the frequency has a moderate effect. Changing the frequency to B has proportionally increased the cost by 15.75%. The cost is affected by the air flow, C, in a very small but significant way.

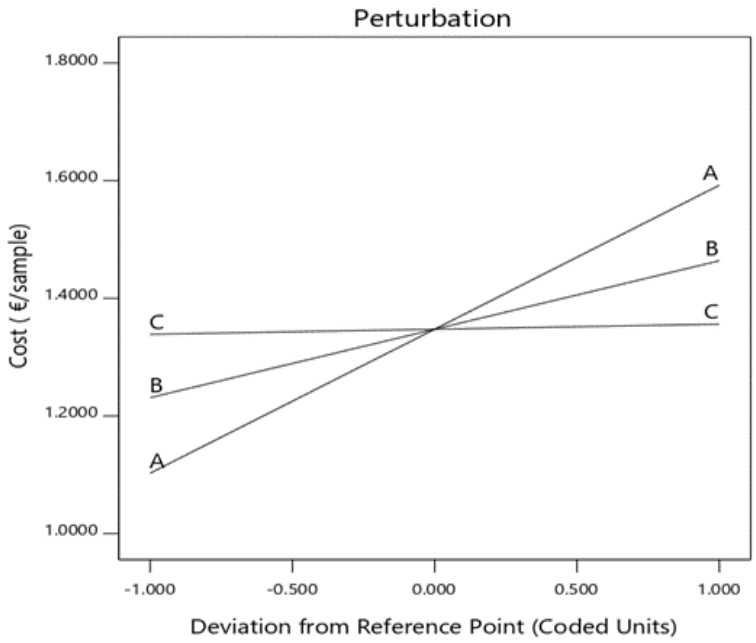

Figure 3.7: Perturbation plot showing the effect of all factors on the COP surface modification cost.

3.6 Optimization

The issue of linking between the surface wettability and treatment cost must be addressed as any increase in the surface wettability is usually reflected in an increase in the cost as a consequence so both are usually studied together. On balance, and based on the above discussion, it is better to run an optimization study

to find out the optimal wettability conditions at which a desirable cost of the treatment can be achieved. Admittedly, once the models are developed and validated, optimization criteria can be established to determine the optimal water contact angle conditions. Throughout this investigation, two criteria were implemented to minimize both the water contact angle and the cost per sample. The first criterion is to reach the minimum water contact angle and no limitation on either the process parameters or the operating cost as shown in Table 3.6. While Table 3.7 shows the second criterion, with which goal was to reach the minimum water contact angle with relatively low-operating cost and maximise profit in the long run.

Table 3.6 Optimal solution as obtained by design-expert based on the first criterion

No	Voltage	Frequency	Air Flow	Distance	WCA	Desirability	
1	209.0	39.74	24.8	3.8	6.25	1	Selected
2	218.4	36.60	24.4	3.4	8.77	1	
3	216.8	38.34	24.9	4.6	6.72	1	
4	202.9	39.83	24.7	3.4	7.59	1	
5	217.6	39.38	23.7	6.5	7.80	1	
6	209.5	39.63	23.2	3.3	7.43	1	
7	206.0	39.71	23.9	4.3	8.18	1	
8	201.4	39.94	24.2	3.2	8.14	1	
9	212.0	39.87	21.9	4.5	8.58	1	
10	219.4	36.09	24.7	3.2	8.87	1	

Table 3.7 Optimal solution as obtained by design-expert based on the second criterion

No	Voltage	Frequency	Air Flow	Distance	WCA	Cost/sample	Desirability	
1	155.0	40.0	25.00	3.0	19.97	1.17	0.83	Selected
2	155.0	40.0	24.90	3.0	19.99	1.17	0.82	
3	155.0	40.0	24.63	3.0	20.06	1.17	0.82	
4	155.0	40.0	24.52	3.0	20.10	1.17	0.82	
5	155.0	40.0	24.38	3.0	20.13	1.17	0.82	
6	155.0	40.0	24.23	3.0	20.16	1.17	0.82	
7	155.0	40.0	23.97	3.0	20.22	1.17	0.82	
8	155.0	39.8	25.00	3.0	20.06	1.17	0.82	
9	155.1	39.9	24.39	3.0	20.14	1.17	0.82	
10	155.0	40.0	23.65	3.0	20.30	1.17	0.82	

3.7 Conclusions

In conclusion, using the plasma jet within the parameters considered in this study the following points can be deduced:

1. Historical data has proven to be an accurate technique for optimising the atmospheric pressure plasma jet process, resulting in the best surface wettability of the polymers surfaces.

2. An input voltage of 200 to 220 V is thought to be the best for obtaining an excellent water contact angle and its interaction with the frequency at the distance is the most effective plasma jet parameter.

3. The graphical optimization results allow for a more efficient search for the best surface treatment settings.

4. If the optimal APPJ conditions are used, the operating cost of plasma surface treatment can be reduced by approximately 30% with acceptable surface wettability. The R2 value of approximately 0.9140 indicates that the model accounts for approximately 91.4 % of the variability in the data. This fact, combined with the satisfactory residual analysis, indicates that the model is a very good fit for the data and that the COP surface water contact angle can be predicted within the

investigated range of parameters. This model will, theoretically, be able to predict the wettability of the sample, which will be useful in comparing the experimental model to the theoretical model. If the optimal APPJ conditions are used, the operating cost of plasma surface treatment can be reduced by approximately 30% with acceptable surface wettability. The R2 value of approximately 0.9140 indicates that the model accounts for approximately 91.4 % of the variability in the data. This fact, combined with the satisfactory residual analysis, indicates that the model is a very good fit for the data and that the COP surface water contact angle can be predicted within the investigated range of parameters. This model will, theoretically, be able to predict the wettability of the sample, which will be useful in comparing the experimental model to the theoretical model

4 Characterization of the Atmospheric Pressure Plasma Jet

4.1 Plasma characterization

This chapter presents the characterization of the plasma jet, the experimental set-up and the methods used to investigate the plasma dynamics of air as a main plume. This is accomplished by analysing voltage peaks at microsecond and nanosecond time scales and through optical emission spectroscopy. Methods have non-intrusive access to the streamer's evolution and the propagation of external parameters.

Electrical measurements were made to evaluate the APPJ's current-voltage characteristics under optimum conditions obtained from DOE; these conditions included voltage, airflow and the distance between the two electrodes.

As previously stated, the plasma jet is comprised of a cylindrical dielectric quartz tube with an electrode bar in the centre and a metal nozzle serving as the anode. Using the nozzle configurations shows that the plasma is a jet which suppresses thermal instabilities and electrical arcing due to the dielectric contact surface and the alternating voltage used. The jet was exhausted into the open ambient air at atmospheric pressure and at room temperature. The discharge tube was filled with air delivered at rates ranging from 5 to 25 standard litters per minute (slm). The flow was controlled by a mass flow controller, model (MKS247). The continuing plume flow is necessary to sustain the plasma discharge and to provide a plume channel to ignite the plasma inside the discharge tube and to propagate beyond it, as illustrated in Figure 4.1.

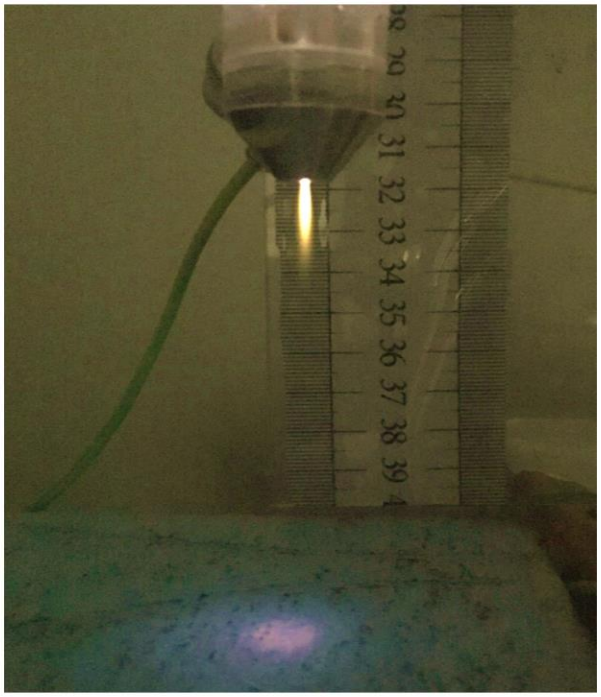

Figure 4.1: **Photograph of the plasma jet plume**

4.2 Experimental Set-up and Investigation

4.2.1 Current-voltage measurements

In this work, the plasma discharge was created using a high voltage power supply model PVM400, which produces high sinusoidal voltages of up to 20 kV at output frequencies of up to 40 kHz. Voltage measurements were made using a Tektronics P6015A high voltage probe with a 1000:1 division ratio. DC Test Voltage: 0 – 20 kV AC, pulse of less than 40 KV peak to peak. The probe was connected at one end to an exposed portion of the high voltage electrode and at the other end to a common ground point. Following that, a BNC cable was used to connect the oscilloscope. The experimental set-up of electrical characteristic measurements is illustrated in Figure 4.2 below.

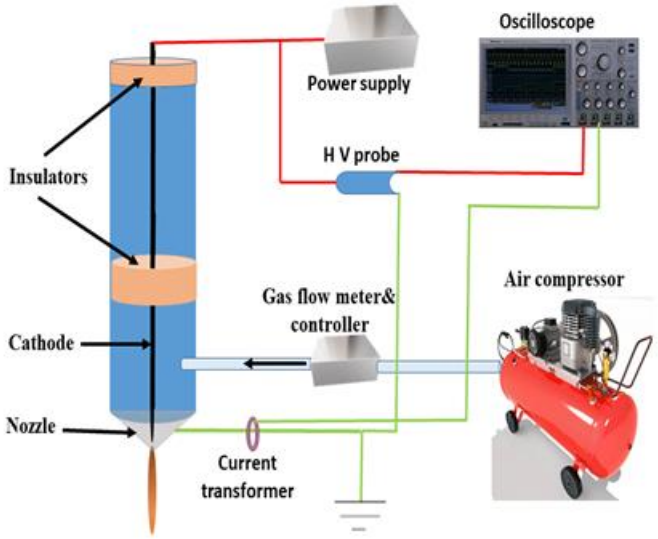

Figure 4.2: The schematic block diagram for measuring current-voltage

When the plasma was active, the oscilloscope was triggered by a current spike. This was done by selecting the oscilloscope's time division to 100 ns and adjusting the oscilloscope's trigger level to be approximately 65 per cent of the current reading, resulting in a stable reading for both current and voltage.

Capacitive load behaviour appears when insufficient voltage is supplied to the gas for breakdown to occur. The waveforms of the current and voltage signals are both sinusoidal, with the current leading the voltage. The period of both the current and the voltage was measured to be 28.7 seconds, which corresponds to a frequency of 34.8 kHz according to $t = 1/f$.

Indicating a small difference between the measured and expected frequency of 34 kHz. The voltage should lag the current by 90° in an ideal capacitive load, which should be 7.17 µs for a period of 28.67 µs, but the calculated phase deference was found to be 6.87 µs, corresponding to a phase difference of approximately 86°. Figure 4.3 shows an example of current and voltage measurements taken pre plasma production.

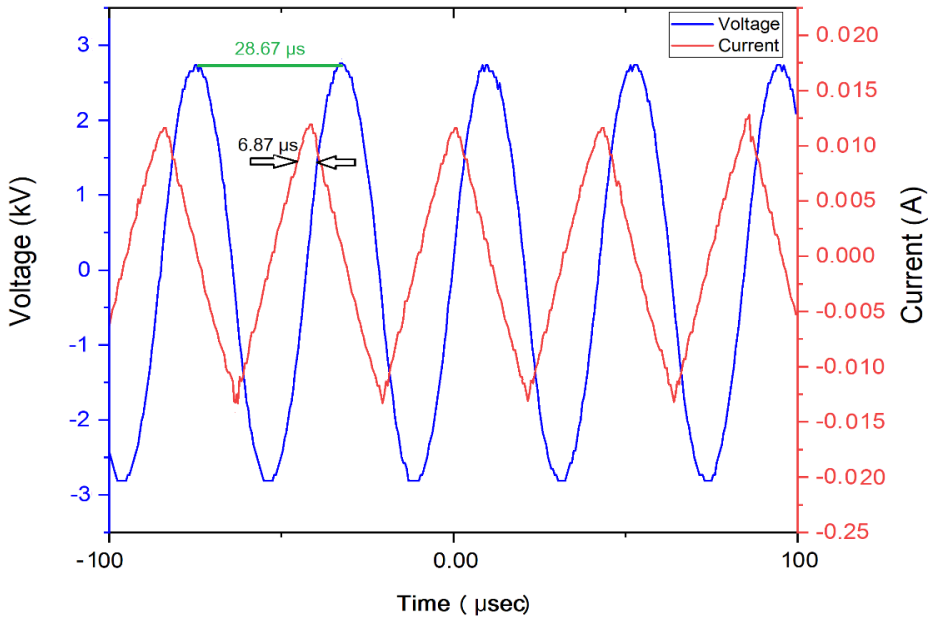

Figure 4.3: Plasma of typical voltage (A) and current (B) waveforms with a 3 kV applied voltage and a 20 slm air flow rate

The optimum APPJ operating conditions were electrically characterised. Figure 4.4 shows standard electrical (Voltage-Current) measurements were obtained at a frequency of around 35 kHz and the applied voltage was increased up to 40 kVp-p. We noticed one sharp distinct peak per half cycle of plasma on voltage. The peak duration is longer in the positive cycle than the negative cycle.

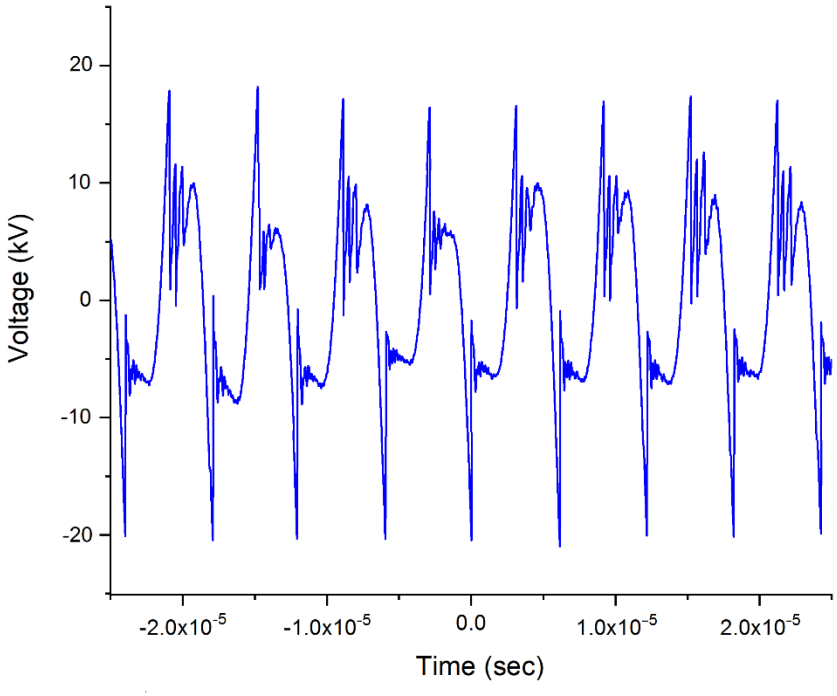

Figure 4.4: The voltage signal observed when the plasma was in the optimal conditions obtained from DOE.

Figure 4.5 and illustrate the accompanying current spike. During the negative half cycle, the voltage drops precipitously, accompanied by a matching rapid, abrupt current spike, generally in the range of 05 - 1 mA and enduring for 5 ns. Throughout this this sentence is not complete.

When a sufficient electric field was applied between the electrodes, the gas was able to break down and switch from a capacitive to a resistive load. During the negative half cycle, the voltage drops sharply in magnitude, accompanied by short, sharp current spikes decreasing gradually lasting around 30 nanoseconds, typically in the range of 1 to 3 A.

A change in voltage polarity from negative to positive was observed after the current surge stopped during this voltage drop. After the voltage drop and polarity

reversal, the voltage quickly reversed back to negative polarity and maintained a long plateau, usually lasting until the moment when the polarity of the applied voltage should change to positive.

Depending on the operating conditions of the APPJ, the plateau remains relatively between 1 - 2 kV, decreasing gradually with cycle length. The applied voltage started to change polarity during the positive half cycle, the voltage dropped to about zero, but the polarity did not change. Waveform distortion also tends to be shorter in duration than the negative half cycle. Whereas the current spikes tend to be shorter than the negative cycle.

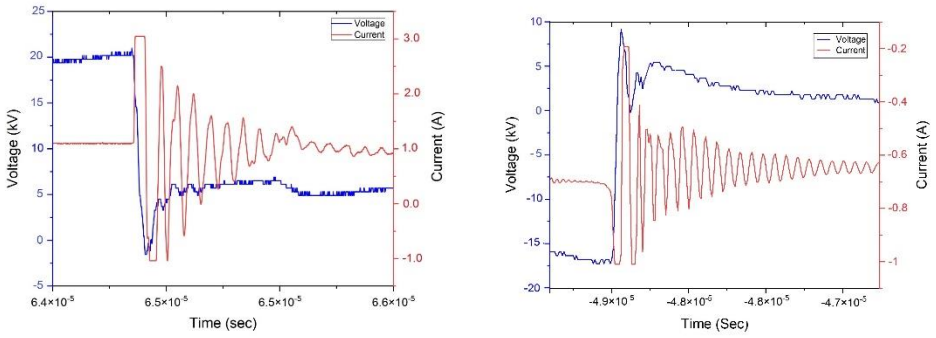

(a) (b)

Figure 4.5: An example of the corresponding voltage drop and current spike (a) the positive half cycle (b) the negative half cycle.

4.2.2 Optical emission spectroscopy measurements

Optical emission spectroscopy OES is one of the most important research tools for atmospheric pressure plasmas. The approach does not interrupt the plasma

discharge and provides direct knowledge about the plasma components by analysing the plasma species that are generated from plasma jets. It presents impeccable results in terms of plasma chemistry and plume temperature. Although it is quick and simple to use, it is capable of detecting a wide variety of elements and concentrations. Accurate and cost-effective, standard optical spectrometers cover a wavelength range of about 200 - 1200 nm, i.e. wavelengths less than 200 nm are invisible to standard spectrometers. This limitation must be taken into account when attempting to interpret plasma spectra acquired using OES. The optical emission spectroscopy is a qualitative technique. If a known concentration of another atom or molecule is intentionally added, it may be semi-quantitative. The technique is also known as actinometry or titration. Extreme caution should be exercised when interpreting actinometry or titration results [153].

Atomic and molecular excited states can be detected by the intensity of light. Since the amplitude of the light intensity at a particular wavelength is inversely proportional to the plasma density, the number of molecules can be calculated simply by measuring the amplitude of the light intensity at that wavelength.

Hence, the width of the spectral line of the atom, ion or molecule gives an indication of the heavy particle temperature in the plasma.

Plasma light emission generally depends on the collisions between plasma particles in excitation. In the process, the electrons transition to the excited state and then return to the lower energy level through a photo-multiplier, emitting photons. In the process, the emission line wavelength represents the energy gap. The light is focused by lenses and then diffused by a series of mirrors in the spectrometer. Light is scattered by the gratings so that a picture multiplier or CCD camera can capture it.

Figure 4.6 depicts an experimental set-up for time-integrated spectroscopy with high resolution and time resolution in a single set-up. An Ocean Optics spectrometer, HR4000, was used to observe and analyse the chemical composition of the plumes generated by the APP, placed perpendicularly to the nozzle's axis of rotation at a distance of 5 mm from the nozzle end. The Spectra Suite is provided with Spectra, which allows us to view and study the spectrum, as well as perform spectral and preliminary analysis of the raw data.

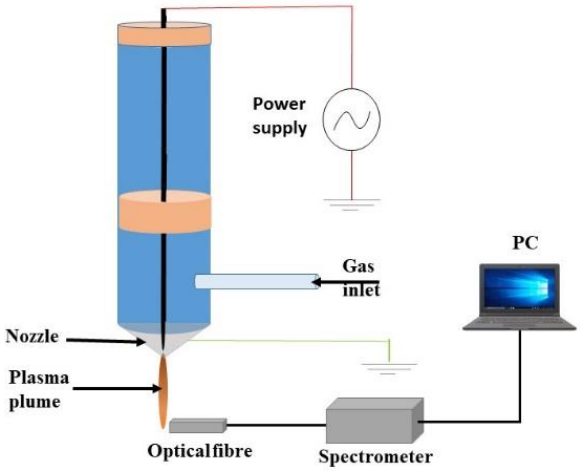

Figure 4.6: Schematic diagram of the optical emission spectroscopy measurements

An optical emission spectroscope at an approximate distance of five millimetres from the nozzle, is represented in Figure. 4.7. As the spectrum shows, the plasma consists of a diverse set of plasma species across a broad wavelength range. As the plasma waves spread through the ambient air, the spectra can be monitored. Frequent nitrogen and oxygen peaks are included in the figure for nitrous oxide. It shows the spectrum of optical radiation emission that occurs 4 mm from the power electrode in the downstream direction. [6,7].

The figure indicates the OES signal collected from the plasma jet over a wavelength range of 200 - 1100 nm. In general, the spectrum consists of emission peaks associated with N2, O, N, OH and H. Several emission peaks correspond to atomic and molecular vibrations of oxygen and nitrogen which were present in the spectrum [17, 18]. The emission peaks in the 280 - 420 nm wavelength region are mostly dominated by the nitrogen vibrational band and those in the 540 - 1100 nm wavelength region corresponding to atomic transitions from nitrogen and oxygen. The emission peaks observed at around 464 and 407 nm are associated with ionized atomic oxygen and those at 525 and 559 nm are related to the ionized molecular oxygen. The OES spectra indicates that the plasma jet produces significant reactive species of interest for surface functionalization of COP polymers.

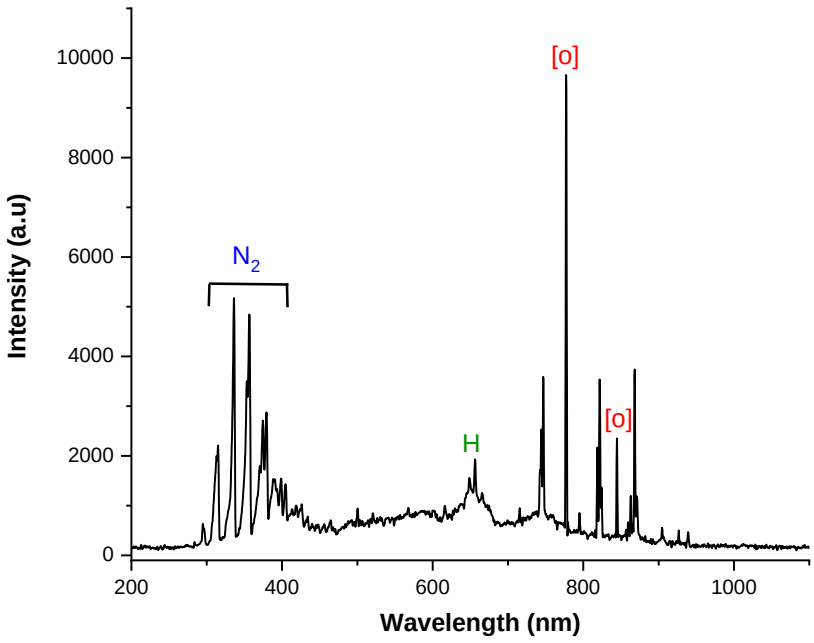

Figure 4.7: Broadband spatially resolved optical emission spectra of APP jet. The measurements were taken at 20 kV applied voltage, a 30 kHz driving frequency, and a 20 slm plume flow rate.

4.2.3 Plasma plume temperature

The surface temperature of the sample as a result of the plasma plume is specified as a critical variable that must be maintained during surface treatment [154]. It must be meticulously measured; as the temperature of the surface gas increases, the species' intensity also increases. Due to the strong correlation between the rotational temperature of the plasma in the atmosphere and the gas temperature [155], [156]. The plasma collisions at atmospheric pressure show that the plume rotational temperature is constant with respect to the rotation of the electron plume, indicating the existence of equilibrium [157].

The temperature of the plume was measured using an infrared thermometer (Fluke, 62 MAX). Measurements were taken at distances between 3 and 20 mm from the plasma jet nozzle at 20 kV applied voltage, 35 kHz and air flow rates of 5 slm to 25 slm, as shown in Figure 4.8. The temperatures measured ranged from 25 to 55°C.

These temperature ranges are ideal for polymer surface modification because they modify the surfaces without causing damage [158].

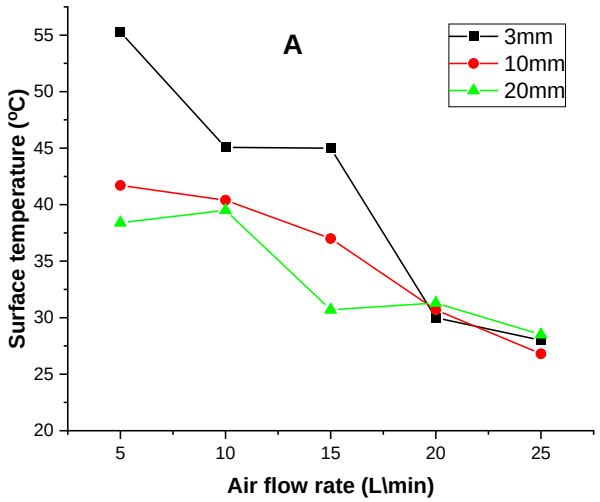

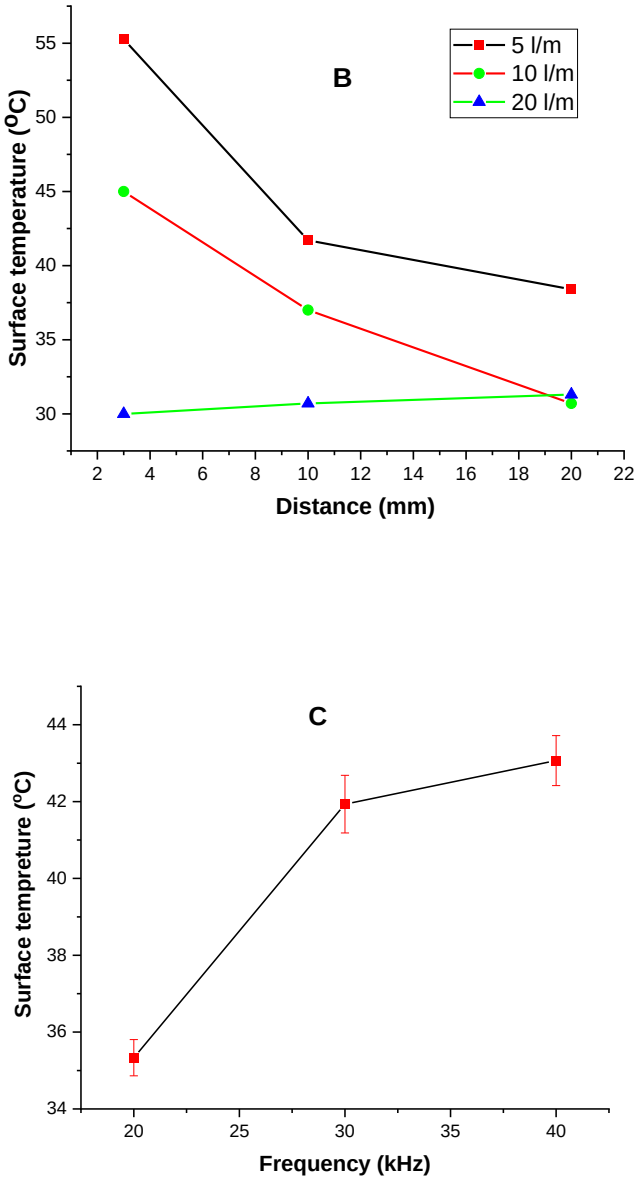

Figure 4.8: Plasma plume temperature at various operating conditions (A, air flow rate), (B, Distance) and (C, Frequency).

4.2.4 APPJ plume length as a function of operating parameters

The expansion of plasma jet plumes into the open air is being studied. The plume length is found to be significantly affected by the applied voltage and frequency, as well as the air flow rate. By adjusting the operating parameters, the length and

intensity of the jet plume can be drastically changed. These experiments are critical for developing a thorough understanding of plume expansion dynamics and enabling a high degree of control over atmospheric pressure plasmas in surface modifications, biomedical, materials synthesis and processing, environmental and other applications.

Figure 4.9 shows how we used a plasma jet device to create a plasma plume that expanded from 0.5 to 1.8 centimetres from the nozzle into the surrounding air. The plume of the plasma jet remains close to room temperature and experiences no thermal increase, which benefits the COP surface modification. Although significant observations and realisations of the APPJs plume have been reported, the physical mechanisms that lead to their generation and the interaction with the surrounding ambient remain poorly understood [159][160].

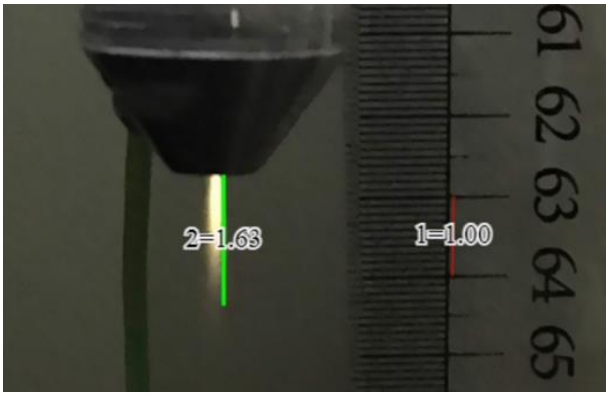

Figure 4.9: Plasma plume length measurement

Our experiment showed that plasma jet control over the plume is possible. In Figure 4.10, the different lengths of the plume are illustrated as the bars along the operating parameters. According to the plasma images, a plume with a length of 1.8 cm at 20

slm, 40 KHz and input voltage 220 v. Increasing both the gas flow and frequency increases the plasma plume.

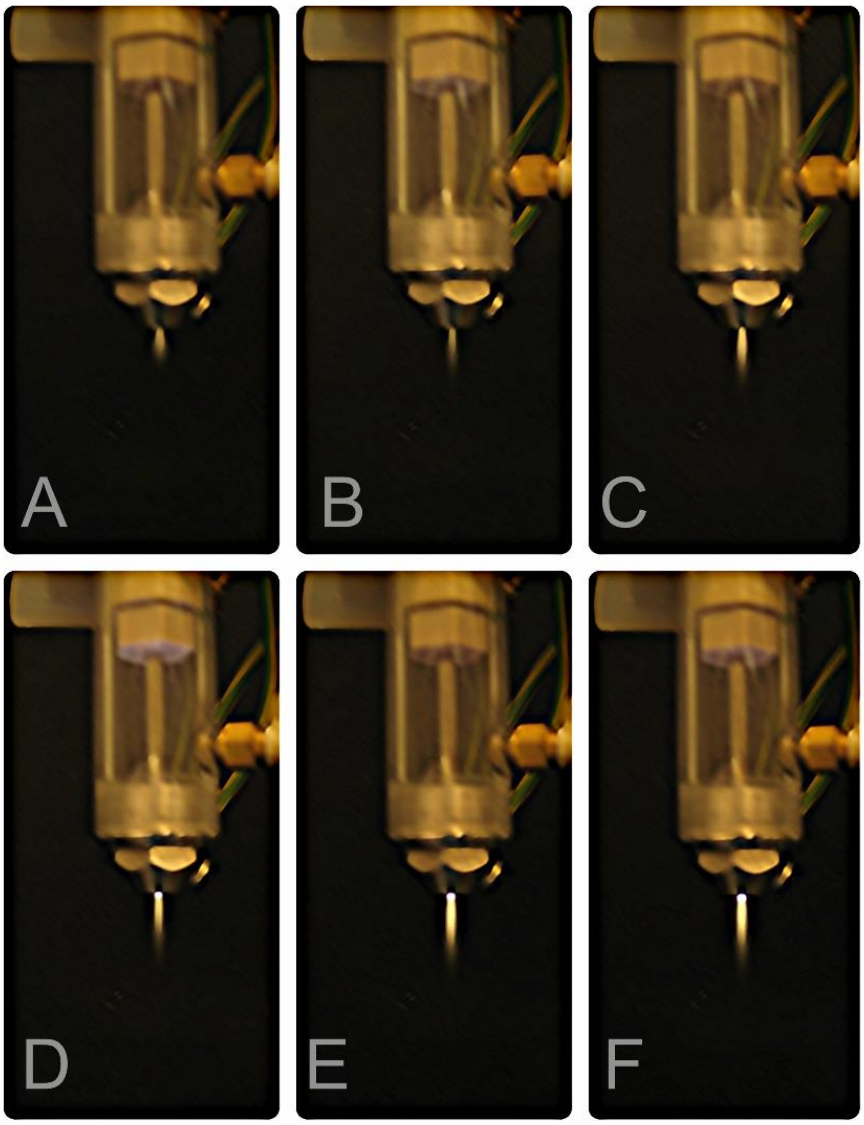

Figure 4.10: Plume length-scale variation in operating conditions, (A) 5 slm 20 kHz 220 V, (B) 10 slm 20 kHz 180V, (C) 10 slm 30 kHz 220 V, (D) 10 slm 40 kHz 220 V, (E) 20 slm 40 kHz 220 V, (F) 25 slm 40 kHz 220 V.

In conclusion, the effects of various operating parameters on the length of the APPJ plume have been studied. The length of the plasma plume is found to be significantly affected by the applied voltage, air flow rate and frequency. Future

research should focus on understanding the interactions between the plasma plume and the surrounding environment, such as air humidity.

4.3 Summary

A detailed description of the experimental set-up, electrical characterization, optical emission spectroscopy measurements and plume thermal and length measurements are presented in this chapter. The goal was to investigate the impact of the plasma jet and improve the role of atmospheric pressure plasma parameters in reducing COP wettability. Various operating parameters were used to generate plasma, a sinusoidal high voltage power supply was used. The electrical parameters of the jet were studied by measuring the discharge current, input and power consumed. It was concluded that under optimal operational conditions (applied voltage of 20 kV, frequency of 35 kHz, and air flow rate of 20 slm), the input and power consumed were 6 W, with the actual plasma current ranging between 2-2.5 mA.

The optical emission spectroscopy of the plasma plume and the main discharge region revealed that at various external parameters, several reactive species were emitted from the atmospheric pressure plasma jet. As a result, the spectra confirmed that the plasma can deliver species like (H, O, N, and OH). A measurement of the plasma plume temperature was presented, which confirmed that the plasma plume temperature was less than 40 °C and that the temperature obtained could be used to treat polymer surfaces.

5 Cyclic Olefin Polymers Post Air Atmospheric Pressure Plasma Treatment

5.1 Introduction:

Surface hydrophilization of polymers treated by plasma and wet chemical processes the functional groups such as hydroxyl groups can be introduced to the polymer surface, this will make the surface more hydrophilic. Combining plasma with wet chemical methods can improve COP's wetting properties. The main challenge was to develop a selective functionalization group, at high surface concentrations, this forms one type of functional group [161]. Plasma and wet chemical processing are two of the most appealing for monotype functionalization [162]. Plasma provides excellent ions, electron waves, and radicals such as hydroxyl and carboxyl bonds for polymers and their application [163]. Atmospheric pressure plasma was found to be a very effective technique for polymer surface modification, but the drawback is that the properties gained will disappear over the time [164].

5.2 Known surface functionalization methods

Surface functionalization via well-defined classical organic chemistry requires primarily suitable polymers that are hydrophilic or hydrophobic in nature. Adhesion-promoting groups can be grafted onto polymers containing the most preferred sites for changing wettability and bond ability, such as the benzene nucleus, hydroxyl groups, double bonds, and halogens [165].

Wet chemical oxidation treatments are one of the most traditional and widely used methods for surface treatment of inert polymers such as polyethylene, polypropylene, and polyester cords, fibres and films [166]. Chromic acid, nitric acid, potassium permanganate, hydrogen peroxide, and peroxydisulfate acid are examples of strong oxidizing agents. A strong oxidizing agent tends to introduce oxygen into all possible chemical combinations, like carbonyls, hydroxyls and

carboxylic acid groups on and into the polymer surfaces. The introduction of all such combinations in the form of oxygen is often sufficient to improve the wettability and adhesion of such inert polymer surfaces.

Reductive treatment is applied to promote the adhesion property of per-fluorinated polymers such as polytetrafluoroethylene (PTFE). Sodium dissolved in naphthalene or ammonia is used as a reducing agent for Teflon and has good bending properties [167].

Plasma treatment is finally the most often used and workable method for polymer surface activation [168], the research focus and purpose of this study. A method with maximum power and versatility, which can be used for cleaning or etching of a polymer surface by removing some of its topmost surface layers, introducing functional groups as well as depositing a thin polymer coating on the polymer substrate.

However, modification is a generic term used for all chemical and physical changes that are introduced to the surfaces of organic and inorganic materials. It could be roughening, coating, oxidizing, etc. Functionalization means the introduction of functional groups on the polymer surface. The process introduces chemically distinct types of functional groups, which is referred to an unspecific functionalization. Specific functionalization refers to consort functional groups, i.e. there is only one type of functional group. The most common functional groups are OH, COOH, epoxy, and so on.

5.3 Surface ageing or hydrophobic recovery

Surface ageing or hydrophobic recovery of plasma-modified polymers is discussed in this chapter. The results of non-thermal plasma activation treatments are not

irreversible. This is because the surface will attempt to return to its original untreated state. It is understood that plasma polymers are vulnerable to oxidation in the atmosphere due to rapid recovery in the air [169]. The so-called surface stability or 'ageing process' has received more attention in science. Many atmospheric pressure plasmas have demonstrated promising results in the application of polymer surface wettability [60], [169]-[171]. The performance of the COP surface immediately after treatment is often not considered. This greatly explains the ageing process of polymers. XPS, FT-IR spectroscopy and water contact angle goniometry have provided data on surface wettability changes in a few air APPJ operating and sample storing conditions. It is agreed that the ageing process starts with these reactions. Oxygen and hydrogen bonds have been shown to be present in freshly treated samples through FT-IR spectroscopy, disappearing steadily when stored in air. The rate and mechanism depend on several factors [172].

The ageing behaviour of cyclic olefin polymer (COPs) surfaces post plasma will be considered in this chapter. Changes in the surface over time were studied by Fourier-transform infrared spectroscopy, FT-IR and water contact angle measurements. We discovered the amount of oxygen incorporated varies. This can be variable in different environments. To better understand the plasma modification properties, the plasma surface has been investigated.

The ageing of some polymer plasma treatments has no lasting impact on the polymer substrates. Rather, the ageing of plasma-treated material, that is, the surface polarity, decays with the time of storage. The thermostatically induced adjustment of inducing d-polar functional groups into bulk materials, to minimise surface energy and the diffusion of polar chemical groups into the polymer matrix, is believed to be responsible for this ageing effect [173]. Many parameters affect

plasma-treated surface ageing, including how much crystallinity in the substance treated, plasma gas used, and storage conditions [174], [175]. A lower crystalline content and a higher storage temperature both contribute to the free circulation of the molecular chain and to the acceleration of the rearrangement of the surface [176]. There have been attempts to restrict ageing phenomena by stabilizing the surface layer enabled by connecting it, which reduces the mobility of the polymer chains [177].

Post plasma treatment stability is one of the main hazards of polymer surface modification, also known as the hydrophobic recovery or ageing phenomenon. Previous investigations have indicated it is through polar group surface reconstruction in bulk, migration of low-molecular weight add-ons from the bulk to the surface and environmental contamination of surfaces, particularly in the case of polymer surface oxidization, due to inadequate storage conditions [59], [60], [178].

Despite the fact that both treatments are surface oxidation processes, the mechanisms of oxidation are vastly different. Because of the limited chain scission associated with flame treatment, more polar groups form on the PP surface. Flame-treated PP is more heavily oxidized after washing with water, and more stable than corona-treated PP, according to insufficient Low Molecular Weight Organic Molecules LMWOM formation.

Plasma surface modification has also carefully examined the effects on the ageing of different surfaces [171], [172], [180]-[182], which have been modified with plasmas of air, oxygen, nitrogen, helium and argon. Although there have been major differences between plasma and corona (DBD filamentary mode) treatments, due to the range of use of plasma sources and gases, it is hard to compare APPJ with other plasma treatments. The hydrophobic recovery effect of APPJs was compared

with corona treatment, particularly in roll to roll process DBD plasma of the glow type [183] and DBD plasma [184]. In both studies, DBD plasma processing produced higher and longer lasting weight resistance on PE surfaces than coronation. In summary, ageing is a complex phenomenon strongly influenced by the method, the nature of the substrates and the conditions for storage (temperature and humidity). As a result, hydrophobic recovery can hardly be generalized or predicted [73].

5.4 Effect of hydrogen peroxide (H_2O_2) treatment on plasma COP polymer surface

The primary objective was to contrast and compare the physical and chemical properties of COP surfaces after being washed with H_2O_2. The water contact angle (WCA) was determined by a COP that had been directly modified by an air APPJ. The unmodified surface was found to have a WCA of 90°, indicating that it is hydrophobic. The treatment did improve the surface's wettability. The changed surfaces were analysed with a WCA of about 30 - 40 on the day after the treatment. The stability of the surface modification was determined over a period of several weeks (Figure 5.1) by analysing the COP substrate's WCA and surface chemistry. In both samples, the WCA continued to rise until it stabilised after approximately 8 weeks. The sample washed with H_2O_2 was slightly more hydrophilic than the sample treated immediately with air APPJ. Both surfaces evolved similarly over time, stabilising at 62 and 77, respectively. Temporal variations in WCA values can be attributed to a variety of factors, including treatment and storage conditions. For H_2O_2, it is most likely the product of COP's surface catalysed oxidation of reactive/charged species.

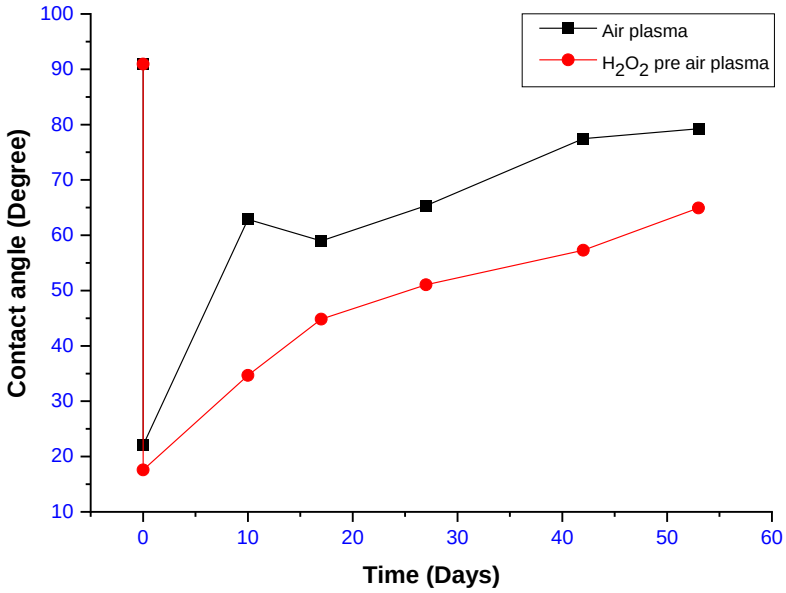

Faraj you need to insert the letter c at the beginning of the vertical axis (contact)

Figure 5.1: Water contact angle as a function of time over a period of 60 days. (Black) sample treated with air APPJ saved in normal room conditions, (Red) sample washed with H_2O_2 then treated with air APPJ saved in normal room conditions.

An ATR-FTIR investigation was applied on unmodified and treated substrates to better classify the COP treated surface (Figure 5.2). Various vibrations can be seen in the ATR-FTIR spectra in two different regions: 3500-2800 cm^{-1} and 1500-750 cm-1. In the first area, there is a broad band between 3750 and 3000 cm^{-1} that can be fitted with two components created at 3565 and 3292 cm^{-1}, which correspond to the associated OH stretching vibrations. The peaks at 2900 and 2800 cm^{-1} can be attributed to asymmetric and symmetric stretching of C=H, respectively. Those peaks arise from the substrate, as they appear on both graphs. In the second region (1700-1550 cm^{-1}), a peak due to the substrate appearing at 1455 cm^{-1} is associated with C=H bending vibrations. This data, alongside WCA data, shows that the

surface is efficiently COP modified with H_2O_2, resulting in greater long-term stability than without the use of H_2O_2.

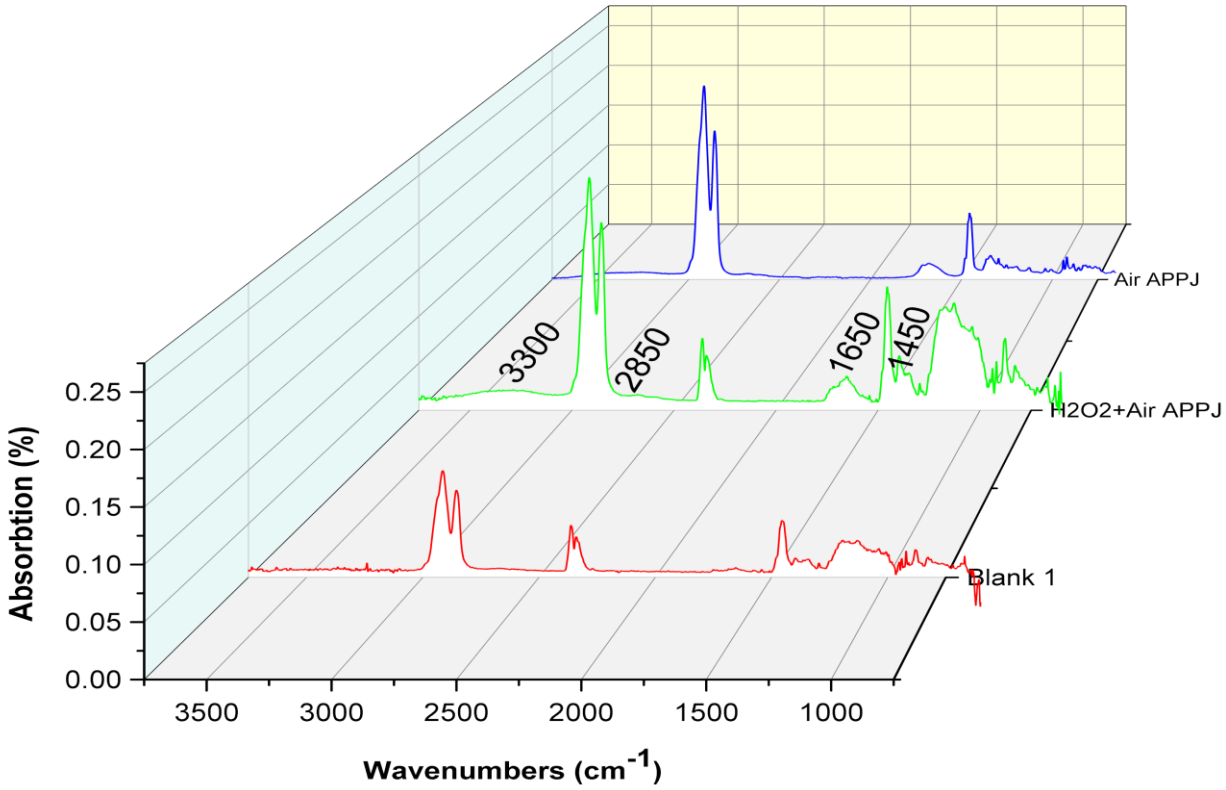

Figure 5.2: COP films treated the air APPJ treatment with and without washing with H_2O_2 for 10 minutes.

5.5 Post-plasma oxidation

Plasma polymers typically react to changes in surface chemistry after treatment. We also found a substantial amount of oxygen incorporation in plasma polymerized COP films after ageing.

5.6 Influence of humidity storage affecting the ageing behaviour of the COP surface

In general, the plasma induced surface modification in polymers is not permanent and stable, called the 'ageing effect', as the treated surface tends to recover hydrophobicity and revert back to the untreated state, which is an important concern. Hence, we will investigate ageing effects as well as factors affecting ageing behaviour in this plasma treated polymer. Here we study the stability of the treated surfaces by controlling the humidity in the storage chamber.

For this experiment, plasma treated polymer samples were stored in two different environments, first in the normal open-air (at room temperature with high humidity of 50-70%) and the second at room temperature with low humidity in the presence of silica gel. Contact angle and FTIR measurements were performed as a function of ageing of the sample up to a period of 180 days. Figure 5.3 indicates the variation of WCA of the plasma treated COP surface as a function of ageing by storing it in both the normal ambient environment and in a closed container with silica gel.

The WCA was found to increase rapidly in the sample stored in the normal ambient (high humidity 50-70%). However, the WCA increase occurs at a slow rate in the presence of a low humidity atmosphere. As shown in the figure, after 180 days, we found a significant increase (~45%) in the WCA of the sample stored in the ambient air compared to that stored in the silica gel atmosphere.

A number of mechanisms have been proposed to explain the hydrophobic recovery of polymer surfaces, including loss of low molecular weight organic material created on the surface during plasma treatment, diffusion and re-orientation of polar surface groups towards the bulk, diffusion and reaction of free radicals and

contamination of the plasma treated surfaces. A number of mechanisms have been proposed to explain the hydrophobic recovery of polymer surfaces, including loss of low molecular weight organic material created on the surface during plasma treatment, diffusion and re-orientation of polar surface groups towards the bulk, diffusion and reaction of free radicals and contamination of the plasma treated surfaces [185], [186].

The ATR-FTIR spectrum of plasma-treated COP surfaces aged for 10 and 60 days in ambient air and silica gel storage containers is shown in Figure 5.4. While the C=O and –OH related peak intensities increased with age in all samples, see Figure 5.4, the peak intensities decreased less when the samples were stored in silica gel containers compared to those stored in open air ambient, which is consistent with a significantly slower hydrophobic recovery rate observed in the silica gel containers.

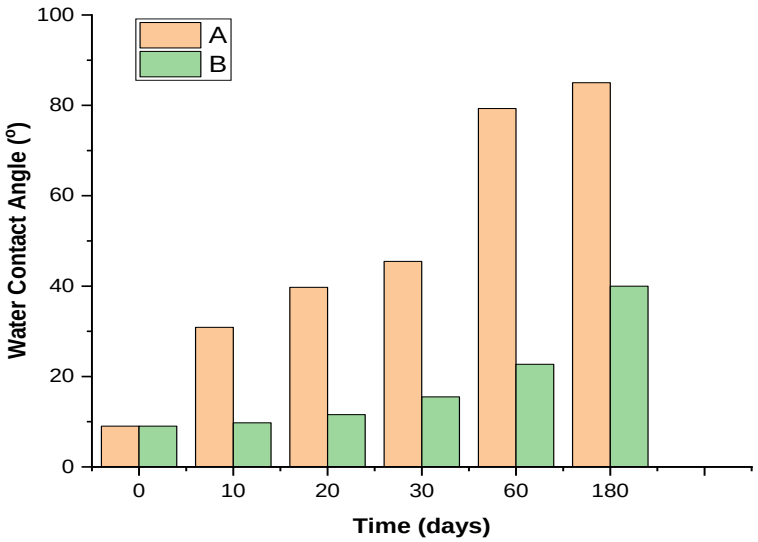

Figure 5. 3: Evolution of the water contact angle of APPJ-treated COP films stored at different humidity ambient (A) stored in room temperature and humidity, (B) stored in room temperature and low humidity.

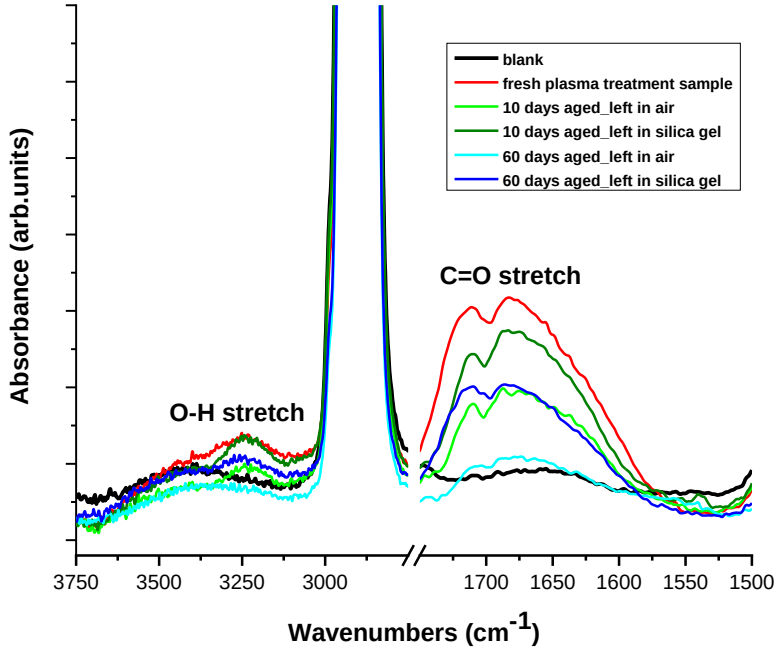

Figure 5.4: ATR-FTIR of COPs samples treated with air APPJ saved in different humidity conditions.

5.3 Conclusion

The chapter proposes an effective and cost-efficient APPJ-based approach for the surface functionalization of COP substrates and an efficacious strategy for the impediment of the hydrophobic recovery of the plasma treated COP surfaces. The indigenous APPJ air plasma treatment improves the wettability of COP substrates and reduces the water contact angle from 90° to as little as 10°.We have found that a number of plasma parameters have a significant influence on controlling the induced hydrophilicity of the COP substrates. We also investigated the long-term stability of the plasma treated COP polymers, by studying the effect of the humidity of the storage container on the hydrophobic recovery rate. We found that the plasma treated polymers remain hydrophilic (WCA < 15o) and stable for up to 20 days, if stored in a container filled with silica gel (low humidity).

6 Air Atmospheric Pressure Plasma Jet Treatment of A Gold-Coated Glass Substrate for Use with Sensors

6.1 Introduction

The term ’noble metal’ refers to a group of several metallic chemical elements that exhibit exceptional resistance to oxidation, even at elevated temperatures; the grouping is not precisely defined, but typically includes rhenium, ruthenium, rhodium, palladium, silver, osmium, iridium, platinum, and gold [184], [185].

The recent increase in nanotechnology is opening up new opportunities for a variety of applications that were impossible just a few decades ago, ranging from chemical detection and imaging (Nejati, Dadashpour et al. 2021, Guo, Zhang et al. 2011), to cancer treatment and drug delivery (Vodnik, Mojić et al. 2021, Awakan, Ohue et al. 2021).

Recent studies show that, in addition to their possible intentional role, these nanomaterials may have unintended or detrimental effects on living cells (McClements 2018). In this case, the ability to precisely prepare NP bio-conjugates is important for understanding how minor differences in their architecture affect their interaction with cells. (Zhang, J., Mou et al., 2020). This, along with scientists' growing demand for higher-quality nanomaterials, makes it critical to examine both the regulated formulation of NP bio-conjugates and the plethora of scenarios that these might have at the nano-bio interface. The majority of plasmon research has been conducted on metal nanostructures containing gold, aluminum, or silver. These noble metals have plasma resonances and practical properties in the visible spectral field. For instance, for oxidation, gold is fairly robust. On the other hand, silver's oxidation strength is less stable, but it has narrower and more powerful LSP resonances. However, as plasmonic has gained popularity, scientists are considering alternatives to noble metals.

The synthesis of gold nanoparticles (Au NPs) has been in the spotlight since Faraday [154] discovered in 1857 the mechanism of formation of pure gold colloids. This synthesis has been the keystone of a large number of chemical routes to obtain Au NPs with a controlled size, shape and surface chemistry. Today, scientists have a wide catalogue of Au NPs available, which can be used as excellent model systems to investigate the nano-bio interface; that is, when Au NPs come into contact with biological components, such as biomolecules, cells, etc. Au NPs have been paired with antibodies or other proteins to attack specific regions of proteins and receptors since the 1970s [186].

Gold nanoparticles (Au NPs) of high quality are used in a variety of applications, including sensors, opto-electronics, medical imaging, and catalysis [187], [188]. Since residual components limit their use, highly distilled surfactant-free Au NPs are critical. Au NP has been synthesised using a variety of approaches, including chemical reduction, biosynthesis, and laser ablation [189], [190]. Despite the low mono dispersibility and the difficulty associated with the manufacturing of their controlled-shape nanoparticles, the synthesis process and the use of toxic reducing agents increase the total cost of their usability [191].

Chemical and biological sensors have received a great deal of attention due to their wide range of applications in contamination detection, medical diagnosis, and other fields. Surface plasmon resonance (SPR) techniques have made significant contributions to the understanding of bimolecular interactions [192]. A relatively simple technique can be used for this form of sensor by using noble metal nanoparticles. The plasmon resonance band of noble metal nanoparticles can be altered by varying physical properties such as size, shape, relative distance, and refractive index of the surrounding medium [193].

The collective oscillation of the conduction electrons within noble metal nanoparticles, referred to as a localized surface plasmon exhibits an absorption spectrum, which depends on the surrounding medium [192]. The sensitivity of a sensor is determined by the ratio of the difference in absorption peak shift to the change in surrounding refractive index, which is dependent on the surrounding refractive index and the binding methods used to adhere the particles to a supporting substrate [194]. The immobilization of the nanoparticles onto the substrate can be achieved by numerous methods which will be described in this chapter. In particular, gold nanoparticles (Au NP) have been used in the form of gold nanospheres (Au NS) and gold nanorods (Au NR) and these immobilized particles could be used as refractive-index sensors.

6.2 SPR Sensor in Planar, Array-based Form

The optical sensor has several key advantages over the conventional SPR sensor. Some of these are simple fabrication, better nanoparticle patterning and a UV-visible spectrometer. Gold colloids and nanorods are used to form an SPR biosensor on a glass substrate for many reasons [192]. Gold nanoparticles are ideal for using visible and near-infrared light for the absorption of light. SPR can be done in transmission or absorption mode, which can be detected by a UV-visible spectrometer. Making SPR sensing accessible to any researcher with a UV-visible spectrophotometer.

6.3 The Use of Noble Metals as a Primary Component of Nanoparticles

Surface plasmon absorption peaks in spherical silver and aluminium particles are more intense than in gold or copper. Silver and aluminium particles, on the other hand, are much more shape-dependent than copper and gold particles in terms of absorption [195]. As a result, they are extremely reliant on the precise spherical contour, size, and shape. Silver has the highest absorption peak, gold has a slightly lower absorption peak, and titanium has an even lower absorption peak. Gold or silver are the best metals for use in SPR sensors. Due to its low oxidation rate and other properties discussed above, gold is preferred in the sensor structure over silver in terms of chemical stability.

6.4 A Brief Overview of Au NP

Spherical gold nanoparticles show a single powerful absorption band that is not present on the substrate in a solid layer of deposited gold. Due to the particle's transverse and longitudinal structures, two distinct absorption bands are observed in elliptical or rod-shaped gold particles. This absorption band occurs when the incident frequency of the photon is resonant with the collective oscillation of the free electron cloud of a particle [195]. The absorption and maximum wavelength are therefore directly commensurate with the change in the LSP's resonance frequency. The sensitivity is determined by the composition of nanoparticles (type, size, form) and the refractive index of the solvent or medium surrounding the medium.

6.5 Plasma and Nanoparticles - Application of Plasma for the Synthesis and Modification of Nanomaterials

Due to their unique physical and chemical properties, nanomaterials for biomedical applications have drawn great attention. In biomedical applications such as cancer therapy, bio-imaging, drug delivery, and tissue engineering, noble metals, transition metals, semi-conductors and carbon-based nanomaterials are widely utilised [196][197]. Even so, the most frequently used strategy for fabricating nanomaterials is chemical synthesis, which requires the use of hazardous and toxic chemical compounds as oxidizing/reducing agents. As a result, it is necessary to develop alternative 'green' methods for restricting the toxicity of nanomaterials. Oftentimes, plasma technology can be used to fabricate nanomaterials [198], In particular, plasma enhanced chemical vapour deposition (PE-CVD) and sputtering. Additionally, air atmospheric pressure plasma can be used to synthesise nanomaterials in ambient room conditions, resulting in large quantities of RONS, which can reduce metal ions in liquid to form metal nanoparticles (NPs). This method is also referred to as a 'green' fabrication method for biomedical research nanomaterials.

Plasmas are extremely versatile and have a wide range of applications. Figure 6.1 illustrates the material types and length scales that are critical for plasma processing of nanomaterials.

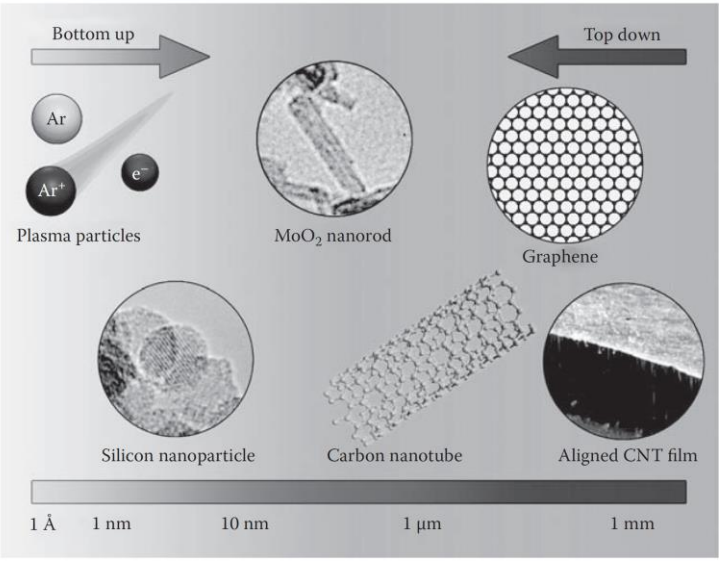

Figure 6.1: Plasma processing of materials at different length scales [199].

6.6 Film Deposition Technique

The transported atom or molecule will begin nucleating and growing in a variety of ways around the substrate. The type of interface formed between the substrate and the atom or molecule is determined by the film's incipient growth. By bombarding the growing thin film with ions from the vapour phase, the composition and microstructure of the thin film can be altered, resulting in sputtering, re-condensation, and nucleation of the film atoms, as well as enhanced surface movement of the film atoms.

There are various types of deposition techniques, however, the focus of this section is on thin film deposition for creating layers of less than one micron in thickness. Physical vapour deposition (PVD) and chemical vapour deposition (CVD) are two of the most common types of deposition techniques. PVD and CVD are distinguished by their vapour phase compositions. The vapour in PVD is composed of atoms and molecules that condense on the substrate and in CVD, the vapour reacts chemically with the substrate, resulting in the formation of a thin film coating

[200], [201]. Figure 6.2 shows thin film deposition types that are purely in the gas, solution and semi-molten or molten state.

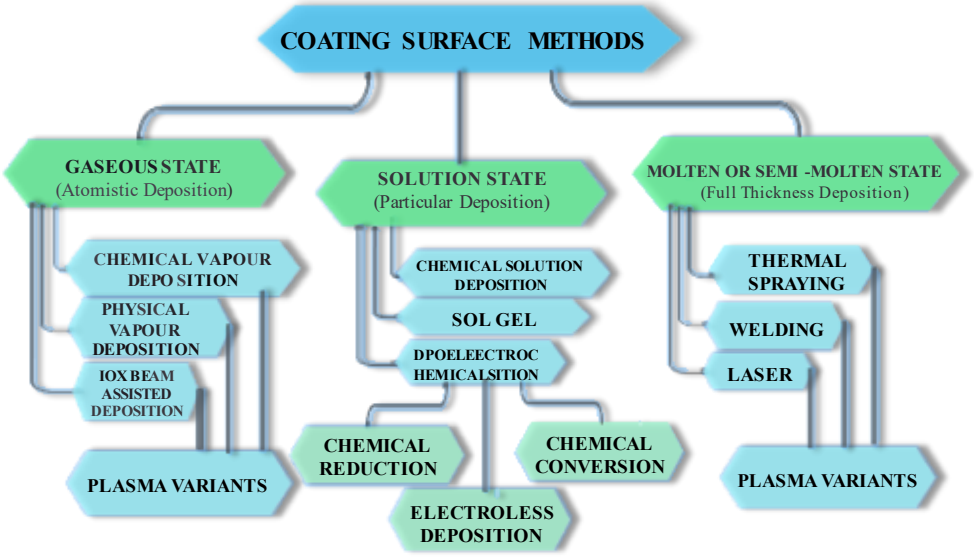

Figure 6.2: Diverse techniques of thin film deposition [200].

6.6.1 Deposition techniques used (vacuum evaporation)

An example of a physical vapour deposition technique is vacuum evaporation. The Au thin films required for the present studies were deposited using an Auto 306 Edwards thermal resistor evaporation system. It is an automated system able to work at a base pressure of 1×10^{-6} mbar by the operation of rotary and oil diffusion pumps. An FTM 6 thickness monitor connected with a water-cooled crystal holder is attached to the evaporation system. This is used to monitor the thickness of the deposited films. The commercially available Si Au powder used in a Tungsten boat is evaporated by the resistive heating of the crucible and the evaporation rate can be controlled by adjusting the current flow through the crucible. The substrates are

placed on a substrate holder about 10 cm away from the heated crucible. Figure 6.3 presents a schematic representation of an evaporation system.

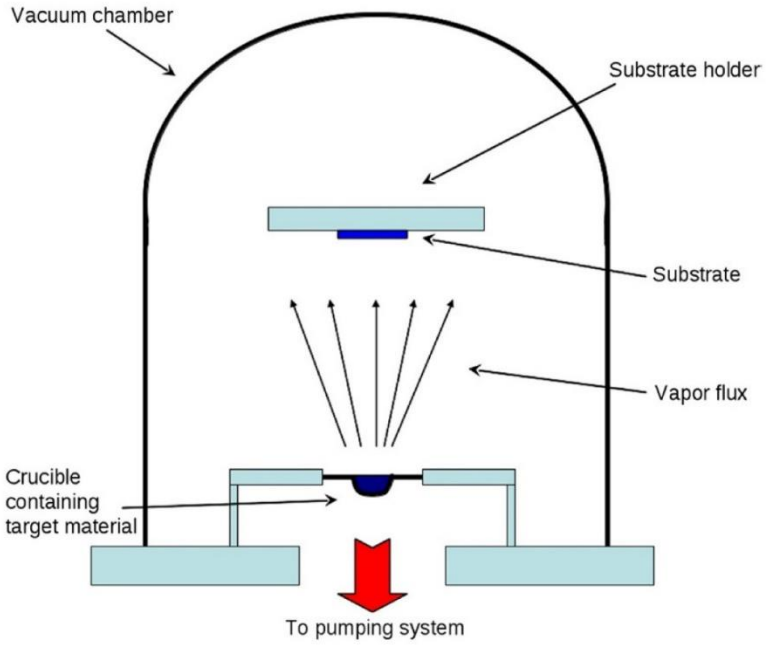

Figure 6.3: A schematic diagram of a vacuum evaporation system [202]

You need to correct the spelling of vapour above.

6.7 Characterisation Methods

Advanced microscopy techniques such as SEM (scanning electron microscopy) methods with a spatial resolution in the nm range are required and commonly used to characterise nanoparticles [203]. It provides valuable data and is required for a comprehensive characterization study and for optical investigations using UV-Vis absorption spectroscopy [204]. The optical interactions of gold nanoparticles can be used to study plasmonic nanoparticles and their applications, most notably the

concepts and applications of surface plasmon resonance (SPR) in Au nanoparticles [205].

6.7.1 UV –VIS absorption spectroscopy

Absorption spectroscopy is a technique for investigating the optical absorption of energy radiations as a feature of wavelength as a result of their contact with a substance. The range of absorbed radiations as a result of wavelength is referred to as the absorption spectrum.

One of the most popular techniques for studying the energy level structure of materials is ultraviolet and visible (UV-Vis) absorption spectroscopy. A Perkin Elmer Lambda 40 spectrometer was used to investigate the UV-Vis absorption spectra of glass samples. In the experiment shown in Figure 6.4, a photograph of the Perkin Elmer Lambda 40 UV-Vis spectrometer was used.

Figure 6.4: Photograph of the Perkin Elmer Lambda 40 UV-Vis spectrometer.

6.7.2 Scanning Electron Microscopy (SEM)

Scanning Electron Microscopy (SEM) is one of the most versatile types of electron microscopy for the investigation of materials' surface topography and chemical composition. The SEM was developed to overcome the optical microscope's limitations, particularly its resolution of 2000 Å. The critical advantage of the SEM over the conventional optical microscope is its significantly higher magnification (> 100,000X) and resolution of 100 Å, which is achieved by imaging with an electron beam rather than visible light.

In this study, a Carl Zeiss EVO LS-15 SEM system was used to examine the gold-coated glass wafer and nanostructures (see Figure 6.5). This system consists of two vacuum chambers: a) the upper chamber, which contains the electron gun column, and b) the lower chamber, which contains the sample holder, stage, and stage control which can be brought to atmospheric pressure without rupturing the upper chamber's vacuum. This is accomplished with the aid of a differential pumping system equipped with pressure-limiting apertures.

Figure 6.5: Photograph of the Zeiss EVO LS-15 SEM system.

6.8 Experimental Set-up

Previously, in Chapter 3, Figure 3.1, an overall block diagram of the atmospheric pressure plasma jet system used was shown. The plasma is created and the plume is expelled from the nozzle when the voltage applied across the gap between the electrode and the grounded nozzle reaches the breakdown voltage. The high voltage power supply (PV400, Information Unlimited, USA). The primary winding of the high voltage step-up transformer was given 0 to 230 Volts via a variac, 50 Hz input.

6.8.1 Sample preparation

Initially, the 1 mm thick gold structures were sputtered on a 5 × 2 cm microscopic glass substrate. To remove any dust or debris, the sample was cleaned with acetone and isopropyl alcohol (IPA) in a beaker. The sample was immersed in acetone for 5 minutes before being washed with IPA. The samples were then dried using dry and clean air.

Samples were then loaded into a vacuum chamber for gold-coating pumping under a pressure of 1 x 10-5 Torr. Different thicknesses of gold investigated on the glass surface were 3, 5 and 25nm. The samples were then treated with an air atmospheric pressure plasma jet. The plasma conditions have been changed to achieve the desired results. Four process parameters were varied: plasma flow rate, plasma input voltage (power), treatment time, and distance between plasma and substrate.

6.9 Results and Dissections

6.9.1 Morphological properties

Glass samples were coated with a 2 nm thickness minutes before being treated with different flow rates (5, 10, and 20 l/min), while the distance between the samples and the nozzle was kept constant (which was chosen to be 2.5 mm) and the treatment time was 1.3 and 10 minutes. Scanning electron microscopy (SEM) was used to identify the types of nanostructures that could be present.

A SEM micrograph with an acceleration voltage of 13.6 kV was used for all measurements. SEM images show an average grain size of micrometres. As shown in Figure 6.6, the gold nanoparticles are selectively positioned within the treated area. As a result, a regular pattern of nanoparticles will be produced. Furthermore, the more nanoparticles produced in the same area, the longer the treatment time. This pattern changed after 20 minutes of treatment with a 25 l/min air flow rate, which could be due to the mechanical effect of treatment time, in which case the pattern is destroyed (Appendix).

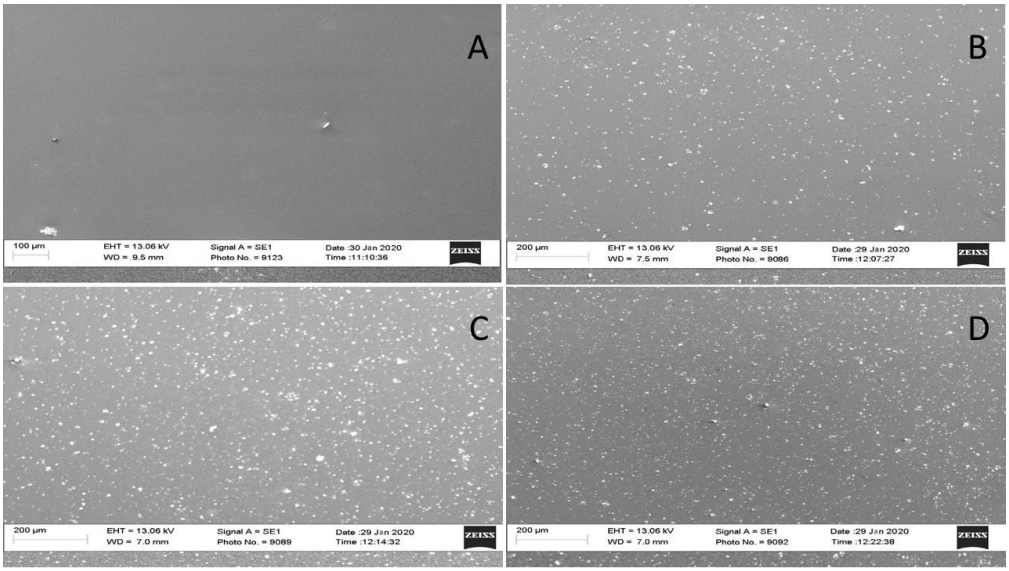

Figure 6.6: SEM images of gold nanoparticle (micro scale patterns on glass obtained from plasma treatment at a flow rate of 20 l/min and a distance of 5mm from the nozzle at various treatment times. (A) coated glass sample; (B) 1 minute treatment time and 5 mm from the nozzle; (C) 3 minute treatment time and 5 mm from the nozzle; (D) 10 minute treatment time and 5 mm from the nozzle

We obtained more precise results by using images at a smaller scale; Figure 6.6 illustrates this in greater detail at a 200 nm scale. Although the Au NPs in (C) and (D) are approximately 20 and 8 nm in diameter, respectively, the amount of Au NPs was very small, which could have a significant effect on the optical properties. We performed UV-INS measurements on these samples and discovered that as the size of the Au NPs increased, the nanostructures' plasmon resonance band shifts [206] (Link, El-Sayed 2000). However, because the nanoparticles are separated, we did not observe the expected shift because the gap between them is greater than 2.5 times their size, as stated in [193] [207].

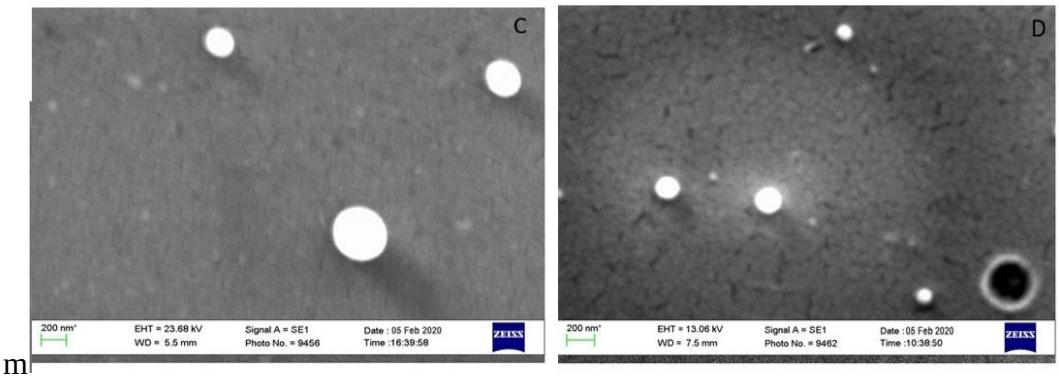

m

Figure 6.7: 200 nm scale of the SEM images of gold nanoparticle patterns on glass obtained from plasma treatment at a flow rate of 20 l/min and a distance of 5 mm from the nozzle at various treatment times. (C) 3 minute treatment time and 5 mm from the nozzle; (D) 10 minute treatment time and 5 mm from the nozzle

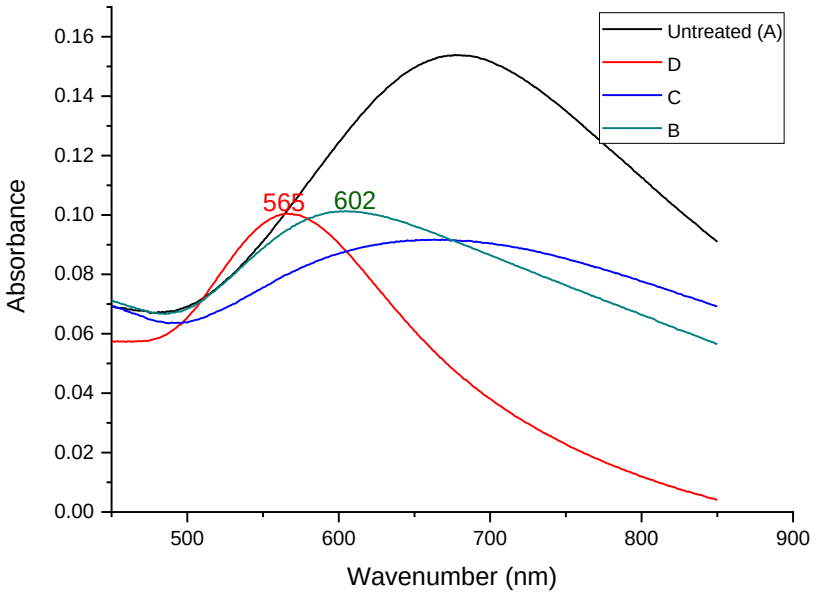

Figure 6.8: Comparison of the UV-vis spectra of as-glass gold coated Au NPs before and after air APPJ treatment with a particle size of (A) before treatment, (B) 3 minute treatment time and 5 mm from the nozzle; (D) 10 minute treatment time and 5 mm from the nozzle, increase in the UV-vis intensity shifted as a function of Au NPs size.

We obtained similar results when the coating thickness was varied between 5 and 25 nanometres; the data is presented in the Appendix.

6.10 Conclusion

In this experiment, gold-coated glass was treated with air atmospheric pressure plasma at various gas flow rates (0.5 l/min to 2 l/min), plasma power, and substrate-to-nozzle distances. SEM and UV-INS were used to characterise the surface morphology and optical properties of control and treated samples. SEM analysis of gold coated glass demonstrates that air plasma jet treatments (different gas flow rates or plasma exposure time) have a small effect on the gold particle measurements of treated samples. Although it is capable of producing small nanoparticles, the quantity produced is insufficient.

7 Conclusion and Recommendations for Future Work

7.1 Conclusions

This work involved the design and construction of an atmospheric pressure plasma jet, as well as the investigation of its chemical, optical and electrical properties.

Chapter 1 discussed the physics and history of APPs. This work aimed to explain the fundamental underlying principles of plasmas, with a particular emphasis on those at atmospheric pressure. The applications of APP are discussed in detail, with an emphasis on modifying the wettability of polymer surfaces, or converting them from hydrophobic to hydrophilic.

Chapter 2 introduced the plasma jet and surface characterisation devices that were used throughout this study. The components used to power the APPJ were described, including the high voltage power supply and the air flow control. Plasma parameters were changed, as well as the distance between the nozzle and the COP substrate, in order to achieve a lower water contact angle. The hydrophobic surface of the COP was modified from 90° to 6° using a simple and inexpensive procedure.

Experimental results were employed in Chapter 3 for modelling using the Response Surface Methodology RSM by means of Design Expert software, and they are practical, accurate and simple to implement. The experimental data was used to develop first and second order mathematical models via regression analysis. These developed mathematical models were optimised for the output responses using the RSM optimization procedure by imposing lower and upper input limits. For air APPJ, it is possible to predict the treated COP wettability. Additionally, optimal conditions can demonstrate that the plasma process is a cost-effective and efficient process. As previously calculated, the additional cost will not exceed 70% of the process without optimization.

In Chapter 4 electrical and optical properties and the emission properties of the plasma were investigated using the experimental method optical emission spectroscopy. Initially the basics of radiative emission theory was presented. The unique spectra of the APPJ were presented and the major features were described. The measurements were token at the optimal parameters obtained from the Design Experiment software.

Chapter 5 demonstrated the treated COP's wettability stability with air APPJ. The wettability of the surface was examined in conjunction with the surface chemistry. This chapter demonstrated experimentally the presence of C=O and O-H bonds on the plasma-treated COP surface. Additionally, the density of these bonds was found to be correlated with the water contact angle, decreasing as the COP surface wettability increased. Additionally, it was demonstrated experimentally that storing the ambient control humidity could prolong the time of stability.

Chapter 6 examined gold nanoparticles coated with glass. We investigated the effect of changing experimental conditions such as the APPJ air flow rate, the applied input voltage, the distance between the nozzle and the substrate and the treatment time on the properties of the resulting nanoparticles. It was discovered that by increasing the concentration of gold nanoparticles, SEM image analysis revealed that when dimension plots indicated that a uniform distribution of nanoparticles had occurred but the maximum density of nanoparticles on the surface had not been reached, the density of nanoparticles could be increased even further.

7.2 Future Work:

The COP film property was developed in this work using extremely cost-effective and commercially viable methods. It is hoped that the process can be improved further with the details provided by this work.

1. Further investigation can be carried out to evaluate the APPJ and the COP properties pre- and post-treatment under various testing and conditions that were not covered in this research, such as the photoelectron spectroscopy (XPS) technique for analyzing the surface chemistry and adhesive properties.

2. Additional research on the Design of Experiment on air APPJ optimization of COP on and other polymers is necessary over a longer time period to establish whether or not they behave similarly under the same APPJ conditions. A modification procedure may incorporate extra process parameters, such as surface roughness, to provide a more precise outcome. Additionally, noise factors in atmospheric pressure plasma, such as room temperature and humidity, must be considered in future DOE research.

3. Future study may concentrate gold nanoparticles on a glass surface, limiting the particle distribution and enabling the application of these low-cost air APPJ as sensing devices

References

[1] S. Cha and Y. Park, "Plasma in dentistry," *Clinical Plasma Medicine,* vol. 2, *(1),* pp. 4-10, 2014.

[2] F. F. Chen, *Introduction to Plasma Physics.* 2012.

[3] X. P. Lu and M. Laroussi, "Electron density and temperature measurement of an atmospheric pressure plasma by millimeter wave interferometer," *Appl. Phys. Lett.,* vol. 92, *(5),* pp. 051501, 2008.

[4] Y. P. Raizer and J. E. Allen, *Gas Discharge Physics.* 1997*2*.

[5] F. Llewellyn-Jones, *Ionization and Breakdown in Gases.* London: Methuen, 1957.

[6] H. Boenig, *Plasma Science and Technology.* 2019.

[7] C. J. McDevitt, Z. Guo and X. Tang, "Avalanche mechanism for runaway electron amplification in a tokamak plasma," *Plasma Phys. Controlled Fusion,* vol. 61, *(5),* pp. 054008, 2019.

[8] A. L. Garner *et al*, "A tutorial on theoretical and computational techniques for gas breakdown in microscale gaps," *IEEE Trans. Plasma Sci.,* vol. 48, *(4),* pp. 808-824, 2020.

[9] M. Radetić, "The influence of low-temperature plasma treatment on some wool properties," in *AIP Conference Proceedings,* 2004, .

[10] S. Thomas *et al*, *Non-Thermal Plasma Technology for Polymeric Materials: Applications in Composites, Nanostructured Materials, and Biomedical Fields.* 2018.

[11] C. Yuan, A. A. Kudryavtsev and V. I. Demidov, "Breakdown and self-sustained discharge ignition in a uniform dc field: the Paschen curves," *Introduction to the Kinetics of Glow Discharges,* pp. 4, 2018.

[12] J. C. Eijkel, H. Stoeri and A. Manz, "An atmospheric pressure dc glow discharge on a microchip and its application as a molecular emission detector," *J. Anal. at. Spectrom.,* vol. 15, *(3),* pp. 297-300, 2000.

[13] M. Tabib-Azar, "Microplasma Field Effect Transistors," *Micro-Plasma Field Effect Transistors,* 2016.

[14] F. F. Chen and J. P. Chang, *Lecture Notes on Principles of Plasma Processing.* 2012.

[15] H. Puliyalil and U. Cvelbar, "Selective Plasma Etching of Polymeric Substrates for Advanced Applications," *Nanomaterials,* vol. 6, *(6),* pp. 108, 2016.

[16] H. Karimabadi *et al*, "Coherent structures, intermittent turbulence, and dissipation in high-temperature plasmas," *Phys Plasmas,* vol. 20, *(1),* pp. 012303, 2013.

[17] P. Gibbon, "Introduction to plasma physics," *arXiv Preprint arXiv:2007.04783,* 2020.

[18] A. Piel, *Plasma Physics: An Introduction to Laboratory, Space, and Fusion Plasmas.* 2017.

[19] R. Mishra *et al*, "Cold plasma: emerging as the new standard in food safety," *Res Inv Int J Eng Sci,* vol. 6, *(2),* pp. 15-20, 2016.

[20] A. Rutscher, "Characteristics of low-temperature plasmas under nonthermal conditions–a short summary," *Low Temperature Plasmas: Fundamentals, Technologies and Techniques,* vol. 1, pp. 1-14, 2008.

[21] C. Tendero *et al*, "Atmospheric pressure plasmas: A review," *Spectrochimica Acta Part B: Atomic Spectroscopy,* vol. 61, *(1),* pp. 2-30, 2006. Available: https://doi.org/10.1016/j.sab.2005.10.003.

[22] K. Wiesemann, "A short introduction to plasma physics," *arXiv Preprint arXiv:1404.0509,* 2014.

[23] R. Chodura, "Plasma–wall transition in an oblique magnetic field," *The Physics of Fluids,* vol. 25, *(9),* pp. 1628-1633, 1982.

[24] X. Lu *et al*, "Guided ionization waves: Theory and experiments," *Physics Reports,* vol. 540, *(3),* pp. 123-166, 2014.

[25] P. Paris, *Initiation of Corona Pulses.* 1994.

[26] T. Iwai *et al*, "Fundamental properties of a non-destructive atmospheric-pressure plasma jet in argon or helium and its first application as an ambient desorption/ionization source for high-resolution mass spectrometry," *J. Anal. at. Spectrom.*, vol. 29, *(3),* pp. 464-470, 2014.

[27] R. A. Wolf, *Atmospheric Pressure Plasma for Surface Modification.* 2012.

[28] J. Hu *et al*, "Dielectric barrier discharge in analytical spectrometry," *Applied Spectroscopy Reviews,* vol. 46, *(5),* pp. 368-387, 2011.

[29] X. Li *et al*, "Enhanced degradation of azo dye in wastewater by pulsed discharge plasma coupled with MWCNTs-TiO 2/γ-Al 2 O 3 composite photocatalyst," *J. Environ. Manage.*, vol. 172, pp. 186-192, 2016.

[30] A. Sobel, "Plasma displays," *IEEE Trans. Plasma Sci.*, vol. 19, *(6),* pp. 1032-1047, 1991.

[31] K. Kunze *et al*, "Diode laser-aided diagnostics of a low-pressure dielectric barrier discharge applied in element-selective detection of molecular species," *Spectrochimica Acta Part B: Atomic Spectroscopy,* vol. 57, *(1),* pp. 137-146, 2002.

[32] M. Miclea *et al*, "The dielectric barrier discharge—a powerful microchip plasma for diode laser spectrometry," *Spectrochimica Acta Part B: Atomic Spectroscopy,* vol. 56, *(1),* pp. 37-43, 2001.

[33] X. Lu, M. Laroussi and V. Puech, "On atmospheric-pressure non-equilibrium plasma jets and plasma bullets," *Plasma Sources Sci. Technol.,* vol. 21, *(3),* pp. 034005, 2012.

[34] U. Kogelschatz, "Dielectric-barrier discharges: their history, discharge physics, and industrial applications," *Plasma Chem. Plasma Process.,* vol. 23, *(1),* pp. 1-46, 2003.

[35] S. Kanazawa *et al*, "Stable glow plasma at atmospheric pressure," *J. Phys. D,* vol. 21, *(5),* pp. 838, 1988.

[36] B. Pashaie, S. K. Dhali and F. I. Honea, "Electrical characteristics of a coaxial dielectric barrier discharge," *J. Phys. D,* vol. 27, *(10),* pp. 2107, 1994.

[37] T. C. Montie, K. Kelly-Wintenberg and J. R. Roth, "An overview of research using the one atmosphere uniform glow discharge plasma (OAUGDP) for sterilization of surfaces and materials," *IEEE Trans. Plasma Sci.,* vol. 28, *(1),* pp. 41-50, 2000.

[38] S. Okazaki *et al*, "Appearance of stable glow discharge in air, argon, oxygen and nitrogen at atmospheric pressure using a 50 Hz source," *J. Phys. D,* vol. 26, *(5),* pp. 889, 1993.

[39] J. Laimer and H. Störi, "Glow Discharges Observed in Capacitive Radio-Frequency Atmospheric-Pressure Plasma Jets," *Plasma Processes and Polymers,* vol. 3, *(8),* pp. 573-586, 2006.

[40] G. S. Selwyn *et al*, "I nsitu plasma contamination measurements by HeNe laser light scattering: A case study," *Journal of Vacuum Science & Technology A: Vacuum, Surfaces, and Films,* vol. 8, *(3),* pp. 1726-1731, 1990.

[41] G. Konesky, "Dwell time considerations for large area cold plasma decontamination," in *SPIE Defense, Security, and Sensing,* 2009, .

[42] A. Salabas, G. Gousset and L. L. Alves, "Charged particle transport modelling in silane–hydrogen radio-frequency capacitively coupled discharges," *Vacuum,* vol. 69, *(1),* pp. 213-219, 2002.

[43] H. Koinuma *et al*, "Development and application of a microbeam plasma generator," *Appl. Phys. Lett.,* vol. 60, *(7),* pp. 816-817, 1992.

[44] A. Schutze *et al*, "The atmospheric-pressure plasma jet: a review and comparison to other plasma sources," *IEEE Trans. Plasma Sci.,* vol. 26, *(6),* pp. 1685-1694, 1998.

[45] M. Teschke *et al*, "High-speed photographs of a dielectric barrier atmospheric pressure plasma jet," *IEEE Trans. Plasma Sci.,* vol. 33, *(2),* pp. 310-311, 2005.

[46] G. Fridman *et al*, "Comparison of direct and indirect effects of non-thermal atmospheric-pressure plasma on bacteria," *Plasma Processes and Polymers,* vol. 4, *(4),* pp. 370-375, 2007.

[47] A. Yamamoto *et al*, "Investigation of gas flow dependence of plasma jet produced by pulsed power," *IEEE Trans. Plasma Sci.,* vol. 43, *(10),* pp. 3451-3455, 2015.

[48] M. Laroussi, "Nonthermal decontamination of biological media by atmospheric-pressure plasmas: review, analysis, and prospects," *IEEE Trans. Plasma Sci.,* vol. 30, *(4),* pp. 1409-1415, 2002.

[49] A. W. Kinandana *et al*, "The comparison of ozone production with dielectric barrier discharge plasma reactors series and parallel at atmospheric pressure," in *Journal of Physics: Conference Series*, 2019, .

[50] G. Speranza, W. Liu and L. Minati, *Applications of Plasma Technologies to Material Processing.* 2019.

[51] R. J. Young and P. A. Lovell, *Introduction to Polymers.* 2011.

[52] N. Casado *et al*, "Current trends in redox polymers for energy and medicine," *Progress in Polymer Science,* vol. 52, pp. 107-135, 2016.

[53] F. Poncin-Epaillard, J. C. Brosse and T. Falher, "Cold plasma treatment: Surface or bulk modification of polymer films" *Macromolecules,* vol. 30, *(15),* pp. 4415-4420, 1997.

[54] M. Mortazavi and M. Nosonovsky, "A model for diffusion-driven hydrophobic recovery in plasma treated polymers," *Appl. Surf. Sci.,* vol. 258, *(18),* pp. 6876-6883, 2012.

[55] N. Recek, "Biocompatibility of plasma-treated polymeric implants," *Materials,* vol. 12, *(2),* pp. 240, 2019.

[56] P. Das *et al*, "Surface modification of electrospun PVA/chitosan nanofibers by dielectric barrier discharge plasma at atmospheric pressure and studies of their mechanical properties and biocompatibility," *Int. J. Biol. Macromol.,* vol. 114, pp. 1026-1032, 2018.

[57] M. C. Coen *et al*, "Modification of the micro-and nanotopography of several polymers by plasma treatments," *Appl. Surf. Sci.,* vol. 207, *(1-4),* pp. 276-286, 2003.

[58] L. J. Gerenser, "XPS studies of in situ plasma-modified polymer surfaces," *J. Adhes. Sci. Technol.,* vol. 7, *(10),* pp. 1019-1040, 1993.

[59] S. K. Nemani *et al*, "Surface modification of polymers: methods and applications," *Advanced Materials Interfaces,* vol. 5, *(24),* pp. 1801247, 2018.

[60] Z. Zhao *et al*, "Controllable modification of polymer membranes by LDDLT plasma flow: Grafting acidic ILs into PPF membrane for catalytic performance," *J. Membr. Sci.,* vol. 553, pp. 99-110, 2018.

[61] K. Orihara *et al*, "Heparin molecularly imprinted polymer thin flm on gold electrode by plasma-induced graft polymerization for label-free biosensor," *J. Pharm. Biomed. Anal.,* vol. 151, pp. 324-330, 2018.

[62] M. Narimisa *et al*, "Atmospheric pressure microwave plasma jet for organic thin film deposition," *Polymers,* vol. 12, *(2),* pp. 354, 2020.

[63] E. M. Liston, L. Martinu and M. R. Wertheimer, "Plasma surface modification of polymers for improved adhesion: a critical review," *J. Adhes. Sci. Technol.,* vol. 7, *(10),* pp. 1091-1127, 1993. Available: https://doi.org/10.1163/156856193X00600.

[64] C. Borcia, I. L. Punga and G. Borcia, "Surface properties and hydrophobic recovery of polymers treated by atmospheric-pressure plasma," *Appl. Surf. Sci.,* vol. 317, pp. 103-110, 2014.

[65] K. G. Kostov *et al*, "Surface modification of polymeric materials by cold atmospheric plasma jet," *Appl. Surf. Sci.,* vol. 314, pp. 367-375, 2014. Available: , https://doi.org/10.1016/j.apsusc.2014.07.009.

[66] S. Wang, W. Cui and J. Bei, "Bulk and surface modifications of polylactide," *Analytical and Bioanalytical Chemistry,* vol. 381, *(3),* pp. 547-556, 2005.

[67] (July 17). *Thermal_barrier_coatings*. Available: http://www.substech.com/.

[68] S. Alberici *et al*, "Organic contamination study for adhesion enhancement between final passivation surface and packaging molding compound," *Microelectronic Engineering,* vol. 76, *(1-4),* pp. 227-234, 2004.

[69] P. Molitor, V. Barron and T. Young, "Surface treatment of titanium for adhesive bonding to polymer composites: a review," *Int J Adhes Adhes,* vol. 21, *(2),* pp. 129-136, 2001.

[70] N. Bhatnagar, "Effect of plasma on adhesion characteristics of high performance polymers," *Reviews of Adhesion and Adhesives,* vol. 1, *(4),* pp. 397-412, 2013.

[71] S. Murab *et al*, "Elucidation of bio-inspired hydroxyapatie crystallization on oxygen-plasma modified 3D printed poly-caprolactone scaffolds," *Materials Science and Engineering: C,* vol. 109, pp. 110529, 2020.

[72] M. B. Borooj *et al*, "Optimization of plasma treatment variables for the improvement of carbon fibres/epoxy composite performance by response surface methodology," *Composites Sci. Technol.,* vol. 128, pp. 215-221, 2016.

[73] F. Poncin-Epaillard and G. Legeay, "Why is the modification of polymer surfaces with electromagnetic discharge so advantageous" in *Annales De Chimie Science Des Materiaux*, 2003, .

[74] T. Li and Z. Suo, "Ductility of thin metal films on polymer substrates modulated by interfacial adhesion," *Int. J. Solids Structures*, vol. 44, *(6)*, pp. 1696-1705, 2007.

[75] D. Hegemann, H. Brunner and C. Oehr, "Plasma treatment of polymers for surface and adhesion improvement," *Nuclear Instruments and Methods in Physics Research Section B: Beam Interactions with Materials and Atoms*, vol. 208, pp. 281-286, 2003.

[76] J. Friedrich *et al*, "Polymer surface modification with monofunctional groups of variable types and densities," *J. Adhes. Sci. Technol.*, vol. 17, *(12)*, pp. 1591-1617, 2003. Available: https://doi.org/10.1163/156856103322396695.

[77] J. Yun *et al*, "Adhesive and Structural Failures of Oxide Coatings on Plasma-Treated Polymers," *Plasma Processes and Polymers*, vol. 8, *(9)*, pp. 815-831, 2011.

[78] C. Chan, *Polymer Surface Modification and Characterization.* 1993.

[79] F. Z. Cui and Z. S. Luo, "Biomaterials modification by ion-beam processing," *Surface and Coatings Technology*, vol. 112, *(1)*, pp. 278-285, 1999.

[80] D. Zhang, Q. Sun and L. C. Wadsworth, "Mechanism of corona treatment on polyolefin films," *Polymer Engineering & Science*, vol. 38, *(6)*, pp. 965-970, 1998.

[81] C. Chan, T. Ko and H. Hiraoka, "Polymer surface modification by plasmas and photons," *Surface Science Reports*, vol. 24, *(1-2)*, pp. 1-54, 1996.

[82] T. S. Williams, H. Yu and R. F. Hicks, "Atmospheric pressure plasma activation of polymers and composites for adhesive bonding," *Reviews of Adhesion and Adhesives*, vol. 1, *(1)*, pp. 46-87, 2013.

[83] J. P. Pascault and R. Williams, "Glass transition temperature versus conversion relationships for thermosetting polymers," *Journal of Polymer Science Part B: Polymer Physics*, vol. 28, *(1)*, pp. 85-95, 1990.

[84] M. Noeske *et al*, "Plasma jet treatment of five polymers at atmospheric pressure: surface modifications and the relevance for adhesion," *Int J Adhes Adhes*, vol. 24, *(2)*, pp. 171-177, 2004. Available: https://doi.org/10.1016/j.ijadhadh.2003.09.006.

[85] J. G. Terlingen *et al*, "Introduction of functional groups on polyethylene surfaces by a carbon dioxide plasma treatment," *J Appl Polym Sci*, vol. 57, *(8)*, pp. 969-982, 1995.

[86] A. Kuwabara, S. Kuroda and H. Kubota, "Polymer surface treatment by atmospheric pressure low temperature surface discharge plasma: Its characteristics and comparison with low pressure oxygen plasma treatment," *Plasma Science and Technology*, vol. 9, *(2)*, pp. 181, 2007.

[87] R. Dorai and M. J. Kushner, "A model for plasma modification of polypropylene using atmospheric pressure discharges," *J. Phys. D*, vol. 36, *(6)*, pp. 666, 2003.

[88] U. Lommatzsch *et al*, "Atmospheric pressure plasma jet treatment of polyethylene surfaces for adhesion improvement," *Plasma Processes and Polymers*, vol. 4, *(S1)*, pp. S1041-S1045, 2007.

[89] J. Zhou, A. V. Ellis and N. H. Voelcker, "Recent developments in PDMS surface modification for microfluidic devices," *Electrophoresis*, vol. 31, *(1)*, pp. 2-16, 2010.

[90] S. Roy *et al*, "Surface analysis, hydrophilic enhancement, ageing behavior and flow in plasma modified cyclic olefin copolymer (COC)-based microfluidic devices," *Sensors Actuators B: Chem.*, vol. 150, *(2)*, pp. 537-549, 2010. Available: http://www.sciencedirect.com/science/article/pii/S0925400510007173. DOI: http://dx.doi.org/10.1016/j.snb.2010.08.043.

[91] J. Cui *et al*, "Synthesis of high performance cyclic olefin polymers (COPs) with ester group via ring-opening metathesis polymerization," *Polymers*, vol. 7, *(8)*, pp. 1389-1409, 2015. Available: . https://doi.org/10.3390/polym7081389.

[92] S. Lee *et al*, "Highly purified cyclic olefin polymer by ROMP and In situ hydrogenation with ruthenium supported catalyst," *Macromolecular Research*, vol. 20, *(8)*, pp. 777-779, 2012.

[93] H. T. Ban *et al*, "Synthesis of cyclo-olefin copolymer latexes and their carbon nanotube composite nanoparticles," *Journal of Polymer Science Part A: Polymer Chemistry*, vol. 51, *(21)*, pp. 4584-4591, 2013.

[94] J. Y. Shin *et al*, "Chemical structure and physical properties of cyclic olefin copolymers (IUPAC technical report)," *Pure and Applied Chemistry*, vol. 77, *(5)*, pp. 801-814, 2005.

[95] K. Obuchi, M. Komatsu and K. Minami, "High performance optical materials cyclo olefin polymer ZEONEX," in *Optical Manufacturing and Testing VII*, 2007, .

[96] M. Sabzekar *et al*, "Cyclic olefin polymer as a novel membrane material for membrane distillation applications," *J. Membr. Sci.*, vol. 621, pp. 118845, 2021.

[97] W. D. Niles and P. J. Coassin, "Cyclic olefin polymers: innovative materials for high-density multiwell plates," *Assay and Drug Development Technologies*, vol. 6, *(4)*, pp. 577-590, 2008. Available: . http://doi.org/10.1089/adt.2008.134.

[98] S. Liu *et al*, "Fabrication of Cyclo-olefin polymer-based microfluidic devices using CO2 laser ablation," *Materials Research Express,* vol. 5, *(9),* pp. 095305, 2018.

[99] A. T. Alsharhan *et al*, "3D microfluidics via cyclic olefin polymer-based in situ direct laser writing," *Lab on a Chip,* vol. 19, *(17),* pp. 2799-2810, 2019.

[100] B. Wang *et al*, "Surface wettability modification of cyclic olefin polymer by direct femtosecond laser irradiation," *Nanomaterials,* vol. 5, *(3),* pp. 1442-1453, 2015. Available: https://doi.org/10.3390/nano5031442.

[101] R. A. Holland *et al*, "A synthesis of the ecosystem services impact of second generation bioenergy crop production," *Renewable and Sustainable Energy Reviews,* vol. 46, *(0),* pp. 30-40, 2015. Available: http://www.sciencedirect.com/science/article/pii/S136403211500091X. DOI: http://dx.doi.org/10.1016/j.rser.2015.02.003.

[102] M. G. Katsikogianni *et al*, "Use of atmospheric plasma jet treatments for the enhancement of cell adhesion to 1 mm internal diameter microwell cell arrays," in *2011 10th International Workshop on Biomedical Engineering,* 2011, .

[103] S. Laib and B. D. MacCraith, "Immobilization of biomolecules on cycloolefin polymer supports," *Anal. Chem.,* vol. 79, *(16),* pp. 6264-6270, 2007.

[104] I. Beaulieu, M. Geissler and J. Mauzeroll, "Oxygen plasma treatment of polystyrene and Zeonor: substrates for adhesion of patterned cells," *Langmuir,* vol. 25, *(12),* pp. 7169-7176, 2009. Available: https://doi.org/10.1021/la9001972.

[105] K. Karahashi and S. Hamaguchi, "Ion beam experiments for the study of plasma–surface interactions," *J. Phys. D,* vol. 47, *(22),* pp. 224008, 2014.

[106] S. Hwang *et al*, "Surface modification of cyclic olefin copolymer substrate by oxygen plasma treatment," *Surface and Coatings Technology,* vol. 202, *(15),* pp. 3669-3674, 2008.

[107] J. Tyczkowski, *Cold Plasma-A Promising Tool for the Development of Electrochemical Cells.* 2012.

[108] D. Nikolova *et al*, "Surface modification of cycloolefinic copolymers for optimization of the adhesion to metals," *Surface and Interface Analysis: An International Journal Devoted to the Development and Application of Techniques for the Analysis of Surfaces, Interfaces and Thin Films,* vol. 36, *(8),* pp. 689-693, 2004.

[109] C. Hurth, R. Lenigk and F. Zenhausern, "A compact LED-based module for DNA capillary electrophoresis," *Applied Physics B,* vol. 93, *(2-3),* pp. 693, 2008.

[110] C. W. Tsao *et al*, "Low temperature bonding of PMMA and COC microfluidic substrates using UV/ozone surface treatment," *Lab on a Chip,* vol. 7, *(4),* pp. 499-505, 2007.

[111] A. ul Haq *et al*, "Corona discharge-induced functional surfaces of polycarbonate and cyclic olefins substrates," *Surface and Coatings Technology*, vol. 362, pp. 185-190, 2019. Available: https://doi.org/10.1016/j.surfcoat.2019.01.073.

[112] S. Bourg *et al*, "Surface functionalization of cyclic olefin copolymer by plasma-enhanced chemical vapor deposition using atmospheric pressure plasma jet for microfluidic applications," *Plasma Processes and Polymers*, vol. 16, *(6)*, pp. 1800195, 2019.

[113] (). *Zeonex*. *www.zeonex.com*. Available: https://www.zeonex.com/life-sciences.aspx.html.

[114] S. H. Lim *et al*, "Resin impregnation and interfacial adhesion behaviors in carbon fiber/epoxy composites: Effects of polymer slip and normalized surface free energy with respect to the sizing agents," *Composites Part A: Applied Science and Manufacturing*, vol. 146, pp. 106424, 2021.

[115] T. Huhtamäki *et al*, "Surface-wetting characterization using contact-angle measurements," *Nature Protocols*, vol. 13, *(7)*, pp. 1521-1538, 2018.

[116] B. Han *et al*, "Simultaneous determination of surface energy and roughness of dense membranes by a modified contact angle method," *Colloids Surf. Physicochem. Eng. Aspects*, vol. 562, pp. 370-376, 2019.

[117] Y. Chen, J. Zhang and Y. Cohen, "Fouling Resistant and Performance Tunable Ultrafiltration Membranes via Surface Graft Polymerization induced by Atmospheric Pressure Air Plasma," *Separation and Purification Technology*, pp. 120490, 2022.

[118] L. A. Belyaeva *et al*, "Hydrophilicity of graphene in water through transparency to polar and dispersive interactions," *Adv Mater*, vol. 30, *(6)*, pp. 1703274, 2018.

[119] Z. Zhang *et al*, "Binary liquid mixture contact-angle measurements for precise estimation of surface free energy," *Langmuir*, vol. 35, *(38)*, pp. 12317-12325, 2019.

[120] C. Hoffmann, C. Berganza and J. Zhang, "Cold Atmospheric Plasma: methods of production and application in dentistry and oncology," *Medical Gas Research*, vol. 3, *(1)*, pp. 21, 2013.

[121] V. I. Pârvulescu, M. Magureanu and P. Lukes, *Plasma Chemistry and Catalysis in Gases and Liquids.* 2012.

[122] J. Friedrich *et al*, "Formation of plasma polymer layers with functional groups of different type and density at polymer surfaces and their interaction with Al atoms," *Plasma Processes and Polymers*, vol. 1, *(1)*, pp. 28-50, 2004. Available: https://doi.org/10.1002/ppap.200400008.

[123] M. M. Dudek *et al*, "Plasma surface modification of cyclo-olefin polymers and its application to lateral flow bioassays," *Langmuir,* vol. 25, *(18),* pp. 11155-11161, 2009.

[124] R. France and R. Short, "Plasma treatment of polymers effects of energy transfer from an argon plasma on the surface chemistry of poly (styrene), low density poly (ethylene), poly (propylene) and poly (ethylene terephthalate)," *Journal of the Chemical Society, Faraday Transactions,* vol. 93, *(17),* pp. 3173-3178, 1997.

[125] P. Nancy *et al*, "Spectroscopic and mass spectrometry analyses of plasma-activated polymeric materials," in *Non-Thermal Plasma Technology for Polymeric Materials*Anonymous 2019, .

[126] A. Vesel *et al*, "Evolution of the surface wettability of PET polymer upon treatment with an atmospheric-pressure plasma jet," *Polymers,* vol. 12, *(1),* pp. 87, 2020.

[127] H. M. Abourayana *et al*, "Evaluation of the effect of plasma treatment frequency on the activation of polymer particles," *Plasma Chem. Plasma Process.,* vol. 37, *(4),* pp. 1223-1235, 2017.

[128] K. Yambe, S. Taka and K. Ogura, "Relation between plasma plume density and gas flow velocity in atmospheric pressure plasma," *Phys Plasmas,* vol. 21, *(4),* pp. 043511, 2014. Available: https://doi.org/10.1063/1.4873384.

[129] A. Van Deynse *et al*, "Surface activation of polyethylene with an argon atmospheric pressure plasma jet: Influence of applied power and flow rate," *Appl. Surf. Sci.,* vol. 328, pp. 269-278, 2015. Available: https://doi.org/10.1016/j.apsusc.2014.12.075.

[130] E. J. Baek *et al*, "Effects of the electrical parameters and gas flow rate on the generation of reactive species in liquids exposed to atmospheric pressure plasma jets," *Phys Plasmas,* vol. 23, *(7),* pp. 073515, 2016. Available: https://doi.org/10.1063/1.4959174.

[131] W. A. Zisman, "Influence of constitution on adhesion," *Industrial & Engineering Chemistry,* vol. 55, *(10),* pp. 18-38, 1963.

[132] Q. Li *et al*, "Understanding the dependence of contact angles of commercially RO membranes on external conditions and surface features," *Desalination,* vol. 309, pp. 38-45, 2013.

[133] Y. Baek *et al*, "Measuring hydrophilicity of RO membranes by contact angles via sessile drop and captive bubble method: A comparative study," *Desalination,* vol. 303, pp. 23-28, 2012.

[134] S. H. Anastasiadis, "Development of functional polymer surfaces with controlled wettability," *Langmuir,* vol. 29, *(30),* pp. 9277-9290, 2013.

[135] D. H. Prajitno, A. Maulana and D. G. Syarif, "Effect of surface roughness on contact angle measurement of nanofluid on surface of stainless steel 304 by sessile drop method," in *Journal of Physics: Conference Series,* 2016, .

[136] C. Mandolfino, E. Lertora and C. Gambaro, "Effect of cold plasma treatment on surface roughness and bonding strength of polymeric substrates," in *Key Engineering Materials,* 2014, .

[137] D. S. Everhart and C. N. Reilley, "Chemical derivatization in electron spectroscopy for chemical analysis of surface functional groups introduced on low-density polyethylene film," *Anal. Chem.*, vol. 53, *(4),* pp. 665-676, 1981.

[138] C. Chen and S. Li, "Spectroscopic measurement of plasma gas temperature of the atmospheric-pressure microwave induced nitrogen plasma torch," *Plasma Sources Sci. Technol.*, vol. 24, *(3),* pp. 035017, 2015. Available: . https://doi.org/10.1088/0963-0252/24/3/035017,.

[139] M. S. Park *et al*, "Selective Wet-Etching of Polymer/Fullerene Blend Films for Surface-and Nanoscale Morphology-Controlled Organic Transistors and Sensitivity-Enhanced Gas Sensors," *Polymers*, vol. 11, *(10),* pp. 1682, 2019. Available: https://doi.org/10.3390/polym11101682.

[140] M. H. Hansen *et al*, "The role of corona discharge treatment in improving polyethylene-aluminum adhesion: an acid-base perspective," *Tappi J.*, vol. 76, *(2),* pp. 171-177, 1993. Available: https://www.bcin.ca/bcin/detail.applid=116557.

[141] F. Agulló-López *et al*, "Ion beam modification of dielectric materials in the electronic excitation regime: cumulative and exciton models," *Progress in Materials Science*, vol. 76, pp. 1-58, 2016. Available: https://doi.org/10.1016/j.pmatsci.2015.06.002.

[142] H. Yamasaki *et al*, "Patternable atmospheric-pressure plasma jets with gas discharge in microfluidic channel array," in *2013 IEEE 26th International Conference on Micro Electro Mechanical Systems (MEMS),* 2013, pp. 205-208.

[143] A. Merenda *et al*, "Assessing the temporal stability of surface functional groups introduced by plasma treatments on the outer shells of carbon nanotubes," *Sci. Rep.*, vol. 6, pp. 31565, 2016. Available: . https://doi.org/10.1038/srep31565.

[144] M. J. Shenton, M. C. Lovell-Hoare and G. C. Stevens, "Adhesion enhancement of polymer surfaces by atmospheric plasma treatment," *J. Phys. D*, vol. 34, *(18),* pp. 2754, 2001. Available: . https://doi.org/10.1088/0022-3727/34/18/307.

[145] D. P. Dowling *et al*, "Influence of dc pulsed atmospheric pressure plasma jet processing conditions on polymer activation," *Plasma Processes and Polymers*, vol. 8, *(8),* pp. 718-727, 2011. Available: , https://doi.org/10.1002/ppap.201000145.

[146] F. Sandon, "Experimental Designs. By WG Cochran and GM Cox. Pp. ix, 454. 46s. 1950.(Wiley & Sons, New York; Chapman & Hall, London)," *The Mathematical Gazette*, vol. 36, *(315)*, pp. 78-79, 1952.

[147] S. L. Lohr, *Sampling: Design and Analysis: Design and Analysis.* 2019.

[148] A. I. Khuri and J. A. Cornell, *Response Surfaces: Designs and Analyses.* 2018.

[149] (). *https://www.statease.com/docs/v12/contents/response-surface-designs/historical-data/*.

[150] R. H. Myers, D. C. Montgomery and C. M. Anderson-Cook, *Response Surface Methodology: Process and Product Optimization using Designed Experiments.* 2016.

[151] K. Y. Benyounis, A. Olabi and M. Hashmi, "Multi-response optimization of CO2 laser-welding process of austenitic stainless steel," *Optics & Laser Technology*, vol. 40, *(1)*, pp. 76-87, 2008. Available: https://doi.org/10.1016/j.optlastec.2007.03.009.

[152] C. L. Rinsch *et al*, "Pulsed radio frequency plasma polymerization of allyl alcohol: Controlled deposition of surface hydroxyl groups," *Langmuir*, vol. 12, *(12)*, pp. 2995-3002, 1996. Available: https://doi.org/10.1021/la950685u.

[153] F. T. O'Neill *et al*, "Generation of active species in a large atmospheric-pressure plasma jet," *IEEE Trans. Plasma Sci.*, vol. 40, *(11)*, pp. 2994-3002, 2012. Available: https://ieeexplore.ieee.org/document/6301740.

[154] H. M. Abourayana and D. P. Dowling, "Plasma processing for tailoring the surface properties of polymers," *Surface Energy*, pp. 123, 2015.

[155] A. Fridman, *Plasma Chemistry.* 2008.

[156] R. Zaplotnik, G. Primc and A. Vesel, "Optical emission spectroscopy as a diagnostic tool for characterization of atmospheric plasma jets," *Applied Sciences*, vol. 11, *(5)*, pp. 2275, 2021.

[157] M. Laroussi and X. Lu, "Room-temperature atmospheric pressure plasma plume for biomedical applications," *Appl. Phys. Lett.*, vol. 87, *(11)*, pp. 113902, 2005.

[158] S. Yoshimura *et al*, "Insights into normothermic treatment with direct irradiation of atmospheric pressure plasma for biological applications," *Japanese Journal of Applied Physics*, 2020.

[159] S. Duarte and B. H. Panariello, "Comprehensive biomedical applications of low temperature plasmas," *Arch. Biochem. Biophys.*, pp. 108560, 2020.

[160] S. Y. Moon and W. Choe, "A comparative study of rotational temperatures using diatomic OH, O2 and N2 molecular spectra emitted from atmospheric plasmas," *Spectrochimica Acta Part B: Atomic Spectroscopy,* vol. 58, *(2),* pp. 249-257, 2003.

[161] C. Cheng, Z. Liye and R. Zhan, "Surface modification of polymer fibre by the new atmospheric pressure cold plasma jet," *Surface and Coatings Technology,* vol. 200, *(24),* pp. 6659-6665, 2006.

[162] Q. Xiong *et al*, "Length control of He atmospheric plasma jet plumes: Effects of discharge parameters and ambient air," *Phys Plasmas,* vol. 16, *(4),* pp. 043505, 2009.

[163] Y. Yu, K. Huang and L. Wu, "Influence of a nearby conductor on shape and length of a microwave plasma jet," *Physical Review E,* vol. 102, *(3),* pp. 031201, 2020.

[164] P. Makvandi *et al*, "Functionalization of polymers and nanomaterials for water treatment, food packaging, textile and biomedical applications: A review," *Environmental Chemistry Letters,* pp. 1-29, 2020.

[165] J. F. Friedrich *et al*, "New plasma techniques for polymer surface modification with monotype functional groups," *Plasma Processes and Polymers,* vol. 5, *(5),* pp. 407-423, 2008.

[166] L. Lin *et al*, "Microfluidic plasmas: Novel technique for chemistry and chemical engineering," *Chem. Eng. J.*, pp. 129355, 2021.

[167] K. Norrman *et al*, "Controlling surface properties of electrospun polyphenylsulfone using plasma treatment and X-ray photoelectron spectroscopy," *Heliyon,* vol. 5, *(6),* pp. e01943, 2019.

[168] K. L. Van Landuyt *et al*, "Systematic review of the chemical composition of contemporary dental adhesives," *Biomaterials,* vol. 28, *(26),* pp. 3757-3785, 2007.

[169] C. Tan and H. Zhang, "Wet-chemical synthesis and applications of non-layer structured two-dimensional nanomaterials," *Nature Communications,* vol. 6, *(1),* pp. 1-13, 2015.

[170] M. Hung and R. R. Burch, "Functionalization and metallization of fluoropolymer surfaces through reduction1, 2," *J Appl Polym Sci,* vol. 55, *(4),* pp. 549-559, 1995.

[171] H. Yasuda, "Plasma for modification of polymers," *Journal of Macromolecular Science—Chemistry,* vol. 10, *(3),* pp. 383-420, 1976.

[172] J. López-García, "Wettability analysis and water absorption studies of plasma activated polymeric materials," in *Non-Thermal Plasma Technology for Polymeric Materials*Anonymous 2019, .

[173] D. J. Guckenberger *et al*, "Induced hydrophobic recovery of oxygen plasma-treated surfaces," *Lab on a Chip,* vol. 12, *(13),* pp. 2317-2321, 2012.

[174] C. Canal *et al*, "Wettability, ageing and recovery process of plasma-treated polyamide 6," *J. Adhes. Sci. Technol.,* vol. 18, *(9),* pp. 1077-1089, 2004.

[175] T. R. Gengenbach, R. C. Chatelier and H. J. Griesser, "Characterization of the ageing of plasma-deposited polymer films: Global analysis of X-ray photoelectron spectroscopy data," *Surface and Interface Analysis: An International Journal Devoted to the Development and Application of Techniques for the Analysis of Surfaces, Interfaces and Thin Films,* vol. 24, *(4),* pp. 271-281, 1996.

[176] F. Lisco *et al*, "Atmospheric-pressure plasma surface activation for solution processed photovoltaic devices," *Solar Energy,* vol. 146, pp. 287-297, 2017.

[177] M. M. Hossain *et al*, "Formation of plasma-polymerized superhydrophobic coating using an atmospheric-pressure plasma jet," *Thin Solid Films,* vol. 675, pp. 34-42, 2019.

[178] K. Li *et al*, "Superhydrophobic thermoplastic surfaces with hierarchical micro-nanostructures fabricated by hot-embossing," in *2020 IEEE 20th International Conference on Nanotechnology (IEEE-NANO),* 2020, pp. 81-84.

[179] D. H. Kim *et al*, "Influences of guide-tube and bluff-body on advanced atmospheric pressure plasma source for single-crystalline polymer nanoparticle synthesis at low temperature," *Phys Plasmas,* vol. 24, *(2),* pp. 023506, 2017.

[180] K. Moraczewski *et al*, "Stability studies of plasma modification effects of polylactide and polycaprolactone surface layers," *Appl. Surf. Sci.,* vol. 377, pp. 228-237, 2016.

[181] D. Bodas and C. Khan-Malek, "Hydrophilization and hydrophobic recovery of PDMS by oxygen plasma and chemical treatment—An SEM investigation," *Sensors Actuators B: Chem.,* vol. 123, *(1),* pp. 368-373, 2007.

[182] T. R. Gengenbach and H. J. Griesser, "Aging of 1, 3-diaminopropane plasma-deposited polymer films: Mechanisms and reaction pathways," *Journal of Polymer Science Part A: Polymer Chemistry,* vol. 37, *(13),* pp. 2191-2206, 1999.

[183] J. M. Strobel *et al*, "Aging of air-corona-treated polypropylene film," *J. Adhes. Sci. Technol.,* vol. 5, *(2),* pp. 119-130, 1991.

[184] Y. Ren, C. Wang and Y. Qiu, "Aging of surface properties of ultra high modulus polyethylene fibers treated with He/O2 atmospheric pressure plasma jet," *Surface and Coatings Technology,* vol. 202, *(12),* pp. 2670-2676, 2008.

[185] T. Schuman *et al*, "Surface treatment and printing properties of dispersion-coated paperboard," *Progress in Organic Coatings,* vol. 54, *(3),* pp. 188-197, 2005.

[186] J. B. Lynch *et al*, "Atmospheric pressure plasma treatment of polyethylene via a pulse dielectric barrier discharge: Comparison using various gas compositions versus corona discharge in air," *J Appl Polym Sci,* vol. 71, *(2),* pp. 319-331, 1999.

[187] C. O'Connell *et al*, "Investigation of the hydrophobic recovery of various polymeric biomaterials after 172 nm UV treatment using contact angle, surface free energy and XPS measurements," *Appl. Surf. Sci.,* vol. 255, *(8),* pp. 4405-4413, 2009. Available: https://doi.org/10.1016/j.apsusc.2008.11.034.

[188] F. Truica-Marasescu *et al*, "Hydrophobic recovery of VUV/NH3 modified polyolefin surfaces: Comparison with plasma treatments in nitrogen," *Nuclear Instruments and Methods in Physics Research Section B: Beam Interactions with Materials and Atoms,* vol. 236, *(1-4),* pp. 117-122, 2005. Available: https://doi.org/10.1016/j.nimb.2005.03.266.

[189] (6 May.). *"noble metal". Encyclopedia Britannica.* Available: https://www.britannica.com/science/noble-metal.

[190] K. P. Kepp, "Chemical causes of metal nobleness," *ChemPhysChem,* vol. 21, *(5),* pp. 360-369, 2020.

[191] W. P. Faulk and G. M. Taylor, "Communication to the editors: an immunocolloid method for the electron microscope," *Immunochemistry,* vol. 8, *(11),* pp. 1081-1083, 1971.

[192] Y. Ma *et al*, "Surface-enhanced Raman spectroscopy on self-assembled Au nanoparticles arrays for pesticides residues multiplex detection under complex environment," *Nanomaterials,* vol. 9, *(3),* pp. 426, 2019.

[193] M. M. Mahan and A. L. Doiron, "Gold nanoparticles as X-ray, CT, and multimodal imaging contrast agents: formulation, targeting, and methodology," *Journal of Nanomaterials,* vol. 2018, 2018.

[194] R. Binaymotlagh *et al*, "In situ generation of the gold nanoparticles–bovine serum albumin (AuNPs–BSA) bioconjugated system using pulsed-laser ablation (PLA)," *Mater. Chem. Phys.,* vol. 177, pp. 360-370, 2016.

[195] Z. Guo *et al*, "Generation of alginate gel particles with AuNPs layers by polydimethylsiloxan template," *Biomicrofluidics,* vol. 5, *(2),* pp. 026502, 2011.

[196] C. Peng *et al*, "Shape-controlled generation of gold nanoparticles assisted by dual-molecules: the development of hydrogen peroxide and oxidase-based biosensors," *Journal of Nanomaterials,* vol. 2014, 2014.

[197] E. E. Bedford *et al*, "Surface plasmon resonance biosensors incorporating gold nanoparticles," *Macromolecular Bioscience,* vol. 12, *(6),* pp. 724-739, 2012.

[198] N. Nath and A. Chilkoti, "Label-free biosensing by surface plasmon resonance of nanoparticles on glass: optimization of nanoparticle size," *Anal. Chem.,* vol. 76, *(18),* pp. 5370-5378, 2004.

[199] S. Jo *et al*, "Localized surface plasmon resonance aptasensor for the highly sensitive direct detection of cortisol in human saliva," *Sensors Actuators B: Chem.,* vol. 304, pp. 127424, 2020.

[200] C. F. Bohren and D. R. Huffman, *Absorption and Scattering of Light by Small Particles.* 2008.

[201] D. Douroumis *et al*, "Mesoporous silica nanoparticles as a drug delivery system," 2011.

[202] Y. K. Mishra and R. Adelung, "ZnO tetrapod materials for functional applications," *Materials Today,* vol. 21, *(6),* pp. 631-651, 2018.

[203] K. Ostrikov, E. C. Neyts and M. Meyyappan, "Plasma nanoscience: from nano-solids in plasmas to nano-plasmas in solids," *Adv. Phys.,* vol. 62, *(2),* pp. 113-224, 2013.

[204] R. M. Sankaran, *Plasma Processing of Nanomaterials.* 2011.

[205] O. O. Abegunde *et al*, "Overview of thin film deposition techniques," *AIMS Materials Science,* vol. 6, *(2),* pp. 174-199, 2019.

[206] R. F. Bunshah, *Deposition Technologies for Films and Coatings: Developments and Applications.* 1982.

[207] R. J. Martín-Palma and A. Lakhtakia, "Vapor-deposition techniques," in *Engineered Biomimicry*Anonymous 2013, .

[208] A. M. Funston *et al*, "Plasmon coupling of gold nanorods at short distances and in different geometries," *Nano Letters,* vol. 9, *(4),* pp. 1651-1658, 2009.

[209] V. Amendola and M. Meneghetti, "Size evaluation of gold nanoparticles by UV− vis spectroscopy," *The Journal of Physical Chemistry C,* vol. 113, *(11),* pp. 4277-4285, 2009.

[210] J. Liu *et al*, "Recent advances of plasmonic nanoparticles and their applications," *Materials,* vol. 11, *(10),* pp. 1833, 2018.

[211] S. Link and M. A. El-Sayed, "Shape and size dependence of radiative, non-radiative and photothermal properties of gold nanocrystals," *International Reviews in Physical Chemistry,* vol. 19, *(3),* pp. 409-453, 2000.

[212] D. Huang *et al*, "Plastic-compatible low resistance printable gold nanoparticle conductors for flexible electronics," *J. Electrochem. Soc.,* vol. 150, *(7),* pp. G412, 2003.

Appendix

Diverse gold thicknesses deposited on glass samples treated with air atmospheric pressure plasma je

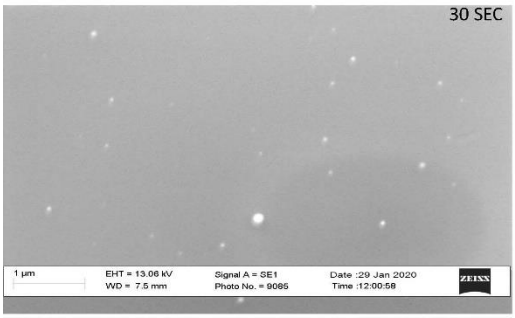
30 SEC
1 µm
EHT = 13.06 kV
WD = 7.5 mm
Signal A = SE1
Photo No. = 9085
Date :29 Jan 2020
Time :12:00:58
ZEISS

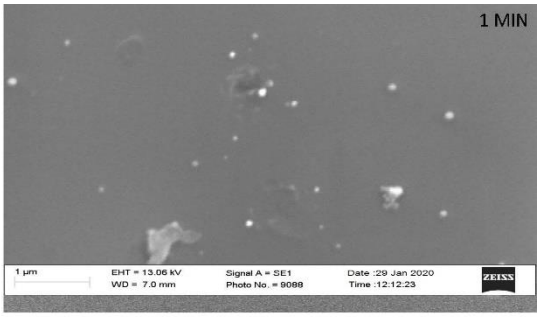
1 MIN
1 µm
EHT = 13.06 kV
WD = 7.0 mm
Signal A = SE1
Photo No. = 9088
Date :29 Jan 2020
Time :12:12:23
ZEISS

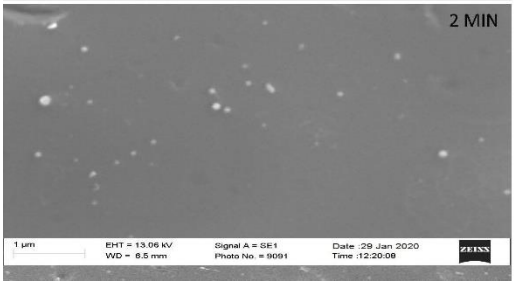
2 MIN
1 µm
EHT = 13.06 kV
WD = 6.5 mm
Signal A = SE1
Photo No. = 9091
Date :29 Jan 2020
Time :12:20:08
ZEISS

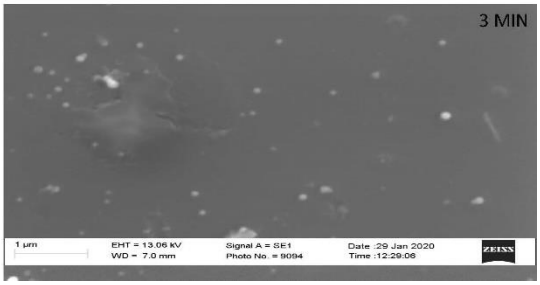
3 MIN
1 µm
EHT = 13.06 kV
WD = 7.0 mm
Signal A = SE1
Photo No. = 9094
Date :29 Jan 2020
Time :12:29:06
ZEISS

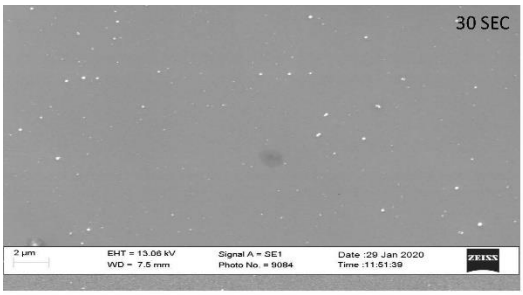
30 SEC
2 µm
EHT = 13.06 kV
WD = 7.5 mm
Signal A = SE1
Photo No. = 9084
Date :29 Jan 2020
Time :11:51:39
ZEISS

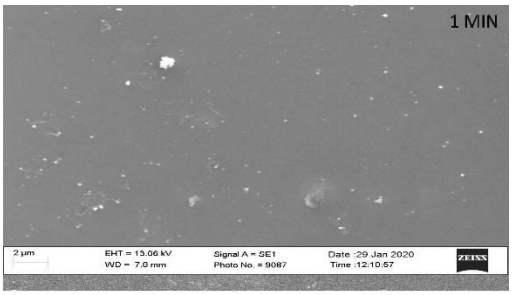
1 MIN
2 µm
EHT = 13.06 kV
WD = 7.0 mm
Signal A = SE1
Photo No. = 9087
Date :29 Jan 2020
Time :12:10:57
ZEISS

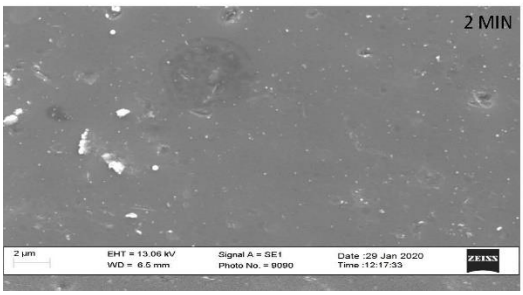
2 MIN
2 µm
EHT = 13.06 kV
WD = 6.5 mm
Signal A = SE1
Photo No. = 9090
Date :29 Jan 2020
Time :12:17:33
ZEISS

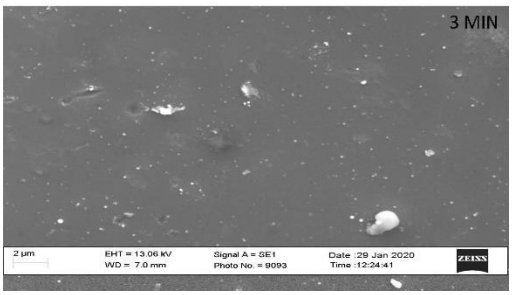
3 MIN
2 µm
EHT = 13.06 kV
WD = 7.0 mm
Signal A = SE1
Photo No. = 9093
Date :29 Jan 2020
Time :12:24:41
ZEISS

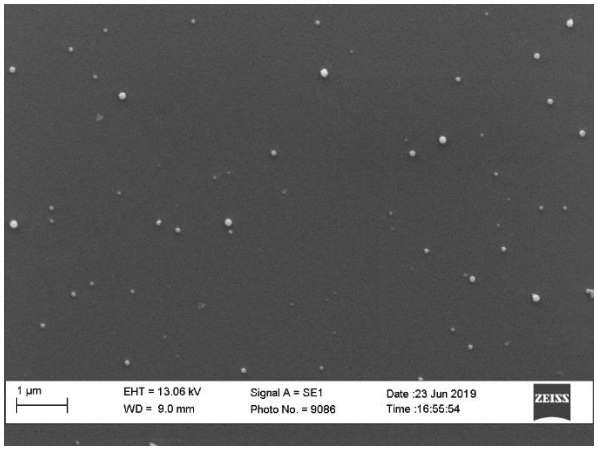

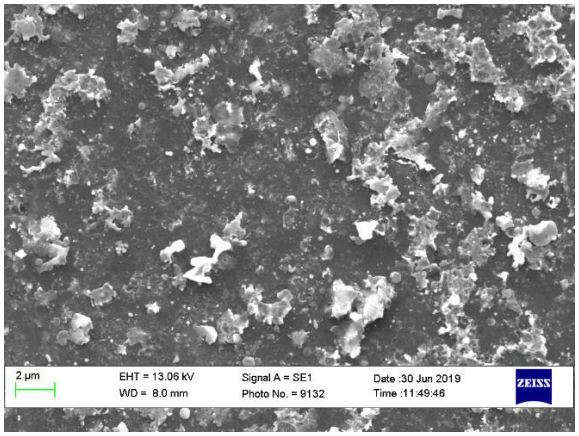

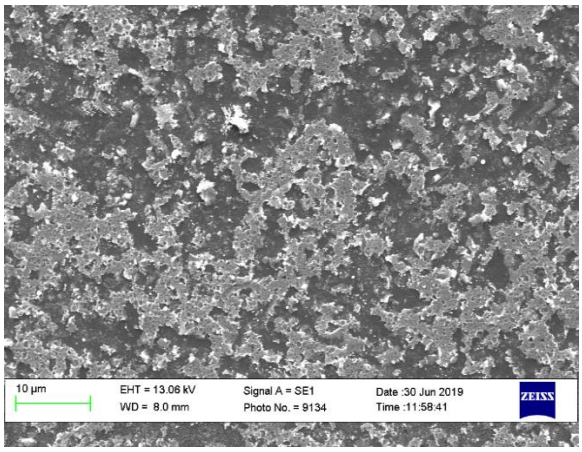

The effect of APPJ plasma on Optical absorption of glass gold deposited with deferent thickness

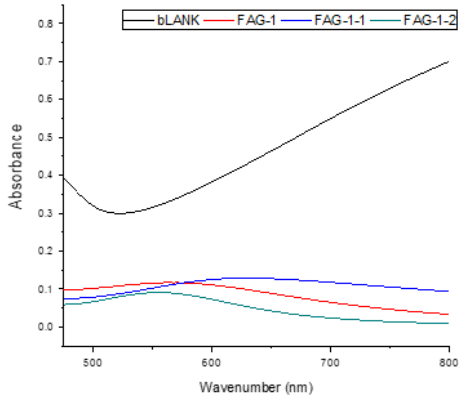

5 minutes deposition
Blank : before treatment
FAG1: Plasma treatment
Vin=180v air flow=20L\ min time=20mins.
FAG1-1 : treated second time
Vin=180v air flow= 10L\ min time=20mins
FAG1-3 : Plasma treatment
Vin=220v air flow=5.5 time=20mins

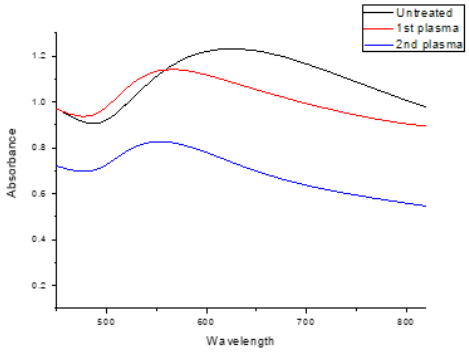

8 minutes deposition
1st: Plasma treatment
Vin=215v air flow=5L \min time=20mins.
2nd : treated second time with same conditions

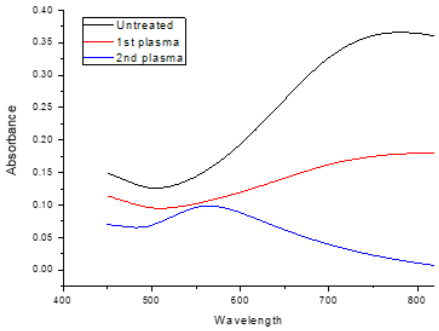

5nm thick gold deposition
1st: Plasma treatment
Vin=215v air flow=5L \min time=20mins.
2nd : treated second time with same conditions+ heated 500c

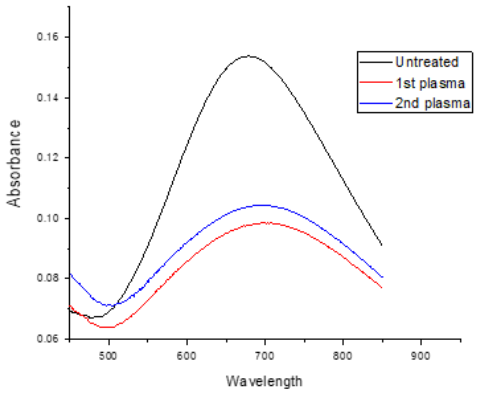

2nm thick gold deposition
1st: Plasma treatment
Vin=215v air flow=5L \min time=20mins.
2nd : treated second time with same conditions